

CERN-EP-2017-193
2018/04/26

CMS-HIN-17-001

Constraints on the chiral magnetic effect using charge-dependent azimuthal correlations in pPb and PbPb collisions at the LHC

The CMS Collaboration*

Abstract

Charge-dependent azimuthal correlations of same- and opposite-sign pairs with respect to the second- and third-order event planes have been measured in pPb collisions at $\sqrt{s_{\text{NN}}} = 8.16$ TeV and PbPb collisions at 5.02 TeV with the CMS experiment at the LHC. The measurement is motivated by the search for the charge separation phenomenon predicted by the chiral magnetic effect (CME) in heavy ion collisions. Three- and two-particle azimuthal correlators are extracted as functions of the pseudorapidity difference, the transverse momentum (p_{T}) difference, and the p_{T} average of same- and opposite-charge pairs in various event multiplicity ranges. The data suggest that the charge-dependent three-particle correlators with respect to the second- and third-order event planes share a common origin, predominantly arising from charge-dependent two-particle azimuthal correlations coupled with an anisotropic flow. The CME is expected to lead to a v_2 -independent three-particle correlation when the magnetic field is fixed. Using an event shape engineering technique, upper limits on the v_2 -independent fraction of the three-particle correlator are estimated to be 13% for pPb and 7% for PbPb collisions at 95% confidence level. The results of this analysis, both the dominance of two-particle correlations as a source of the three-particle results and the similarities seen between PbPb and pPb, provide stringent constraints on the origin of charge-dependent three-particle azimuthal correlations and challenge their interpretation as arising from a chiral magnetic effect in heavy ion collisions.

Published in Physical Review C as doi:10.1103/PhysRevC.97.044912.

1 Introduction

It has been suggested that in high-energy nucleus-nucleus (AA) collisions, metastable domains of gluon fields with nontrivial topological configurations may form [1–4]. These domains can carry an imbalance between left- and right-handed quarks arising from interactions of chiral quarks with topological gluon fields, leading to a local parity (P) violation [3, 4]. This chirality imbalance, in the presence of the extremely strong magnetic field, which can be produced in a noncentral AA collision, is expected to lead to an electric current perpendicular to the reaction plane, resulting in a final-state charge separation phenomenon known as the chiral magnetic effect (CME) [5–7]. Such macroscopic phenomena arising from quantum anomalies are a subject of interest for a wide range of physics communities. The chiral-anomaly-induced phenomena have been observed in magnetized relativistic matter in three-dimensional Dirac and Weyl materials [8–10]. The search for the charge separation from the CME in AA collisions was first carried out at RHIC at BNL [11–15] and later at the CERN LHC [16] at various center-of-mass energies. In these measurements, a charge-dependent azimuthal correlation with respect to the reaction plane was observed, which is qualitatively consistent with the expectation of charge separation from the CME. No strong collision energy dependence of the signal is observed going from RHIC to LHC energies, although some theoretical predictions suggested that the possible CME signal could be much smaller at the LHC than at RHIC because of a shorter lifetime of the magnetic field [17]. Nevertheless, theoretical estimates of the time evolution of the magnetic field have large uncertainties [17].

The experimental evidence for the CME in heavy ion collisions remains inconclusive because of several identified sources of background correlations that can account for part or all of the observed charge-dependent azimuthal correlations [18–20]. Moreover, the charge-dependent azimuthal correlation in high-multiplicity pPb collisions has been recently found to have a nearly identical value to that observed in PbPb collisions [21]. This is a strong indication that the observed effect in heavy ion collisions might predominantly result from background contributions. The CME-induced charge separation effect is predicted to be negligible in pPb collisions, as the angle between the magnetic field direction and the event plane is expected to be randomly distributed [21, 22].

The charge separation can be characterized by the first P -odd sine term (a_1) in a Fourier decomposition of the charged-particle azimuthal distribution [23]:

$$\frac{dN}{d\phi} \propto 1 + 2 \sum_n \{v_n \cos[n(\phi - \Psi_{\text{RP}})] + a_n \sin[n(\phi - \Psi_{\text{RP}})]\}, \quad (1)$$

where $\phi - \Psi_{\text{RP}}$ represents the particle azimuthal angle with respect to the reaction plane angle Ψ_{RP} in heavy ion collisions (determined by the impact parameter and beam axis), and v_n and a_n denote the coefficients of P -even and P -odd Fourier terms, respectively. Although the reaction plane is not an experimental observable, it can be approximated in heavy ion collisions by the second-order event plane, Ψ_2 , determined by the direction of the beam and the maximal particle density in the elliptic azimuthal anisotropy. The P -odd terms will vanish after averaging over events, because the sign of the chirality imbalance changes event by event. Therefore, the observation of such an effect is only possible through the measurement of particle azimuthal correlations. An azimuthal three-particle correlator, γ_{112} , proposed to explore the first coefficient, a_1 , of the P -odd Fourier terms characterizing the charge separation [23] is:

$$\gamma_{112} \equiv \langle \cos(\phi_\alpha + \phi_\beta - 2\Psi_2) \rangle = \langle \cos(\phi_\alpha - \Psi_2) \cos(\phi_\beta - \Psi_2) \rangle - \langle \sin(\phi_\alpha - \Psi_2) \sin(\phi_\beta - \Psi_2) \rangle. \quad (2)$$

Here, α and β denote particles with the same or opposite electric charge sign and the angle brackets reflect an averaging over particles and events. Assuming particles α and β are uncorrelated, except for their individual correlations with respect to the event plane, the first term on the right-hand side of Eq. (2) becomes $\langle v_{1,\alpha} v_{1,\beta} \rangle$, which is generally small and independent of the charge [12], while the second term is sensitive to the charge separation and can be expressed as $\langle a_{1,\alpha} a_{1,\beta} \rangle$.

While the similarity of the pPb and PbPb data at 5.02 TeV analyzed by the CMS experiment pose a considerable challenge to the CME interpretation of the charge-dependent azimuthal correlations observed in AA collisions [21], important questions still remain to be addressed: is the correlation signal observed in pPb collisions entirely a consequence of background correlations? What is the underlying mechanism for those background correlations that are almost identical in pPb and PbPb collisions? Can the background contribution be quantitatively constrained with data and, if so, is there still evidence for a statistically significant CME signal?

In particular, among the proposed mechanisms for background correlations, one source is related to the charge-dependent two-particle correlation from local charge conservation in decays of resonances or clusters (e.g., jets) [20]. By coupling with the anisotropic particle emission, an effect resembling charge separation with respect to the reaction plane can be generated. The observed characteristic range of the two-particle correlation in data is around one unit of rapidity, consistent with short-range cluster decays. In this mechanism of local charge conservation coupled with the elliptic flow, a background contribution to the three-particle correlator, γ_{112} , is expected to be [24]:

$$\gamma_{112}^{\text{bkg}} = \kappa_2 \langle \cos(\phi_\alpha - \phi_\beta) \rangle \langle \cos 2(\phi_\beta - \Psi_{\text{RP}}) \rangle = \kappa_2 \delta v_2. \quad (3)$$

Here, $\delta \equiv \langle \cos(\phi_\alpha - \phi_\beta) \rangle$ represents the charge-dependent two-particle azimuthal correlator and κ_2 is a constant parameter, independent of v_2 , but mainly determined by the kinematics and acceptance of particle detection [24]. As both the charge conservation effect and anisotropic flow are known to be present in heavy ion collisions, the primary goal of this paper is to conduct a systematic investigation of how much of the observed charge-dependent correlations in the data can be accounted for by this mechanism.

Although the background contribution from local charge conservation is well defined in Eq. (3) and has been long recognized [17, 20, 24], it is still not known to what extent background contributions account for the observed γ_{112} correlator. The main difficulty lies in determining the unknown value of κ_2 in a model-independent way. The other difficulty is to demonstrate directly the linear dependence on v_2 of $\gamma_{112}^{\text{bkg}}$, which is nontrivial as one has to ensure the magnetic field, and thus the CME, does not change when selecting events with different v_2 values. Therefore, selecting events with a quantity that directly relates to the magnitude of v_2 is essential.

This paper aims to overcome the difficulties mentioned above and achieve a better understanding as to the contribution of the local charge conservation background to the charge-dependent azimuthal correlation data. The results should serve as a new baseline for the search for the CME in heavy ion collisions. Two approaches are employed as outlined below.

1. Higher-order harmonic three-particle correlator: in heavy ion collisions, the charge separation effect from the CME is only expected along the direction of the induced magnetic field normal to the reaction plane, approximated by the second-order event plane, Ψ_2 . As the symmetry plane of the third-order Fourier term (“triangular flow” [25]), Ψ_3 , is expected to have a weak correlation with Ψ_2 [26], the charge separation effect with respect

to Ψ_3 is expected to be negligible. By constructing a charge-dependent correlator with respect to the third-order event plane,

$$\gamma_{123} \equiv \langle \cos(\phi_\alpha + 2\phi_\beta - 3\Psi_3) \rangle, \quad (4)$$

charge-dependent background effects unrelated to the CME can be explored. In particular, in the context of the local charge conservation mechanism, the γ_{123} correlator is also expected to have a background contribution, with

$$\gamma_{123}^{\text{bkg}} = \kappa_3 \langle \cos(\phi_\alpha - \phi_\beta) \rangle \langle \cos 3(\phi_\beta - \Psi_3) \rangle = \kappa_3 \delta v_3, \quad (5)$$

similar to that for the γ_{112} correlator as given in Eq. (3). As the κ_2 and κ_3 parameters mainly depend on particle kinematics and detector acceptance effects, they are expected to be similar, largely independent of harmonic event plane orders. The relation in Eq. (5) can be generalized for all ‘‘higher-order harmonic’’ three-particle correlators, $\gamma_{1,n-1,n} = \kappa_n \delta v_n$. Derivation of Eq. (5) as well as generalization to all higher-order harmonics can be found in Appendix A, which follows similar steps as for that of Eq. (3) given in Ref. [24]. One caveat here is that when averaging over a wide η and p_T range, the κ_n value may also depend on the η and p_T dependence of the v_n harmonic, which is similar, but not exactly identical between the v_2 and v_3 coefficients [27, 28].

By taking the difference of correlators between same- and opposite-sign pairs (denoted as $\Delta\gamma_{112}$ and $\Delta\gamma_{123}$ among three particles, and $\Delta\delta$ between two particles) to eliminate all charge-independent background sources, the following relation is expected to hold if the charge dependence of three-particle correlators is dominated by the effect of local charge conservation coupled with the anisotropic flow:

$$\frac{\Delta\gamma_{112}}{\Delta\delta v_2} \approx \frac{\Delta\gamma_{123}}{\Delta\delta v_3}. \quad (6)$$

Therefore, an examination of Eq. (6) will quantify to what extent the proposed background from charge conservation contributes to the γ_{112} correlator, and will be a critical test of the CME interpretation in heavy ion collisions.

2. Event shape engineering (ESE): to establish directly a linear relationship between the γ correlators and v_n coefficients, the ESE technique [29] is employed. In a narrow centrality or multiplicity range (so that the magnetic field does not change significantly), events are further classified based on the magnitude of the event-by-event Fourier harmonic related to the anisotropy measured in the forward rapidity region. Within each event class, the γ correlators and v_n values are measured and compared to test the linear relationship. A nonzero intercept value of the γ correlators with a linear fit would reflect the strength of the CME.

With a higher luminosity pPb run at $\sqrt{s_{\text{NN}}} = 8.16$ TeV and using the high-multiplicity trigger in CMS, the pPb data sample gives access to multiplicities comparable to those in peripheral PbPb collisions, allowing for a detailed comparison and study of the two systems with very different expected CME contributions in the collisions [21]. Measurements of three-particle correlators, γ_{112} and γ_{123} , and the two-particle correlator, δ , are presented in different charge combinations as functions of the pseudorapidity (η) difference ($|\Delta\eta|$), the transverse momentum (p_T) difference ($|\Delta p_T|$), and the average p_T of correlated particles (\bar{p}_T). Integrated over η and p_T , the event multiplicity dependence of three- and two-particle correlations is also presented in pPb and PbPb collisions. In pPb collisions, the particle correlations are explored separately with

respect to the event planes that are obtained using particles with $4.4 < |\eta| < 5.0$ from the p- and Pb-going beam directions. The ESE analysis is performed for γ_{112} as a function of v_2 in both pPb and PbPb collisions.

This paper is organized as follows. After a brief description of the detector and data samples in Section 2, the event and track selections are discussed in Section 3, followed by the discussion of the analysis technique in Section 4. The results are presented in Section 5, and the paper is summarized in Section 6.

2 Detector and data samples

The central feature of the CMS apparatus is a superconducting solenoid of 6 m internal diameter, providing a magnetic field of 3.8 T. Within the solenoid volume, there are four primary subdetectors, including a silicon pixel and strip tracker detector, a lead tungstate crystal electromagnetic calorimeter (ECAL), and a brass and scintillator hadron calorimeter (HCAL), each composed of a barrel and two endcap sections. The silicon tracker measures charged particles within the range $|\eta| < 2.5$. Iron and quartz-fiber Cherenkov hadron forward (HF) calorimeters cover the range $2.9 < |\eta| < 5.2$. The HF calorimeters are constituted of towers, each of which is a two-dimensional cell with a granularity of 0.5 units in η and 0.349 radians in ϕ . For charged particles with $1 < p_T < 10$ GeV and $|\eta| < 1.4$, the track resolutions are typically 1.5% in p_T and 25–90 (45–150) μm in the transverse (longitudinal) impact parameter [30]. A detailed description of the CMS detector, together with a definition of the coordinate system used and the relevant kinematic variables, can be found in Ref. [31].

The pPb data at $\sqrt{s_{\text{NN}}} = 8.16$ TeV used in this analysis were collected in 2016, and correspond to an integrated luminosity of 186 nb^{-1} . The beam energies are 6.5 TeV for the protons and 2.56 TeV per nucleon for the lead nuclei. The data were collected in two different run periods: one with the protons circulating in the clockwise direction in the LHC ring, and one with them circulating in the counterclockwise direction. By convention, the proton beam rapidity is taken to be positive when combining the data from the two run periods. A subset of PbPb data at $\sqrt{s_{\text{NN}}} = 5.02$ TeV collected in 2015 (30–80% centrality, where centrality is defined as the fraction of the total inelastic cross section, with 0% denoting the most central collisions) is used. The PbPb data were reprocessed using the same reconstruction algorithm as the pPb data, in order to compare directly the two colliding systems at similar final-state multiplicities. The three-particle correlator, γ_{112} , data for pPb collisions at $\sqrt{s_{\text{NN}}} = 8.16$ TeV are compared to those previously published at $\sqrt{s_{\text{NN}}} = 5.02$ TeV [21] to examine any possible collision energy dependence. Because of statistical limitations, new analyses of higher-order harmonic three-particle correlator and event shape engineering introduced in this paper cannot be performed with the 5.02 TeV pPb data.

3 Selection of events and tracks

The event reconstruction, event selections, and the triggers, including the dedicated triggers to collect a large sample of high-multiplicity pPb events at $\sqrt{s_{\text{NN}}} = 8.16$ TeV, are similar to those used in previous CMS particle correlation measurements at lower energies [28, 32–34], as discussed below. For PbPb events, they are identical to those in Ref. [21].

Minimum bias pPb events at 8.16 TeV were selected by requiring energy deposits in at least one of the two HF calorimeters above a threshold of approximately 1 GeV and the presence of at least one track with $p_T > 0.4$ GeV in the pixel tracker. In order to collect a large sample of

high-multiplicity pPb collisions, a dedicated trigger was implemented using the CMS level-1 (L1) and high-level trigger (HLT) systems. At L1, the total number of towers of ECAL+HCAL above a threshold of 0.5 GeV in transverse energy (E_T) was required to be greater than a given threshold (120 and 150 towers), where a tower is defined by $\Delta\eta \times \Delta\phi = 0.087 \times 0.087$ radians. Online track reconstruction for the HLT was based on the same offline iterative tracking algorithm to maximize the trigger efficiency. For each event, the vertex reconstructed with the greatest number of tracks was selected. The number of tracks with $|\eta| < 2.4$, $p_T > 0.4$ GeV, and a distance of closest approach less than 0.12 cm to this vertex, was determined for each event and required to exceed a certain threshold (120, 150, 185, 250).

In the offline analysis of pPb (PbPb) collisions, hadronic events are selected by requiring the presence of at least one (three) energy deposit(s) greater than 3 GeV in each of the two HF calorimeters. Events are also required to contain a primary vertex within 15 cm of the nominal interaction point along the beam axis and 0.15 cm in the transverse direction. In the pPb data sample, the average pileup (number of interactions per bunch crossing) varied between 0.1 to 0.25 pPb interactions per bunch crossing. A procedure similar to that described in Ref. [28] is used for identifying and rejecting pileup events. It is based on the number of tracks associated with each reconstructed vertex and the distance between multiple vertices. The pileup in PbPb data is negligible.

For track selections, the impact parameter significance of the track with respect to the primary vertex in the direction along the beam axis and in the transverse plane, $d_z/\sigma(d_z)$ and $d_T/\sigma(d_T)$, are required to be less than 3. The relative uncertainty in p_T , $\sigma(p_T)/p_T$, must be less than 10%. Primary tracks, i.e., tracks that originate at the primary vertex and satisfy the high-purity criteria of Ref. [30], are used to define the event charged-particle multiplicity ($N_{\text{trk}}^{\text{offline}}$). To perform correlation measurements, each track is also required to leave at least one hit in one of the three layers of the pixel tracker. Only tracks with $|\eta| < 2.4$ and $p_T > 0.3$ GeV are used in this analysis to ensure high tracking efficiency.

The pPb and PbPb data are compared in classes of $N_{\text{trk}}^{\text{offline}}$, where primary tracks with $|\eta| < 2.4$ and $p_T > 0.4$ GeV are counted. To compare with results from other experiments, the PbPb data are also analyzed based on centrality classes for the 30–80% centrality range.

4 Analysis technique

The analysis technique of three-particle correlations employed in this paper is based on that established in Ref. [21], with the extension of charge-dependent two-particle correlations, higher-order harmonic three-particle correlations, and correlation studies in different event shape classes (i.e., ESE analysis). The details are outlined below.

4.1 Calculations of two- and three-particle correlators

Without directly reconstructing the event plane, the expression given in Eq. (2) can be alternatively evaluated using a three-particle correlator with respect to a third particle [11, 12], $\langle \cos(\phi_\alpha + \phi_\beta - 2\phi_c) \rangle / v_{2,c}$, where $v_{2,c}$ is the elliptic flow anisotropy of particle c with inclusive charge sign. The three-particle correlator is measured via the scalar-product method of Q vectors. A complex Q vector for each event is defined as $Q_n \equiv \sum_{i=1}^M w_i e^{in\phi_i} / W$, where ϕ_i is the azimuthal angle of particle i , n is the Fourier harmonic order, M is the number of particles in the Q_n calculation in each event, w_i is a weight assigned to each particle for efficiency correction, which is derived from a simulation using the HIJING event generator [35]. The $W = \sum_{i=1}^M w_i$ represents the weight of the Q vector. In this way, the three-particle correlator can be expressed

in terms of the product of Q vectors, i.e., $Q_{1,\alpha}$ and $Q_{1,\beta}$, when particles α and β are chosen from different detector phase-space regions or carry different charge signs,

$$\gamma_{112} = \frac{\langle \cos(\phi_\alpha + \phi_\beta - 2\phi_c) \rangle}{v_{2,c}} = \frac{\langle Q_{1,\alpha} Q_{1,\beta} Q_{2,\text{HF}\pm}^* \rangle}{\sqrt{\frac{\langle Q_{2,\text{HF}\pm} Q_{2,\text{HF}\mp}^* \rangle \langle Q_{2,\text{HF}\pm} Q_{2,\text{trk}}^* \rangle}{\langle Q_{2,\text{HF}\mp} Q_{2,\text{trk}}^* \rangle}}, \quad (7)$$

where the angle brackets on the right-hand side denote an event average of the Q -vector products, weighted by the product of their respective total weights W . Here $Q_{2,\text{trk}}$ is the charge inclusive Q_2 vector of all particles in the tracker region, and $Q_{2,\text{HF}\pm}$ denotes the Q_2 -vector for particles c detected in the HF towers. When particles α and β are of the same sign and share the same phase space region (denoted as $\alpha = \beta$), an extra term is needed to remove the contribution of a particle pairing with itself, so evaluation of the three-particle correlator is modified as

$$\gamma_{112} = \frac{\langle \cos(\phi_\alpha + \phi_\beta - 2\phi_c) \rangle}{v_{2,c}} = \frac{\langle Q_{112} Q_{2,\text{HF}\pm}^* \rangle}{\sqrt{\frac{\langle Q_{2,\text{HF}\pm} Q_{2,\text{HF}\mp}^* \rangle \langle Q_{2,\text{HF}\pm} Q_{2,\text{trk}}^* \rangle}{\langle Q_{2,\text{HF}\mp} Q_{2,\text{trk}}^* \rangle}}, \quad (8)$$

where the Q_{112} is defined as,

$$Q_{112} \equiv \frac{\left(\sum_{i=1} w_i e^{i\phi_i} \right)^2 - \sum_{i=1} w_i^2 e^{i2\phi_i}}{\left(\sum_{i=1} w_i \right)^2 - \sum_{i=1} w_i^2}, \quad (9)$$

and the denominator of Eq. (9) is the respective event weight associated with Q_{112} .

In the numerators of Eqs. (7) and (8), the particles α and β are identified in the tracker, with $|\eta| < 2.4$ and $0.3 < p_T < 3 \text{ GeV}$, and are assigned a weight factor w_i to correct for tracking inefficiency. The particle c is selected by using the tower energies and positions in the HF calorimeters with $4.4 < |\eta| < 5.0$. This choice of η range for the HF towers imposes an η gap of at least 2 units with respect to particles α and β from the tracker, to minimize possible short-range correlations. To account for any occupancy effect of the HF detectors resulting from the large granularities in η and ϕ , each tower is assigned a weight factor w_i corresponding to its E_T value when calculating the Q vector. The denominator of the right-hand side of Eqs. (7) and (8) corresponds to the $v_{2,c}$ using the scalar-product method [11, 12], with $Q_{2,\text{trk}}$ and $Q_{2,\text{HF}\pm}$ denoting Q_2 vectors obtained from the tracker and the two HF detectors (positive and negative η side) with the same kinematic requirements as for the numerator. The three-particle correlator is evaluated for particles α and β carrying the same sign (SS) and opposite sign (OS). The SS combinations, $(+, +)$ and $(-, -)$, give consistent results and are therefore combined. For pPb collisions, the three-particle correlator is also measured with particle c from HF+ and HF-, corresponding to the p- and Pb-going direction, respectively. For symmetric PbPb collisions, the results from HF+ and HF- are consistent with each other and thus combined.

The higher-order harmonic three-particle correlator, γ_{123} , defined in Eq. (4), is evaluated in exactly the same way as the γ_{112} correlator as follows when particles α and β do not overlap,

$$\gamma_{123} = \frac{\langle \cos(\phi_\alpha + 2\phi_\beta - 3\phi_c) \rangle}{v_{3,c}} = \frac{\langle Q_{1,\alpha} Q_{2,\beta} Q_{3,\text{HF}\pm}^* \rangle}{\sqrt{\frac{\langle Q_{3,\text{HF}\pm} Q_{3,\text{HF}\mp}^* \rangle \langle Q_{3,\text{HF}\pm} Q_{3,\text{trk}}^* \rangle}{\langle Q_{3,\text{HF}\mp} Q_{3,\text{trk}}^* \rangle}}, \quad (10)$$

with higher-order Q vectors for particles α and β of SS and OS. Similarly to Eq. (8) when particles α and β can overlap, the γ_{123} can be evaluated via

$$\gamma_{123} = \frac{\langle \cos(\phi_\alpha + 2\phi_\beta - 3\phi_c) \rangle}{v_{3,c}} = \frac{\langle Q_{123} Q_{3,\text{HF}\pm}^* \rangle}{\sqrt{\frac{\langle Q_{3,\text{HF}\pm} Q_{3,\text{HF}\mp}^* \rangle \langle Q_{3,\text{HF}\pm} Q_{3,\text{trk}}^* \rangle}{\langle Q_{3,\text{HF}\mp} Q_{3,\text{trk}}^* \rangle}}, \quad (11)$$

where Q_{123} is defined as

$$Q_{123} \equiv \frac{\left(\sum_{i=1} w_i e^{i\phi_i} \sum_{i=1} w_i e^{i2\phi_i} \right) - \sum_{i=1} w_i^2 e^{i3\phi_i}}{\left(\sum_{i=1} w_i \right)^2 - \sum_{i=1} w_i^2}, \quad (12)$$

and the respective event weight associated with Q_{123} is the denominator of Eq. (12).

Similarly, the charge-dependent two-particle correlator, $\delta \equiv \langle \cos(\phi_\alpha - \phi_\beta) \rangle$, is also evaluated with Q vectors as $\delta = \langle Q_{1,\alpha} Q_{1,\beta}^* \rangle$ when particles α and β are chosen from different detector phase-space regions or have opposite signs, or otherwise,

$$\delta = \left\langle \frac{\left(\sum_{i=1} w_i e^{i\phi_i} \sum_{i=1} w_i e^{-i\phi_i} \right) - \sum_{i=1} w_i^2}{\left(\sum_{i=1} w_i \right)^2 - \sum_{i=1} w_i^2} \right\rangle, \quad (13)$$

and the respective event weight is the denominator of Eq. (13).

The effect of the nonuniform detector acceptance is corrected by evaluating the cumulants of Q -vector products [36]. While the correction is found to be negligible for the γ_{112} and δ correlators, there is a sizable effect of 5–10% correction to the γ_{123} correlator.

4.2 Event shape engineering

In the ESE analysis, within each multiplicity range of pPb or centrality range of PbPb data, events are divided into different q_2 classes, where q_2 is defined as the magnitude of the Q_2 vector. In this analysis, the q_2 value is calculated from one side of the HF region within the range $3 < \eta < 5$ for both pPb and PbPb collisions (weighted by the tower E_T), where in pPb collisions only the Pb-going side of HF is used because of the poor resolution from a relatively low charged-particle multiplicity on the proton-going side. In each q_2 class, the v_2 harmonic is measured with the scalar product method using a common resolution term ($v_{2,c}$) as in the γ_{112} correlator. Therefore, the v_2 from the tracker region can be expressed in terms of the Q -vectors as

$$v_2 = \frac{\langle Q_{2,\alpha} Q_{2,\text{HF}\pm}^* \rangle}{\sqrt{\frac{\langle Q_{2,\text{HF}\pm} Q_{2,\text{HF}\mp}^* \rangle \langle Q_{2,\text{HF}\pm} Q_{2,\text{trk}}^* \rangle}{\langle Q_{2,\text{HF}\mp} Q_{2,\text{trk}}^* \rangle}}, \quad (14)$$

where particles from the HF are selected from the same region as particle c in the γ_{112} correlator.

In PbPb collisions, the particle c in the γ_{112} correlator is taken from the HF detector that is at the opposite η side to the one used to calculate q_2 . However, the results are in good agreement with those where the particle c for γ_{112} and q_2 is measured from the same side of the HF detector,

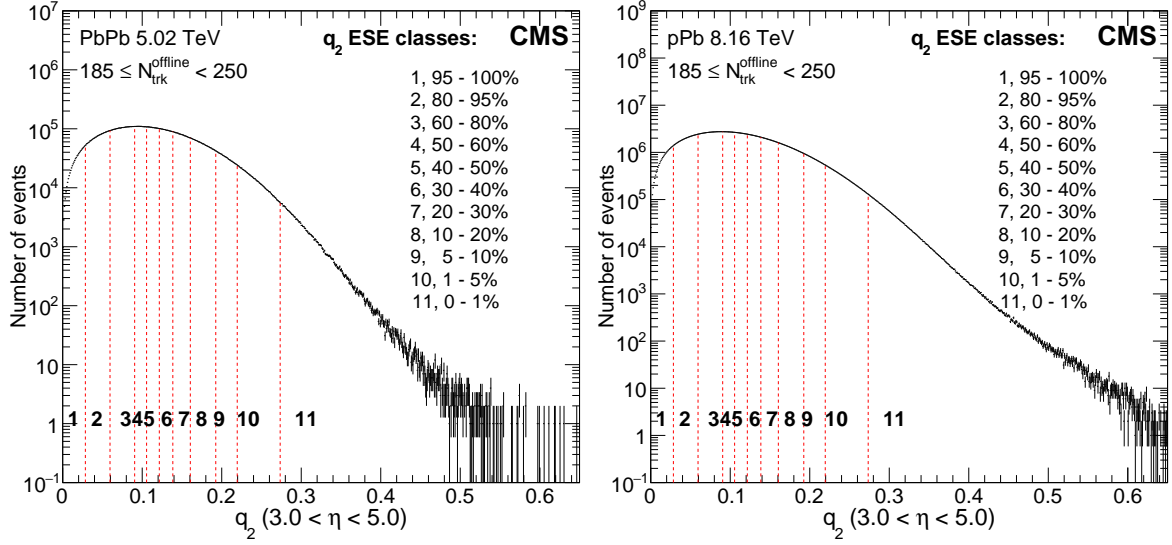


Figure 1: The q_2 classes are shown in different fractions with respect to the total number of events in multiplicity range $185 \leq N_{\text{trk}}^{\text{offline}} < 250$ in PbPb (left) and pPb (right) collisions at $\sqrt{s_{\text{NN}}} = 5.02$ and 8.16 TeV, respectively.

which can be found in Appendix B. In pPb collisions, the particle c in the γ_{112} correlator with respect to the Pb- and p-going sides is studied, when q_2 is measured only in the Pb-going side. The results are found to be independent of the side in which the particle c is detected.

In Fig. 1, the HF q_2 distributions are shown for PbPb and pPb collisions in the multiplicity range $185 \leq N_{\text{trk}}^{\text{offline}} < 250$, where most of the high-multiplicity pPb events were recorded by the high-multiplicity trigger in this range. As indicated by the vertical dashed lines, the distribution is divided into several intervals with each corresponding to a fraction of the full distribution, where 0–1% represents the highest q_2 class. For each q_2 class, the three-particle γ_{112} is calculated with the default kinematic regions for particles α, β , and c , and the v_2 harmonics from the tracker ($|\eta| < 2.4$) are also obtained by the scalar-product method [37]. The pPb and PbPb results are presented in Section 5 for both SS and OS pairs, as well as the differences found for the two charge combinations.

In Fig. 2, the v_2 values for tracker particles as a function of the average q_2 in each HF q_2 class are shown. A proportionality close to linear is seen, indicating the two quantities are strongly correlated because of the initial-state geometry [38].

4.3 Systematic uncertainties

The absolute systematic uncertainties of the two-particle correlator δ , and three-particle correlators γ_{112} and γ_{123} , have been studied. Varying the $d_z/\sigma(d_z)$ and $d_T/\sigma(d_T)$ from less than 3 (default) to less than 2 and 5, and the $\sigma(p_T)/p_T < 10\%$ (default) to $\sigma(p_T)/p_T < 5\%$, together yield the systematic uncertainties of $\pm 1.0 \times 10^{-5}$ for the γ_{112} , $\pm 4.0 \times 10^{-5}$ for the γ_{123} , and $\pm 1.0 \times 10^{-4}$ for the δ correlator. The longitudinal primary vertex position (V_z) has been varied, using ranges $|V_z| < 3$ cm and $3 < |V_z| < 15$ cm, where the differences with respect to the default range $|V_z| < 15$ cm are $\pm 1.0 \times 10^{-5}$ for the γ_{112} , $\pm 3.0 \times 10^{-5}$ for the γ_{123} , and $\pm 1.0 \times 10^{-4}$ for the δ correlator, taken as the systematic uncertainty. In the pPb collisions only, using the lower-threshold of the high-multiplicity trigger with respect to the default trigger, yields a systematic uncertainty of $\pm 3.0 \times 10^{-5}$ for all three correlators, which accounts for the possible trigger bias from the inefficiency of the default trigger around the threshold. In the

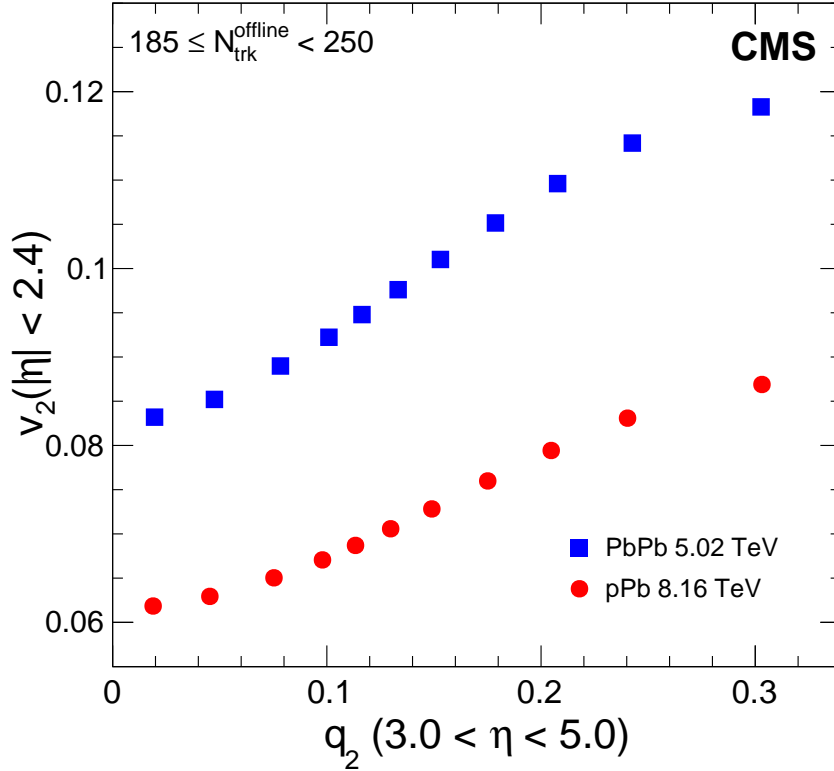


Figure 2: The correlation between the tracker v_2 and the HF q_2 is shown for pPb and PbPb collisions at collisions at $\sqrt{s_{\text{NN}}} = 8.16$ and 5.02 TeV, respectively.

pPb data sample, the average pileup can be as high as 0.25 and therefore the systematic effects from pileup have been evaluated. The full sample has been split into 4 different sets of events with different average pileup, according to their instantaneous luminosity during each run. The systematic effects for γ_{112} and δ have been found to be $\pm 1.0 \times 10^{-5}$, and for γ_{123} is to be $\pm 3.0 \times 10^{-5}$.

A final test of the analysis procedures is done by comparing “known” charge-dependent signals based on the EPOS event generator [39] to those found after events are passed through a GEANT4 [40, 41] simulation of the CMS detector response. Based on this test, a systematic uncertainty of $\pm 2.5 \times 10^{-5}$ is assigned for the γ_{112} , $\pm 4.0 \times 10^{-5}$ for the γ_{123} , and $\pm 5.0 \times 10^{-4}$ for the δ correlators, by taking the difference in the correlators between the reconstructed and the generated level. Note that this uncertainty for the δ correlator is based on differential variables, where the uncertainty covers the maximum deviation from the closure test. For results that averaged over $|\Delta\eta| < 1.6$, the systematic uncertainty is found to be $\pm 2.0 \times 10^{-4}$ when directly evaluating the average. The tracking efficiency and acceptance of positively and negatively charged particles have been evaluated separately, and the difference has been found to be negligible. All sources of systematic uncertainty are uncorrelated and added in quadrature to obtain the total absolute systematic uncertainty. No dependence of the systematic uncertainties on the sign combination, multiplicity, $\Delta\eta$, Δp_T , or average- p_T is found. The systematic uncertainties in our results are point-to-point correlated. In pPb collisions, the systematic uncertainty is also observed to be independent of particle c pointing to the Pb- or p-going direction, and thus it is quoted to be the same for these two situations. The systematic uncertainties are summarized in Table 1.

Table 1: Summary of systematic uncertainties in SS and OS three-particle correlators γ_{112} and γ_{123} , and two-particle correlator δ in pPb collisions at $\sqrt{s_{\text{NN}}} = 8.16$ TeV and PbPb collisions at 5.02 TeV.

| Source | $\gamma_{112} (\times 10^{-5})$ | $\gamma_{123} (\times 10^{-5})$ | $\delta (\times 10^{-4})$ |
|---|---------------------------------|---------------------------------|---------------------------|
| Track selections | 1.0 | 4.0 | 1.0 |
| Vertex Z position | 1.0 | 3.0 | 1.0 |
| Pileup (pPb only) | 1.0 | 3.0 | 0.1 |
| High multiplicity trigger bias (pPb only) | 3.0 | 3.0 | 0.3 |
| MC closure | 2.5 | 4.0 | 5.0 |
| Total in pPb | 4.3 | 7.7 | 5.2 |
| Total in PbPb | 2.9 | 6.4 | 5.2 |

5 Results

5.1 Charge-dependent two- and three-particle correlators

Measurements of the charge-dependent three-particle (γ_{112} , γ_{123}) and two-particle (δ) correlators are shown in Fig. 3 as functions of the pseudorapidity difference ($|\Delta\eta| \equiv |\eta_\alpha - \eta_\beta|$) between SS and OS particles α and β , in the multiplicity range $185 \leq N_{\text{trk}}^{\text{offline}} < 250$ for pPb collisions at $\sqrt{s_{\text{NN}}} = 8.16$ TeV and PbPb collisions at 5.02 TeV. The SS and OS of δ correlators are shown with different markers to differentiate the two-particle correlation from the three-particle correlation with a particle c in the forward rapidity. The pPb data are obtained with particle c in the Pb- and p-going sides separately. The multiplicity range $185 \leq N_{\text{trk}}^{\text{offline}} < 250$ for PbPb data roughly corresponds to the centrality range 60–65%.

Similar to the observation reported in Ref. [21], the three-particle γ_{112} (Figs. 3a and 3b) and γ_{123} (Figs. 3c and 3d) correlators show a charge dependence for $|\Delta\eta|$ up to about 1.6, in both pPb (5.02 [21] and 8.16 TeV) and PbPb (5.02 TeV) systems. Little collision energy dependence of the γ_{112} data for pPb collisions is found from $\sqrt{s_{\text{NN}}} = 5.02$ TeV to 8.16 TeV within uncertainties (as will be shown later in Figs. 6 and 8 as a function of event multiplicity). For $|\Delta\eta| > 1.6$, the SS and OS correlators converge to a common value, which is weakly dependent on $|\Delta\eta|$ out to about 4.8 units. In pPb collisions, the γ_{112} correlator obtained with particle c from the p-going side is shifted toward more positive values than that from the Pb-going side by approximately the same amount for both the SS and OS pairs. This trend is reversed for the higher-order harmonic γ_{123} correlator, where the Pb-going side data are more positive than the p-going side data. The Pb-going side results for the γ_{112} correlator for the pPb collisions are of similar magnitude as the results for PbPb collisions, although a more pronounced peak structure at small $|\Delta\eta|$ is observed in pPb collisions. The common shift of SS and OS correlators between the p- and Pb-going side reference (c) particle may be related to sources of correlation that are charge independent, such as directed flow (the first-order azimuthal anisotropy in Eq. (1)) and the momentum conservation effect, the latter being sensitive to the difference in multiplicity between p- and Pb-going directions. The two-particle δ correlators (Figs. 3e and 3f) for both SS and OS pairs also show a decreasing trend as $|\Delta\eta|$ increases and converge to the same values at $|\Delta\eta| \approx 1.6$, similar to that for the three-particle correlators. The values of both OS and SS δ correlators are found to be larger in pPb than in PbPb collisions at similar multiplicities. As the δ correlator is sensitive to short-range jet-like correlations, reflected by the low- $|\Delta\eta|$ region, this effect may be related to the higher- p_T jets or clusters in pPb compared to PbPb collisions at similar multiplicities, as suggested in Ref. [28], because of short-range two-particle $\Delta\eta$ - $\Delta\phi$ correlations.

To provide more detailed information on the particle p_T dependence of the correlations, the

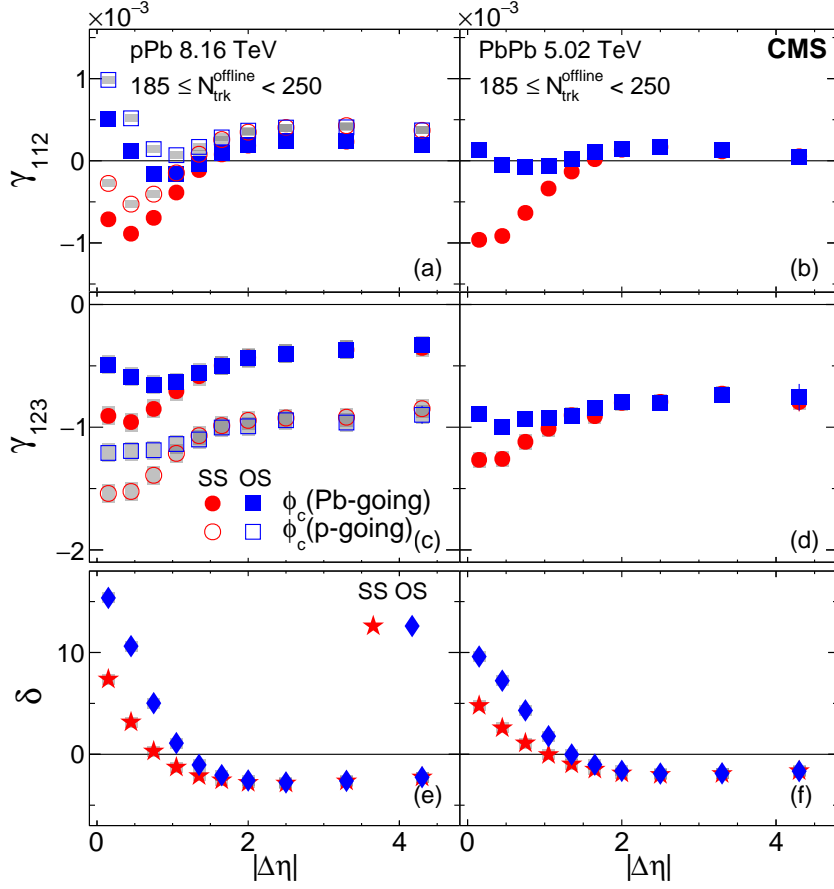


Figure 3: The SS and OS three-particle correlators, γ_{112} (upper) and γ_{123} (middle), and two-particle correlator, δ (lower), as a function of $|\Delta\eta|$ for $185 \leq N_{\text{trk}}^{\text{offline}} < 250$ in pPb collisions at $\sqrt{s_{\text{NN}}} = 8.16$ TeV (left) and PbPb collisions at 5.02 TeV (right). The pPb results obtained with particle c in Pb-going (solid markers) and p-going (open markers) sides are shown separately. The SS and OS two-particle correlators are denoted by different markers for both pPb and PbPb collisions. Statistical and systematic uncertainties are indicated by the error bars and shaded regions, respectively.

γ_{112} , γ_{123} , and δ correlators are measured as functions of the p_T difference ($|\Delta p_T| \equiv |p_{T,\alpha} - p_{T,\beta}|$) and average ($\bar{p}_T \equiv (p_{T,\alpha} + p_{T,\beta})/2$) of the SS and OS pairs in pPb and PbPb collisions, and shown in Figs. 4 and 5. The $|\Delta p_T|$ - and \bar{p}_T -dependent results are averaged over the full $|\eta| < 2.4$ range. In particular, the charge-dependent correlations from the CME are expected to be strongest in the low- p_T region [6].

For all correlators, similar behaviors between pPb and PbPb data are again observed. The trends in $|\Delta p_T|$ for γ_{112} and γ_{123} correlators seem to be opposite. The γ_{112} correlator increases as a function of $|\Delta p_T|$, while a decreasing trend is seen for the γ_{123} correlator up to $|\Delta p_T| \approx 2$ GeV, where γ_{123} becomes constant in $|\Delta p_T|$. The opposite behavior observed between the γ_{112} and γ_{123} correlators is related to back-to-back jet-like correlations, which give a positive (negative) contribution to even- (odd-) order Fourier harmonics [42]. The δ correlators decrease monotonically as functions of $|\Delta p_T|$ for both SS and OS pairs in pPb and PbPb collisions. This trend of decreasing for δ is consistent with the expectation from either transverse momentum conservation or back-to-back jet correlations [19].

In terms of the \bar{p}_T dependence in Fig. 5, all three correlators for both SS and OS pairs show very similar behaviors in the low- \bar{p}_T region, which is likely a consequence of the same physical

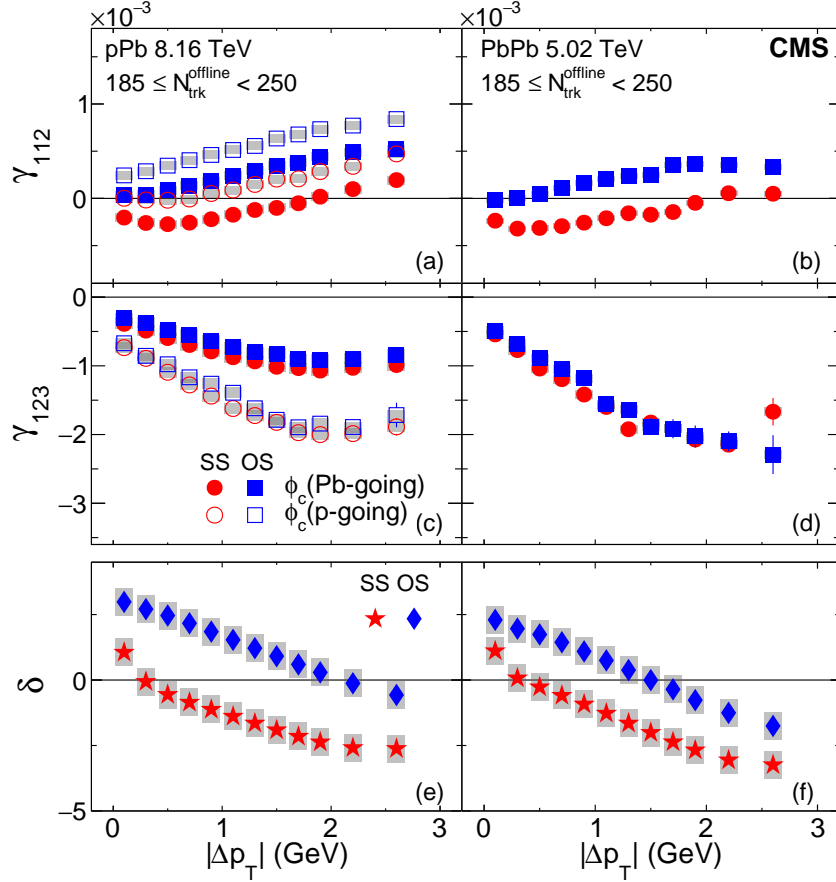


Figure 4: The SS and OS three-particle correlators, γ_{112} (upper) and γ_{123} (middle), and two-particle correlator, δ (lower), as a function of $|\Delta p_T|$ for $185 \leq N_{\text{trk}}^{\text{offline}} < 250$ in pPb collisions at $\sqrt{s_{\text{NN}}} = 8.16$ TeV (left) and PbPb collisions at 5.02 TeV (right) collisions. The pPb results obtained with particle c in Pb-going (solid markers) and p-going (open markers) sides are shown separately. The SS and OS two-particle correlators are denoted by different markers for both pPb and PbPb collisions. Statistical and systematic uncertainties are indicated by the error bars and shaded regions, respectively.

origin. However, an opposite trend starts emerging at $\bar{p}_T \approx 1.6$ GeV, most evidently for γ_{112} and δ . Within the $0.3 < p_T < 3$ GeV range, as \bar{p}_T increases toward 3 GeV, both particles of a pair tend to be selected with a high- p_T value, while for low- \bar{p}_T or any $|\Delta p_T|$ values, the pair usually consists of at least one low- p_T particle. This may be the reason for a different trend seen at high \bar{p}_T . The qualitative behavior of the data is captured by the A Multi-Phase Transport model [43, 44]. In Appendix C, all three correlators as functions of $|\Delta\eta|$, Δp_T , and \bar{p}_T in different multiplicity and centrality ranges in pPb and PbPb collisions, can be found.

To explore the multiplicity or centrality dependence of the three- and two-particle correlators, an average of the data is taken over $|\Delta\eta| < 1.6$, corresponding to the region in Fig. 3 which exhibits charge dependence. The average over $|\Delta\eta| < 1.6$ is weighted by the density of particle pairs in $|\Delta\eta|$, and all further plots averaged over $|\Delta\eta| < 1.6$ are weighted similarly. The resulting $|\Delta\eta|$ -averaged data of γ_{112} , γ_{123} and δ are shown in Fig. 6 for both OS and SS pairs, as functions of $N_{\text{trk}}^{\text{offline}}$ for pPb collisions at $\sqrt{s_{\text{NN}}} = 8.16$ TeV (particle c from the Pb-going side) and PbPb collisions at 5.02 TeV. Previously published pPb data at 5.02 TeV are also shown for comparison [21]. The centrality scale on the top of Fig. 6 relates to the PbPb experimental results. Up to $N_{\text{trk}}^{\text{offline}} = 400$, the pPb and PbPb results are measured in the same $N_{\text{trk}}^{\text{offline}}$ ranges. The

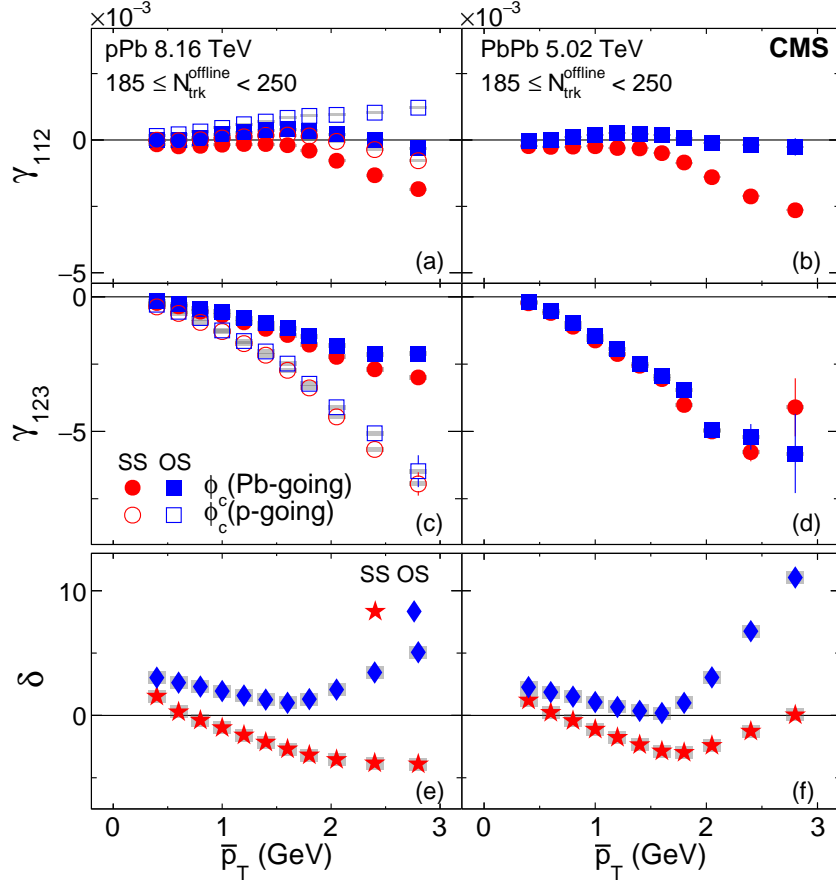


Figure 5: The SS and OS three-particle correlators, γ_{112} (upper) and γ_{123} (middle), and two-particle correlator, δ (lower), as a function of \bar{p}_T for $185 \leq N_{\text{trk}}^{\text{offline}} < 250$ in pPb collisions at $\sqrt{s_{\text{NN}}} = 8.16$ TeV (left) and PbPb collisions at 5.02 TeV (right). The pPb results obtained with particle c in Pb-going (solid markers) and p-going (open markers) sides are shown separately. The SS and OS two-particle correlators are denoted by different markers for both pPb and PbPb collisions. Statistical and systematic uncertainties are indicated by the error bars and shaded regions, respectively.

new pPb data at 8.16 TeV extend the multiplicity reach further than the previously published pPb data at 5.02 TeV (which stopped at $N_{\text{trk}}^{\text{offline}} \approx 300$).

Within the uncertainties, the SS and OS γ_{112} correlators in pPb and PbPb collisions exhibit the same magnitude and trend as functions of event multiplicity. The pPb data are independent of collision energy from 5.02 to 8.16 TeV at similar multiplicities. This justifies the comparison of new pPb data and PbPb data at somewhat different energies. For both pPb and PbPb collisions, the OS correlator reaches a value close to zero for $N_{\text{trk}}^{\text{offline}} > 200$, while the SS correlator remains negative, but the magnitude gradually decreases as $N_{\text{trk}}^{\text{offline}}$ increases. Part of the observed multiplicity (or centrality) dependence is understood as a dilution effect that falls with the inverse of event multiplicity [12]. The notably similar magnitude and multiplicity dependence of the three-particle correlator, γ_{112} , observed in pPb collisions relative to that in PbPb collisions again indicates that the dominant contribution of the signal is not related to the CME. The results of SS and OS three-particle correlators as functions of centrality in PbPb collisions at $\sqrt{s_{\text{NN}}} = 5.02$ TeV are also found to be consistent with the results from lower energy AA collisions [12, 16]. However, values of γ_{123} correlators between pPb and PbPb are observed to be different, unlike those for γ_{112} correlators. As the CME contribution to γ_{123} is not expected, the

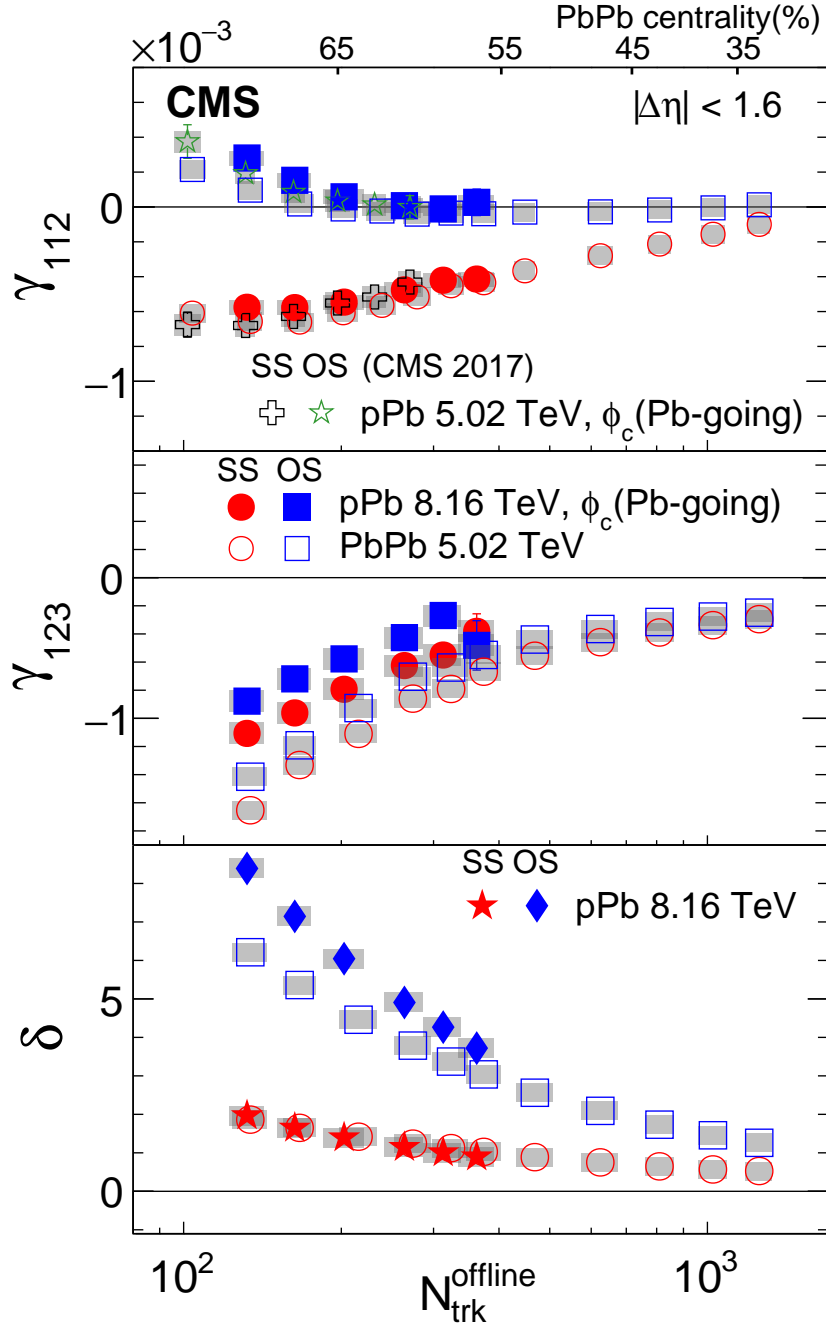


Figure 6: The SS and OS three-particle correlators, γ_{112} (upper) and γ_{123} (middle), and two-particle correlator, δ (lower), averaged over $|\Delta\eta| < 1.6$ as a function of $N_{\text{trk}}^{\text{offline}}$ in pPb collisions at $\sqrt{s_{\text{NN}}} = 8.16$ TeV and PbPb collisions at 5.02 TeV. The SS and OS two-particle correlators are denoted by different markers for pPb collisions. The results of γ_{112} for pPb collisions at 5.02 TeV from CMS Collaboration (CMS 2017: [21]), are also shown for comparison. Statistical and systematic uncertainties are indicated by the error bars and shaded regions, respectively.

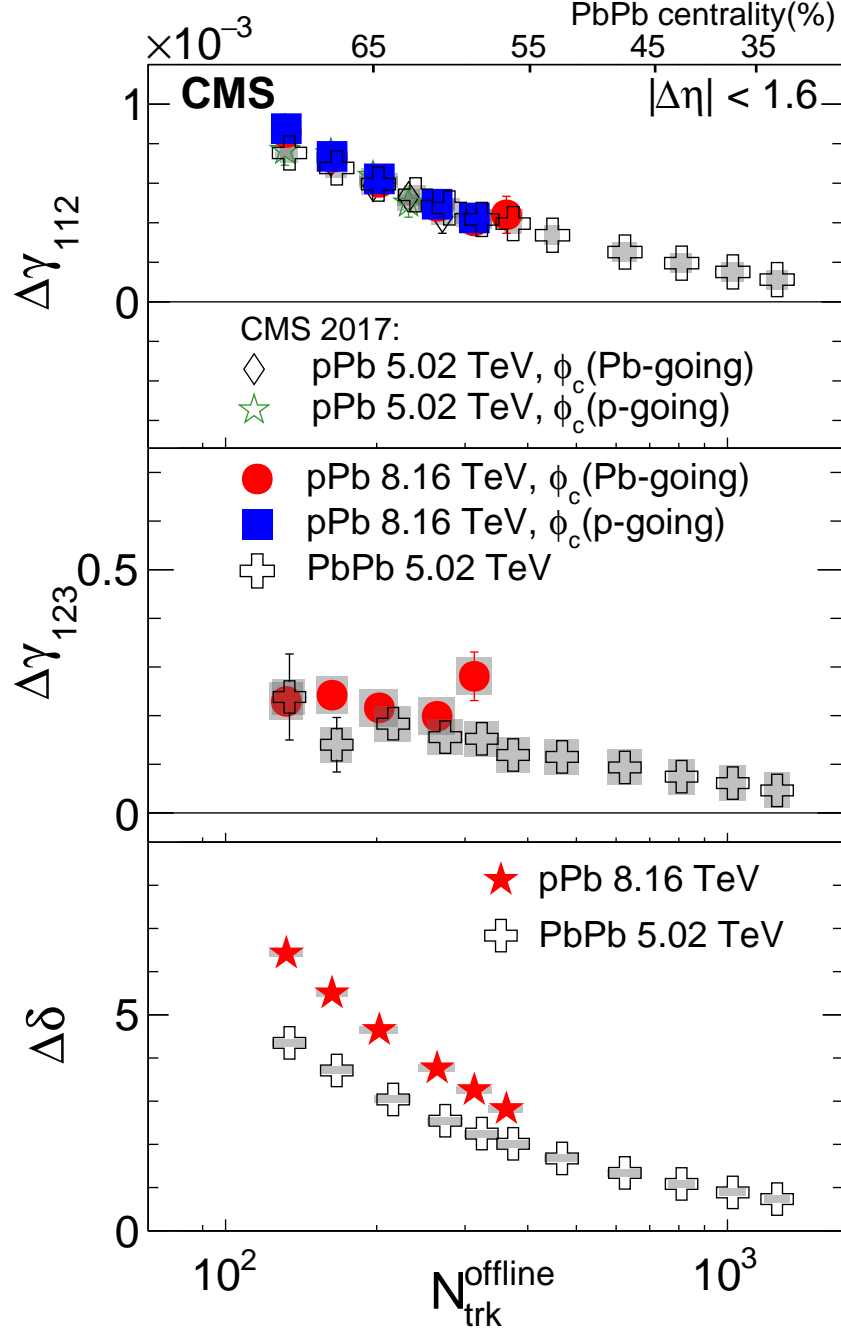


Figure 8: The difference of the OS and SS three-particle correlators, γ_{112} (upper) and γ_{123} (middle), and two-particle correlator, δ (lower), averaged over $|\Delta\eta| < 1.6$ as a function of $N_{\text{trk}}^{\text{offline}}$ in pPb collisions at $\sqrt{s_{\text{NN}}} = 8.16$ TeV and PbPb collisions at 5.02 TeV. The pPb results are obtained with particle c from Pb- and p-going sides separately. The $\Delta\delta$ correlator is denoted by a different marker for pPb collisions. The results of γ_{112} for pPb collisions at 5.02 TeV from CMS Collaboration (CMS 2017: [21]), are also shown for comparison. Statistical and systematic uncertainties are indicated by the error bars and shaded regions, respectively.

origin. As argued in Ref. [21], a strong charge separation signal from the CME is not expected in a very high-multiplicity pPb collisions, and not with respect to Ψ_3 (for the γ_{123} correlator) in either the pPb or PbPb system. The similarity seen between high-multiplicity pPb and peripheral PbPb collisions for both $\Delta\gamma_{112}$ and $\Delta\gamma_{123}$ further challenges the attribution of the observed charge-dependent correlations to the CME. The two-particle correlator, $\Delta\delta$, on the other hand, is found to show a larger value in pPb than in PbPb collisions.

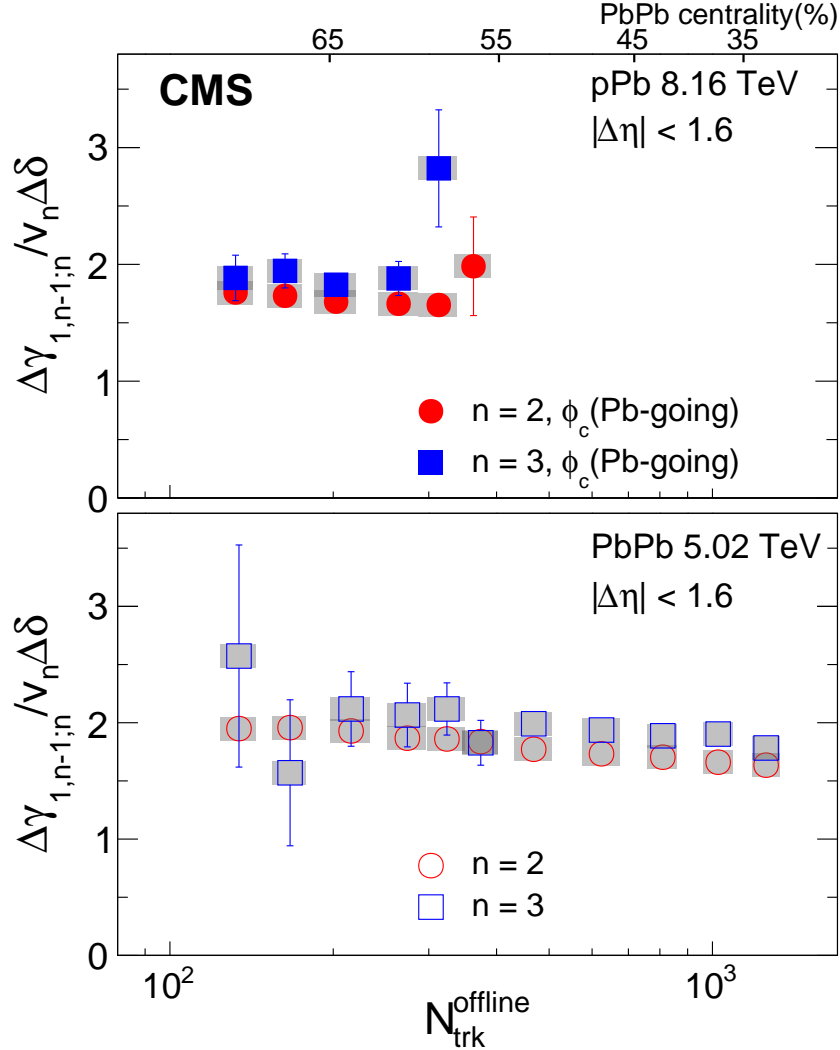


Figure 9: The ratio of $\Delta\gamma_{112}$ and $\Delta\gamma_{123}$ to the product of v_n and δ , averaged over $|\Delta\eta| < 1.6$, in pPb collisions for the Pb-going direction at $\sqrt{s_{\text{NN}}} = 8.16$ TeV (upper) and PbPb collisions at 5.02 TeV (lower). Statistical and systematic uncertainties are indicated by the error bars and shaded regions, respectively.

The differences of three-particle correlators, $\Delta\gamma_{112}$ and $\Delta\gamma_{123}$, and two-particle correlator, $\Delta\delta$, between OS and SS are shown in Fig. 8 as functions of $N_{\text{trk}}^{\text{offline}}$ averaged over $|\Delta\eta| < 1.6$ for pPb collisions at $\sqrt{s_{\text{NN}}} = 8.16$ TeV and PbPb collisions at 5.02 TeV. For comparison, previously published pPb data at 5.02 TeV are also shown [21]. Similar to those shown in Fig. 7, the observed difference between OS and SS pairs in $\Delta\gamma_{112}$ and $\Delta\gamma_{123}$ is strikingly similar in pPb and PbPb collisions over the entire overlapping multiplicity range (and also independent of collision energy for $\Delta\gamma_{112}$ in pPb), while higher values of an OS-SS difference in $\Delta\delta$ are found for the pPb system.

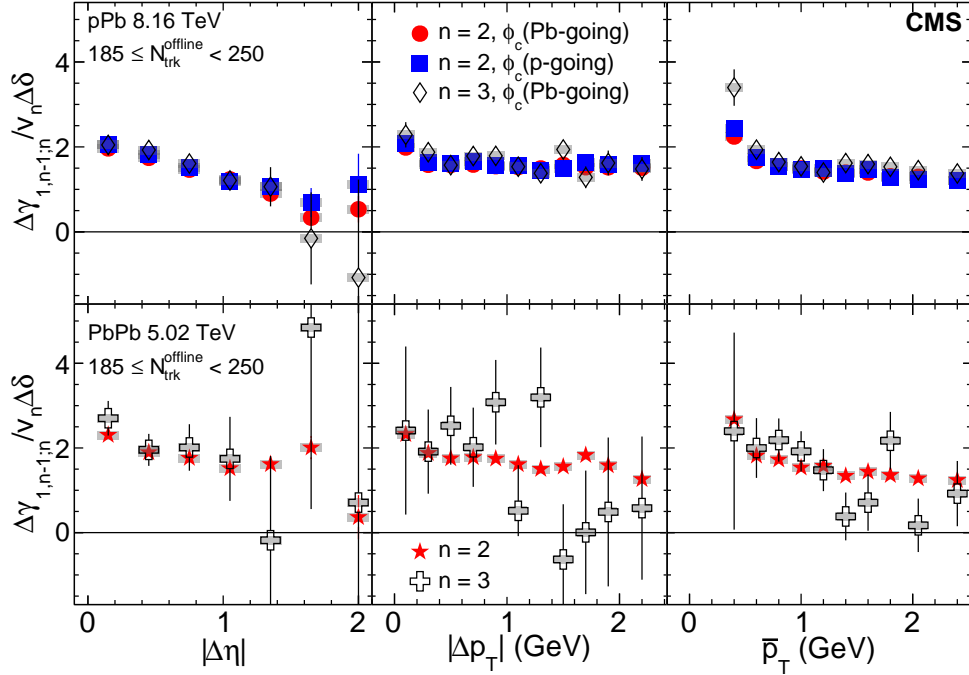


Figure 10: The ratio of $\Delta\gamma_{112}$ and $\Delta\gamma_{123}$ to the product of v_n and δ , as functions of $|\Delta\eta|$ (left), $|\Delta p_T|$ (middle), and \bar{p}_T (right) for $185 \leq N_{\text{trk}}^{\text{offline}} < 250$ in pPb collisions at $\sqrt{s_{\text{NN}}} = 8.16$ TeV (upper) and PbPb collisions at 5.02 TeV (lower). Statistical and systematic uncertainties are indicated by the error bars and shaded regions, respectively.

To check if the mechanism of local charge conservation coupled with anisotropic flow can explain the observed charge dependence of the $\Delta\gamma_{112}$ and $\Delta\gamma_{123}$ correlators, the relation in Eq. (6) is used. The ratios of $\Delta\gamma_{112}$ and $\Delta\gamma_{123}$ to the product of $\Delta\delta$ and v_n are shown in Fig. 9, averaged over $|\Delta\eta| < 1.6$, as functions of event multiplicity in pPb and PbPb collisions. The v_2 and v_3 values for particles α or β are calculated with the scalar-product method with respect to the particle c . In pPb collisions, only results with the Pb-going direction are shown because the p-going direction data lack statistical precision, except for the multiplicity range $185 \leq N_{\text{trk}}^{\text{offline}} < 250$.

The ratios shown in Fig. 9 for both systems are found to be similar between $n=2$ and $n=3$, on average with values slightly less than 2. This observation indicates that the measured charge dependence of three-particle correlators is consistent with mostly being dominated by charge-dependent two-particle correlations (e.g., from local charge conservation) coupled with the anisotropic flow v_n . For a given n value, the ratios are also similar between pPb and PbPb collisions (and may reflect similar particle kinematics and acceptances), and approximately constant as functions of event multiplicity. Notably, the $\Delta\delta$ in Fig. 8 are different between the pPb and PbPb systems. However, the anisotropic flow harmonics v_n are larger for PbPb collisions than for pPb collisions [28]. As a result, the product of $\Delta\delta$ and v_n leads to similar values of $\Delta\gamma_{112}$ and $\Delta\gamma_{123}$ correlators between the pPb and PbPb systems, implying the κ_2 is similar to κ_3 .

The ratios of $\Delta\gamma_{112}$ and $\Delta\gamma_{123}$ to the product of $\Delta\delta$ and v_n can also be studied as functions of $|\Delta\eta|$, $|\Delta p_T|$, and \bar{p}_T in pPb and PbPb collisions, as shown in Fig. 10 for the multiplicity range of $185 \leq N_{\text{trk}}^{\text{offline}} < 250$. Here, the v_n are calculated as the average v_n of particles α and β , $v_n = (v_{n,\alpha} + v_{n,\beta})/2$ (based on the relation derived in Eq. (21) in Appendix A), and are weighted by the number of pairs of particles α and β in the given kinematic ranges when averaged over η or p_T . The ratios involving $\Delta\gamma_{112}$ and $\Delta\gamma_{123}$ are again found to be similar differentially for all

three variables in both pPb and PbPb collisions. This observation further supports a common origin of $\Delta\gamma_{112}$ and $\Delta\gamma_{123}$ from charge-dependent two-particle correlations coupled with the anisotropic flow.

5.2 Event shape engineering

To explore directly the background scenario in Eq. (3) in terms of a linear dependence on v_2 for the γ_{112} correlator, results based on the ESE analysis are presented in this section.

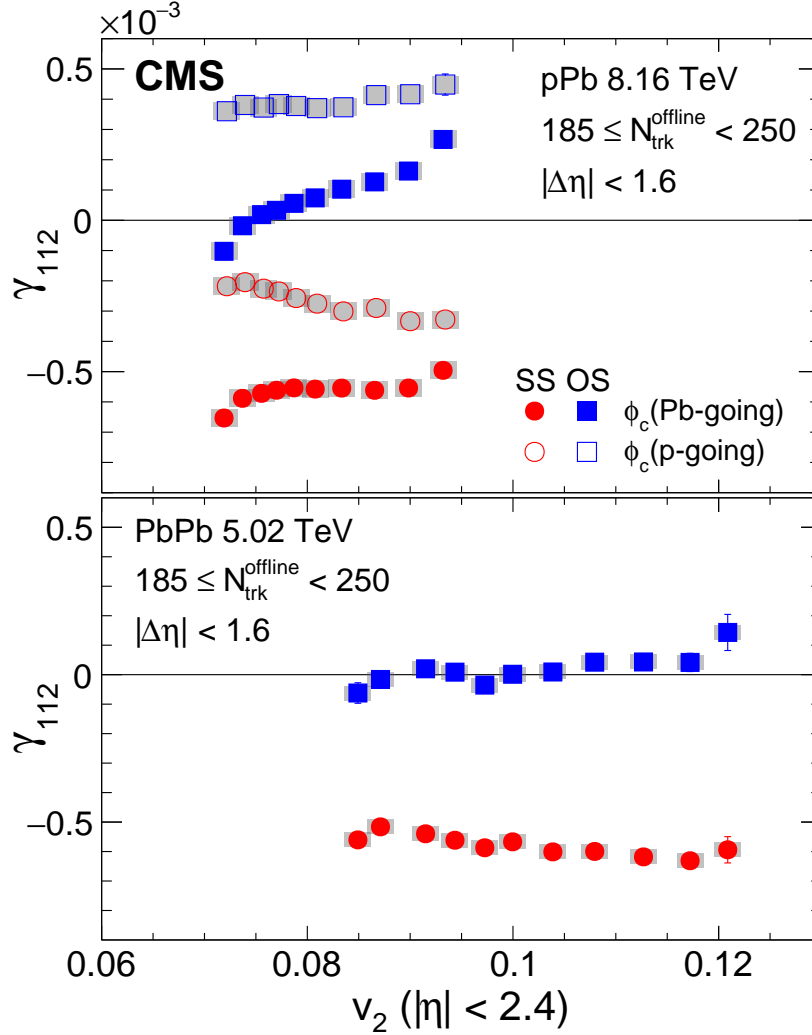


Figure 11: The SS and OS three-particle correlators, γ_{112} , averaged over $|\Delta\eta| < 1.6$ as a function of v_2 (evaluated as the average v_2 value for each corresponding q_2 event class), for the multiplicity range $185 \leq N_{\text{trk}}^{\text{offline}} < 250$ in pPb collisions at $\sqrt{s_{\text{NN}}} = 8.16$ TeV (upper) and PbPb collisions at 5.02 TeV (lower). The pPb results are obtained with particle c from Pb- and p-going sides separately. Statistical and systematic uncertainties are indicated by the error bars and shaded regions, respectively.

The SS and OS three-particle correlators, γ_{112} , averaged over $|\Delta\eta| < 1.6$, are shown as a function of v_2 (evaluated as the average v_2 value for each corresponding q_2 event class in Fig. 11), for the multiplicity range $185 \leq N_{\text{trk}}^{\text{offline}} < 250$ in pPb collisions at $\sqrt{s_{\text{NN}}} = 8.16$ TeV (upper) and PbPb collisions at 5.02 TeV (lower). The pPb results are obtained with particle c from the Pb- and p-going sides separately.

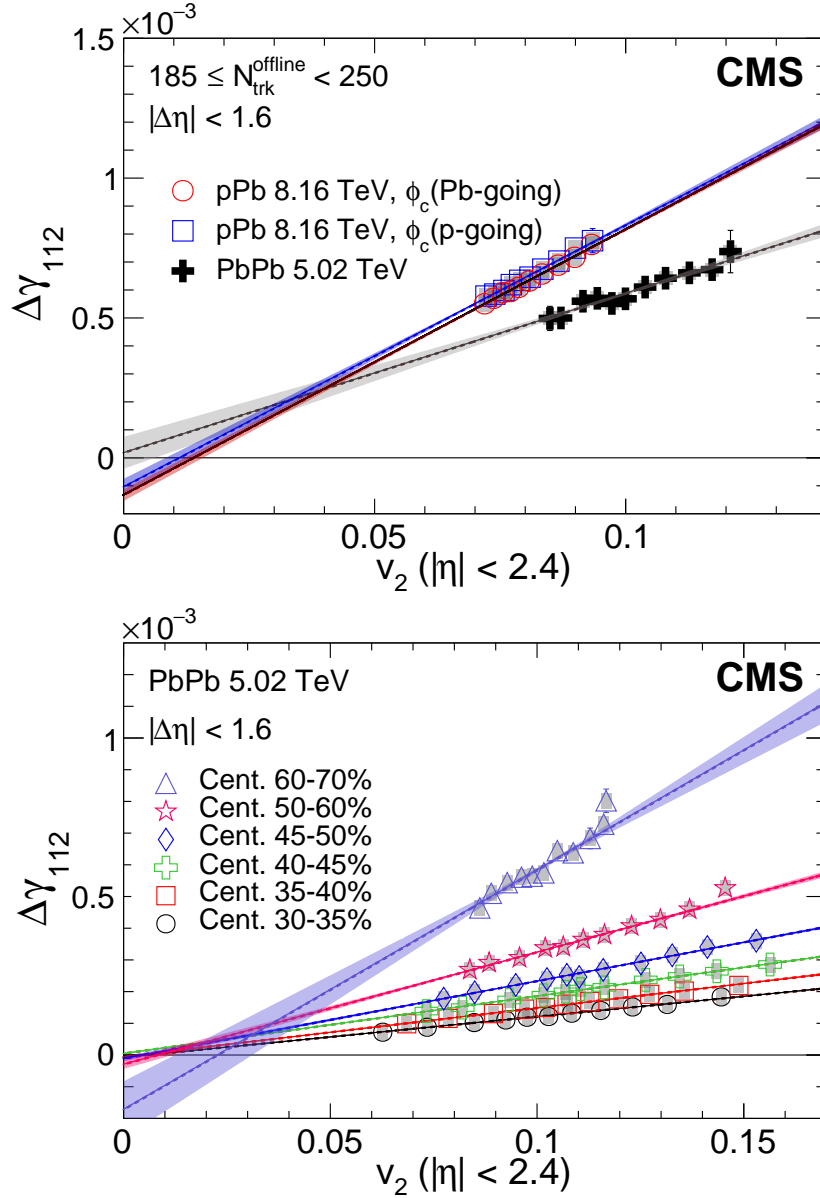


Figure 12: The difference of the OS and SS three-particle correlators, γ_{112} , averaged over $|\Delta\eta| < 1.6$ as a function of v_2 evaluated in each q_2 class, for the multiplicity range $185 \leq N_{\text{trk}}^{\text{offline}} < 250$ in pPb collisions at $\sqrt{s_{\text{NN}}} = 8.16$ TeV and PbPb collisions at 5.02 TeV (upper), and for different centrality classes in PbPb collisions at 5.02 TeV (lower). Statistical and systematic uncertainties are indicated by the error bars and shaded regions, respectively. A one standard deviation uncertainty from the fit is also shown.

Both SS and OS γ_{112} correlators in both pPb (both beam directions for particle c) and PbPb collisions show a dependence on v_2 . A clear linear dependence on the v_2 value is not seen for any of the SS and OS correlators studied.

Similar to the analysis in Section 5.1, the difference between OS and SS correlators is taken in order to eliminate the charge-independent sources of the correlators. The results, averaged over $|\Delta\eta| < 1.6$, are shown in Fig. 12 (upper), as a function of v_2 evaluated in each q_2 class, for the multiplicity range $185 \leq N_{\text{trk}}^{\text{offline}} < 250$ in pPb collisions at $\sqrt{s_{\text{NN}}} = 8.16$ TeV and PbPb collisions at 5.02 TeV. The results obtained in each centrality class of PbPb collisions at 5.02 TeV are also presented in Fig. 12 (lower). The lines are linear fits to the data,

$$\Delta\gamma_{112} = a v_2 + b, \quad (15)$$

where the first term corresponds to the v_2 -dependent background contribution with the slope parameter a equal to $\kappa_2\Delta\delta$ (from Eq. (3)), which is assumed to be v_2 independent. The intercept parameter b denotes the v_2 -independent contribution (when linearly extrapolating to $v_2 = 0$) in the γ_{112} correlator. In particular, as the CME contribution to the $\Delta\gamma_{112}$ is expected to be largely v_2 -independent within narrow multiplicity (centrality) ranges, the b parameter may provide an indication to a possible observation of the CME, or set an upper limit on the CME contribution.

As shown in Fig. 12, for both pPb and PbPb collisions in each multiplicity or centrality range, a clear linear dependence of the $\Delta\gamma_{112}$ correlator as a function of v_2 is observed. Fitted by a linear function, the intercept parameter, b , can be extracted. A one standard deviation uncertainty band is also shown for the linear fit. Taking the statistical uncertainties into account, the values of b are found to be nonzero for multiplicity range $185 \leq N_{\text{trk}}^{\text{offline}} < 250$ in pPb and 60–70% centrality in PbPb collisions.

Observing a nonzero intercept b from Fig. 12 may or may not lead to a conclusion of a finite CME signal, as an assumption is made for the background contribution term, namely that $\Delta\delta$ is independent of v_2 . To check this assumption explicitly, the $\Delta\delta$ correlator is shown in Fig. 13 as a function of v_2 in different multiplicity and centrality ranges in pPb (upper) and PbPb (lower) collisions. It is observed that the value of $\Delta\delta$ remains largely constant as a function of v_2 in low- or intermediate- q_2 classes, but starts rising as v_2 increases in high- q_2 classes. The multiplicity, within a centrality or multiplicity range, decreases slightly with increasing q_2 , which qualitatively could contribute to the rising $\Delta\delta$ due to a multiplicity dilution effect. However, this is only found to be true for PbPb collisions, but not for pPb collisions. The other reason may be related to larger jet-like correlations selected by requiring large q_2 values. Events with higher multiplicities show a weaker dependence on v_2 than those with lower multiplicities, which is consistent with the expectation that short-range jet-like correlations are stronger in peripheral events. Because of the possible bias towards larger jet-like correlations at higher q_2 from the ESE technique, the v_2 dependence of $\Delta\delta$ is hard to completely eliminate. This presents a challenge to the interpretation of the intercept values from the linear fits in Fig. 12.

In order to avoid the issue of $\Delta\delta$ being dependent on v_2 , the ratio $\Delta\gamma_{112}/\Delta\delta$ as function of v_2 is shown in Fig. 14 for different multiplicity ranges in pPb collisions at $\sqrt{s_{\text{NN}}} = 8.16$ TeV (upper) and for different centrality classes in PbPb collisions at 5.02 TeV (lower). Particularly in the scenario of a pure v_2 -dependent background, the ratio $\Delta\gamma_{112}/\Delta\delta$ is expected to be proportional to v_2 . A linear function is fitted again using

$$\frac{\Delta\gamma_{112}}{\Delta\delta} = a_{\text{norm}} v_2 + b_{\text{norm}}. \quad (16)$$

Here, comparing to the intercept parameter b in Eq. (15), the b_{norm} parameter is equivalent to b scaled by the $\Delta\delta$ factor. The fitted linear slope and intercept parameters, a_{norm} and b_{norm} , are

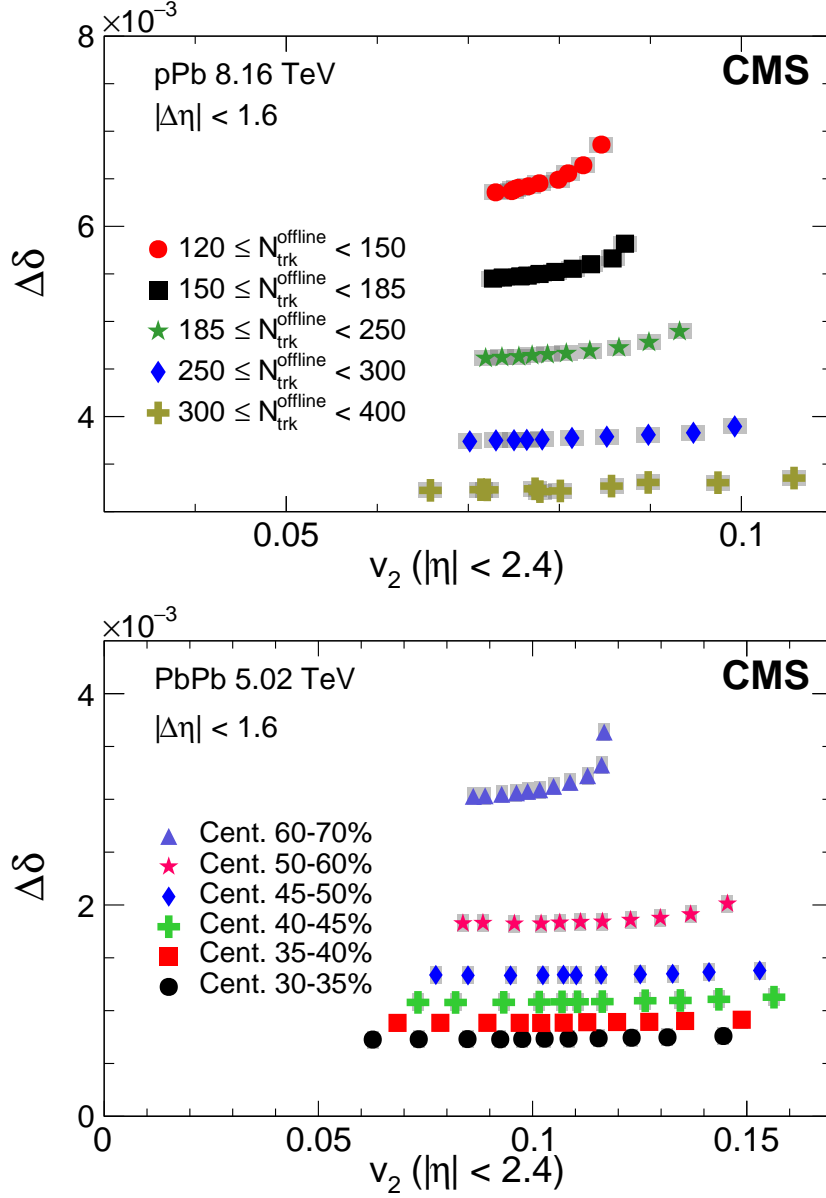


Figure 13: The difference of the OS and SS two-particle correlators, δ , averaged over $|\Delta\eta| < 1.6$ as a function of v_2 evaluated in each q_2 class, for different multiplicity ranges in pPb collisions at $\sqrt{s_{\text{NN}}} = 8.16$ TeV (upper), and for different centrality classes in PbPb collisions at 5.02 TeV (lower). Statistical and systematic uncertainties are indicated by the error bars and shaded regions, respectively.

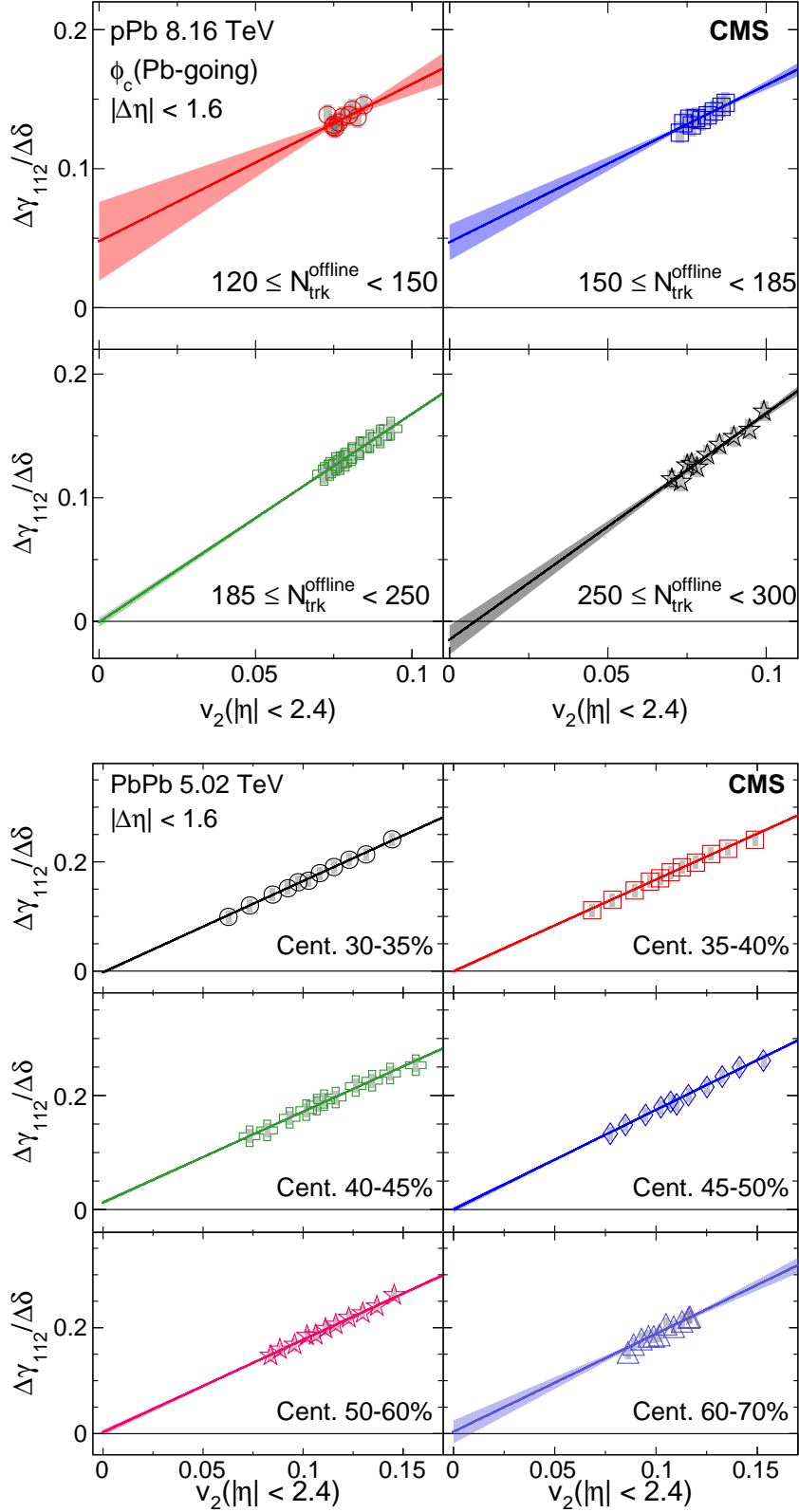


Figure 14: The ratio between the difference of the OS and SS three-particle correlators and the difference of OS and SS in δ correlators, $\Delta\gamma_{112}/\Delta\delta$, averaged over $|\Delta\eta| < 1.6$ as a function of v_2 evaluated in each q_2 class, for different multiplicity ranges in pPb collisions at $\sqrt{s_{\text{NN}}} = 8.16$ TeV (upper), and for different centrality classes in PbPb collisions at 5.02 TeV (lower). Statistical and systematic uncertainties are indicated by the error bars and shaded regions, respectively. A one standard deviation uncertainty from the fit is also shown.

Table 2: The summary of slope and intercept parameter a_{norm} and b_{norm} for different $N_{\text{trk}}^{\text{offline}}$ classes in pPb collisions, and the goodness of fit χ^2 per degree of freedom (ndf). The statistical and systematic uncertainties are shown after the central values, respectively.

| $N_{\text{trk}}^{\text{offline}}$ | a_{norm} | b_{norm} | χ^2/ndf |
|-----------------------------------|--------------------------|---------------------------------|---------------------|
| 120–150 | $1.13 \pm 0.24 \pm 0.14$ | $0.048 \pm 0.019 \pm 0.012$ | 16.3/8 |
| 150–185 | $1.13 \pm 0.19 \pm 0.04$ | $0.047 \pm 0.016 \pm 0.008$ | 4.9/8 |
| 185–250 | $1.69 \pm 0.06 \pm 0.01$ | $-0.0009 \pm 0.0050 \pm 0.0078$ | 4.5/8 |
| 250–300 | $1.83 \pm 0.13 \pm 0.15$ | $-0.015 \pm 0.011 \pm 0.016$ | 8.1/8 |

Table 3: The summary of slope and intercept parameter a_{norm} and b_{norm} for different centrality classes in PbPb collisions, and the goodness of fit χ^2 per degree of freedom (ndf). The statistical and systematic uncertainties are shown after the central values, respectively.

| Centrality | a_{norm} | b_{norm} | χ^2/ndf |
|------------|--------------------------|---------------------------------|---------------------|
| 60–70% | $1.85 \pm 0.17 \pm 0.21$ | $0.003 \pm 0.017 \pm 0.023$ | 12.3/9 |
| 50–60% | $1.75 \pm 0.04 \pm 0.01$ | $0.002 \pm 0.004 \pm 0.010$ | 11.8/9 |
| 45–50% | $1.74 \pm 0.04 \pm 0.03$ | $0.000 \pm 0.005 \pm 0.011$ | 8.4/9 |
| 40–45% | $1.59 \pm 0.03 \pm 0.01$ | $0.012 \pm 0.003 \pm 0.011$ | 9.1/9 |
| 35–40% | $1.68 \pm 0.03 \pm 0.01$ | $-0.001 \pm 0.003 \pm 0.010$ | 15.1/9 |
| 30–35% | $1.67 \pm 0.04 \pm 0.01$ | $-0.0026 \pm 0.0036 \pm 0.0095$ | 6.9/9 |

summarized in Tables 2 and 3 in $N_{\text{trk}}^{\text{offline}}$ and centrality classes for pPb and PbPb collisions, respectively.

The values of the intercept parameter b_{norm} are shown as a function of event multiplicity in Fig. 15 (upper), for both pPb and PbPb collisions. The $\pm 1\sigma$ and $\pm 2\sigma$ systematic uncertainty is shown, which correspond to a 68% and 95% confidence level (CL), respectively. Within statistical and systematic uncertainties, no significant positive value for b_{norm} is observed for most multiplicities in pPb or centralities in PbPb collisions. For multiplicity ranges $120 \leq N_{\text{trk}}^{\text{offline}} < 150$ and $150 \leq N_{\text{trk}}^{\text{offline}} < 185$ in pPb collisions, an indication of positive values with significances of more than two standard deviations is seen. However, results in these multiplicity ranges are likely to be highly sensitive to the very limited v_2 coverage using the ESE technique, as shown in the upper panel of Fig. 14. Overall, the result suggests that the v_2 -independent contribution to the $\Delta\gamma_{112}$ correlator is consistent with zero, and correlation data are consistent with the background-only scenario of charge-dependent two-particle correlations plus an anisotropic flow, v_n . This conclusion is consistent with that drawn from the study of higher-order harmonic three-particle correlators discussed earlier.

Based on the assumption of a nonnegative CME signal, the upper limit of the v_2 -independent fraction in the $\Delta\gamma_{112}$ correlator is obtained from the Feldman–Cousins approach [45] with the measured statistical and systematic uncertainties. In Fig. 15 (lower), the upper limit of the fraction f_{norm} , where f_{norm} is the ratio of the b_{norm} value to the value of $\langle \Delta\gamma_{112} \rangle / \langle \Delta\delta \rangle$, is presented at 95% CL as a function of event multiplicity. The v_2 -independent component of the $\Delta\gamma_{112}$ correlator is less than 8–15% for most of the multiplicity or centrality range. The combined limits from all presented multiplicities and centralities are also shown in pPb and PbPb collisions. An upper limit on the v_2 -independent fraction of the three-particle correlator, or possibly the CME signal contribution, is estimated to be 13% in pPb and 7% in PbPb collisions, at 95% CL. Note that the conclusion here is based on the assumption of a CME signal independent of v_2 in a narrow multiplicity or centrality range. As pointed out in a study by the ALICE collaboration after this manuscript was submitted [46], the observed CME signal may

be reduced as v_2 decreases for small v_2 values (e.g., $<6\%$), due to a weaker correlation between magnetic field and event-plane orientations as a result of initial-state fluctuations. Depending on specific models of initial-state fluctuations, the upper limits obtained in this paper may increase relatively by about 20%, although still well within a few % level. On the other hand, covering a wide range of v_2 values in this analysis (6–15%), the v_2 dependence of the observed CME signal is minimized to the largest extent, especially for more central events. The data also rule out any significant nonlinear v_2 dependence of the observed CME signal, as suggested by Ref. [46]. Therefore, the high-precision data presented in this paper indicate that the charge-dependent three-particle azimuthal correlations in pPb and PbPb collisions are consistent with a v_2 -dependent background-only scenario, posing a significant challenge to the search for the CME in heavy ion collisions using three-particle azimuthal correlations.

6 Summary

Charge-dependent azimuthal correlations of same- and opposite-sign (SS and OS) pairs with respect to the second- and third-order event planes have been studied in pPb collisions at $\sqrt{s_{\text{NN}}}=8.16$ TeV and PbPb collisions at 5.02 TeV by the CMS experiment at the LHC. The correlations are extracted via three-particle correlators as functions of pseudorapidity difference, transverse momentum difference, and p_{T} average of SS and OS particle pairs, in various multiplicity or centrality ranges of the collisions. The differences in correlations between OS and SS particles with respect to both second- and third-order event planes as functions of $\Delta\eta$ and multiplicity are found to agree for pPb and PbPb collisions, indicating a common underlying mechanism for the two systems. Dividing the OS and SS difference of the three-particle correlator by the product of the v_n harmonic of the corresponding order and the difference of the two-particle correlator, the ratios are found to be similar for the second- and third-order event planes, and show a weak dependence on event multiplicity. These observations support a scenario in which the charge-dependent three-particle correlator is predominantly a consequence of charge-dependent two-particle correlations coupled to an anisotropic flow signal.

To establish the relation between the three-particle correlator and anisotropic flow harmonic in detail, an event shape engineering technique is applied. A linear relation for the ratio of three- to two-particle correlator difference as a function of v_2 is observed, which extrapolates to an intercept that is consistent with zero within uncertainties for most of multiplicities. An upper limit on the v_2 -independent fraction of the three-particle correlator, or the possible CME signal contribution (assumed independent of v_2 within the same narrow multiplicity or centrality range), is estimated to be 13% for pPb data and 7% for PbPb data at a 95% confidence level. The data presented in this paper provide new stringent constraints on the nature of the background contribution to the charge-dependent azimuthal correlations, and establish a new baseline for the search for the chiral magnetic effect in heavy ion collisions.

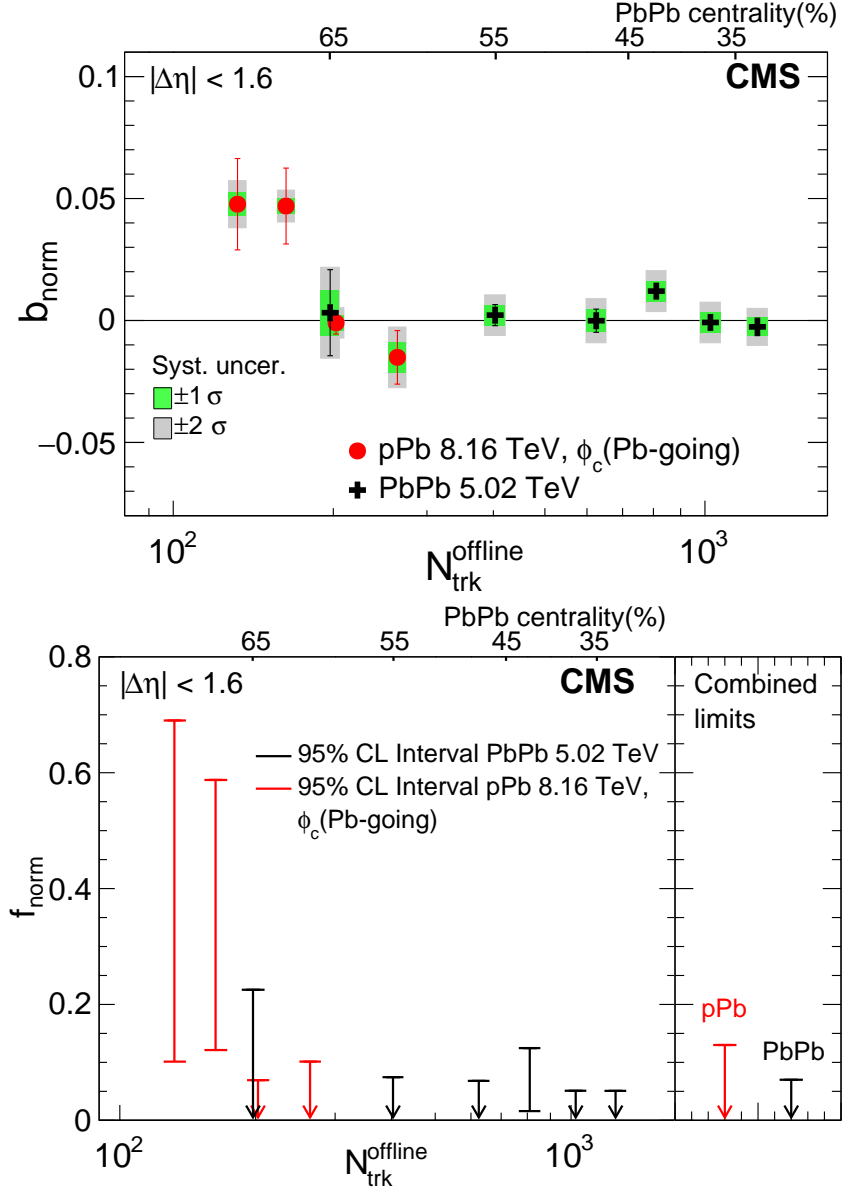


Figure 15: Extracted intercept parameter b_{norm} (upper) and corresponding upper limit of the fraction of v_2 -independent γ_{112} correlator component (lower), averaged over $|\Delta\eta| < 1.6$, as a function of $N_{\text{trk}}^{\text{offline}}$ in pPb collisions at $\sqrt{s_{\text{NN}}} = 8.16$ TeV and PbPb collisions at 5.02 TeV. Statistical and systematic uncertainties are indicated by the error bars and shaded regions in the top panel, respectively.

Acknowledgments

We congratulate our colleagues in the CERN accelerator departments for the excellent performance of the LHC and thank the technical and administrative staffs at CERN and at other CMS institutes for their contributions to the success of the CMS effort. In addition, we gratefully acknowledge the computing centers and personnel of the Worldwide LHC Computing Grid for delivering so effectively the computing infrastructure essential to our analyses. Finally, we acknowledge the enduring support for the construction and operation of the LHC and the CMS detector provided by the following funding agencies: BMWFW and FWF (Austria); FNRS and FWO (Belgium); CNPq, CAPES, FAPERJ, and FAPESP (Brazil); MES (Bulgaria); CERN; CAS, MoST, and NSFC (China); COLCIENCIAS (Colombia); MSES and CSF (Croatia); RPF (Cyprus); SENESCYT (Ecuador); MoER, ERC IUT, and ERDF (Estonia); Academy of Finland, MEC, and HIP (Finland); CEA and CNRS/IN2P3 (France); BMBF, DFG, and HGF (Germany); GSRT (Greece); OTKA and NIH (Hungary); DAE and DST (India); IPM (Iran); SFI (Ireland); INFN (Italy); MSIP and NRF (Republic of Korea); LAS (Lithuania); MOE and UM (Malaysia); BUAP, CINVESTAV, CONACYT, LNS, SEP, and UASLP-FAI (Mexico); MBIE (New Zealand); PAEC (Pakistan); MSHE and NSC (Poland); FCT (Portugal); JINR (Dubna); MON, RosAtom, RAS, RFBR and RAEP (Russia); MESTD (Serbia); SEIDI, CPAN, PCTI and FEDER (Spain); Swiss Funding Agencies (Switzerland); MST (Taipei); ThEPCenter, IPST, STAR, and NSTDA (Thailand); TUBITAK and TAEK (Turkey); NASU and SFFR (Ukraine); STFC (United Kingdom); DOE and NSF (USA).

Individuals have received support from the Marie-Curie program and the European Research Council and Horizon 2020 Grant, contract No. 675440 (European Union); the Leventis Foundation; the A. P. Sloan Foundation; the Alexander von Humboldt Foundation; the Belgian Federal Science Policy Office; the Fonds pour la Formation à la Recherche dans l'Industrie et dans l'Agriculture (FRIA-Belgium); the Agentschap voor Innovatie door Wetenschap en Technologie (IWT-Belgium); the Ministry of Education, Youth and Sports (MEYS) of the Czech Republic; the Council of Science and Industrial Research, India; the HOMING PLUS program of the Foundation for Polish Science, cofinanced from European Union, Regional Development Fund, the Mobility Plus program of the Ministry of Science and Higher Education, the National Science Center (Poland), contracts Harmonia 2014/14/M/ST2/00428, Opus 2014/13/B/ST2/02543, 2014/15/B/ST2/03998, and 2015/19/B/ST2/02861, Sonata-bis 2012/07/E/ST2/01406; the National Priorities Research Program by Qatar National Research Fund; the Programa Clarín-COFUND del Principado de Asturias; the Thalís and Aristeia programs cofinanced by EU-ESF and the Greek NSRF; the Rachadapisek Sompot Fund for Postdoctoral Fellowship, Chulalongkorn University and the Chulalongkorn Academic into Its 2nd Century Project Advancement Project (Thailand); and the Welch Foundation, contract C-1845.

Appendices

A General relation of v_n harmonics, two- and three-particle azimuthal correlations

In Section 1, Eq. (5) can be derived in a way similar to Eq. (3), with details which can be found in Ref. [24]. Here, a general derivation of Eq. (5) for all higher-order-harmonic correlators is given.

Similar to Eq. (40) in Ref. [24], the general relation between the n th order anisotropy harmonic v_n and the three-particle correlator with respect to the n th order event plane can be derived

starting from,

$$\begin{aligned}\gamma_{1,n-1;n} &\equiv \langle \cos(\phi_\alpha + (n-1)\phi_\beta - n\Psi_n) \rangle \\ &= \frac{\int \rho_2 \cos(\phi_\alpha + (n-1)\phi_\beta - n\Psi_n) d\phi_\alpha d\phi_\beta dx_\alpha dx_\beta}{\int \rho_2 d\phi_\alpha d\phi_\beta dx_\alpha dx_\beta} \\ &= \frac{\int \rho_2 \cos(\phi_\alpha - \phi_\beta + n(\phi_\beta - \Psi_n)) d\phi_\alpha d\phi_\beta dx_\alpha dx_\beta}{\int \rho_2 d\phi_\alpha d\phi_\beta dx_\alpha dx_\beta},\end{aligned}\quad (17)$$

where x denotes (p_T, η) and $dx = p_T dp_T d\eta$. ρ_2 is the two-particle pair density distribution, which can be expressed in terms of the single-particle density distribution and its underlying two-particle correlation function (see Section 2 in Ref. [24]),

$$\rho_2 = \rho(\phi_\alpha, x_\alpha)\rho(\phi_\beta, x_\beta) [1 + C(\phi_\alpha, \phi_\beta, x_\alpha, x_\beta)].\quad (18)$$

In presence of collective anisotropy flow, the single-particle azimuthal distribution can be expressed in terms of a Fourier series with respect to the event plane of the corresponding order,

$$\rho(\phi, x) = \frac{\rho_0(x)}{2\pi} \left[1 + \sum_{n=1}^{\infty} n v_n(x) \cos n(\phi - \Psi_n) \right],\quad (19)$$

where $\rho_0(x)$ depends on p_T and η only.

The two-particle correlation function C describes intrinsic correlations that are insensitive to the event plane Ψ_n , but only involve azimuthal angle difference $\Delta\phi = \phi_\alpha - \phi_\beta$. It can be also expanded in Fourier series [24],

$$C(\Delta\phi, x_\alpha, x_\beta) = \sum_{n=1}^{\infty} a_n(x_\alpha, x_\beta) \cos(n\Delta\phi),\quad (20)$$

where $a_n(x_\alpha, x_\beta)$ is the two-particle Fourier coefficient. By definition, $a_1(x_\alpha, x_\beta)$ is equal to the two-particle correlator $\delta(x_\alpha, x_\beta)$, introduced in Section 1, as a function of x_α and x_β (i.e., p_T and η of both particles).

Therefore, we substitute Eqs. (20) and (18) into (17) and obtain,

$$\begin{aligned}\gamma_{1,n-1;n} &= \frac{1}{2N^2} \int \rho_0(x_\alpha)\rho_0(x_\beta)a_1(x_\alpha, x_\beta) \\ &\quad [v_n(x_\alpha) + v_n(x_\beta)] dx_\alpha dx_\beta \\ &= \frac{1}{2N^2} \int \rho_0(x_\alpha)\rho_0(x_\beta)\delta(x_\alpha, x_\beta) \\ &\quad [v_n(x_\alpha) + v_n(x_\beta)] dx_\alpha dx_\beta\end{aligned}\quad (21)$$

where $N = \int \rho_0(x)dx$. This is the general equation explaining why a nonzero two-particle correlation $\delta(x_\alpha, x_\beta)$ plus an anisotropy flow of n th order $v_n(x)$ contribute to the three-particle correlator, $\gamma_{1,n-1;n}$.

Therefore, this general form of $\gamma_{1,n-1;n}$ can be applied to any order n and decomposed into the two-particle correlator δ and the n th order harmonic v_n , where $n = 2$ and 3 are studied in detail in Section 5.1.

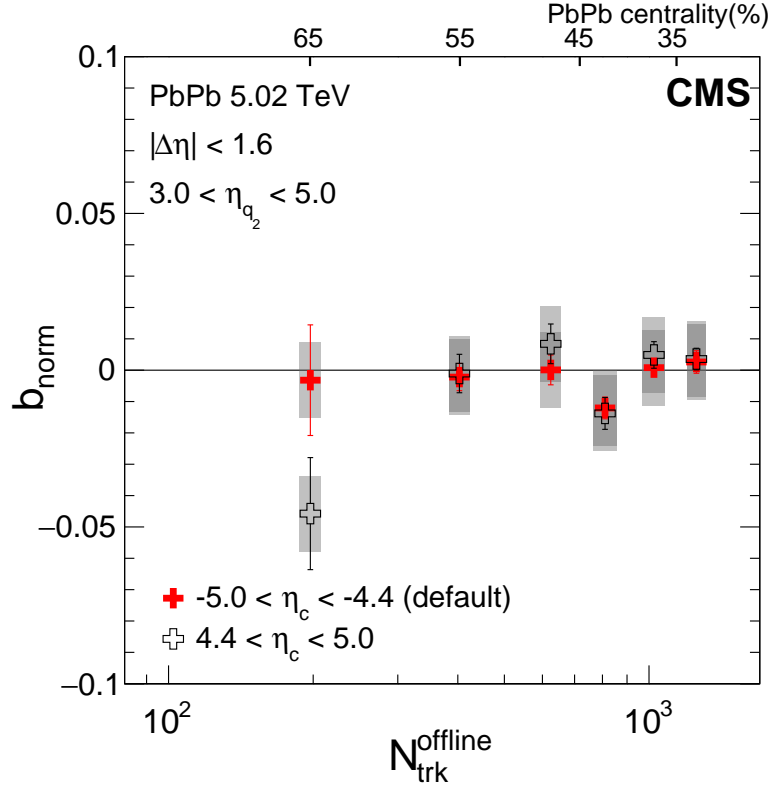


Figure 16: The intercepts b_{norm} of v_2 -independent γ_{112} correlator component using particle c from HF+ and HF– data, averaged over $|\Delta\eta| < 1.6$, are shown as a function of $N_{\text{trk}}^{\text{offline}}$ in PbPb collisions at $\sqrt{s_{\text{NN}}} = 5.02$ TeV. Statistical and systematic uncertainties are indicated by the error bars and shaded regions, respectively.

B Supporting results of the event shape engineering method

As stated in Section 4.2, the Q_2 vector is calculated using one side of the HF detector within the η range of 3 to 5 units. The default result in Section 5.2 presents the $\Delta\gamma_{112}$ as a function of v_2 , where the particle c in the γ_{112} correlator corresponds to the η range -5.0 to -4.4 . However, the results are found to be independent of where the particle c is reconstructed, as it is shown in Fig. 16.

In Figs. 17 and 18, the denominators of Eq. (7), $v_{2,c}$, for different Q_2 classes with respect to HF+ and HF– in PbPb collisions at $\sqrt{s_{\text{NN}}} = 5.02$ TeV, and the Pb-going side of the HF in pPb collisions at 8.16 TeV, are shown as a function of v_2 in the tracker region. Here $v_{2,c}$ is a measure of elliptic anisotropy of the transverse energy registered in the HF detectors without being corrected to the particle-level elliptic flow. It serves as the resolution correction factor when deriving the three-particle correlators or the v_2 values in the tracker region using the scalar-product method.

In Fig. 19, the average $N_{\text{trk}}^{\text{offline}}$ is shown as a function of v_2 in different multiplicity and centrality ranges in pPb (upper) and PbPb collisions (lower), respectively. The average $N_{\text{trk}}^{\text{offline}}$ is found to be weakly dependent on v_2 , but with a slight decreasing trend as v_2 increases. Similar to Fig. 13, the effect at low multiplicities is stronger than that at high multiplicities. Overall, this effect is negligible for the results shown in Section 5.2.

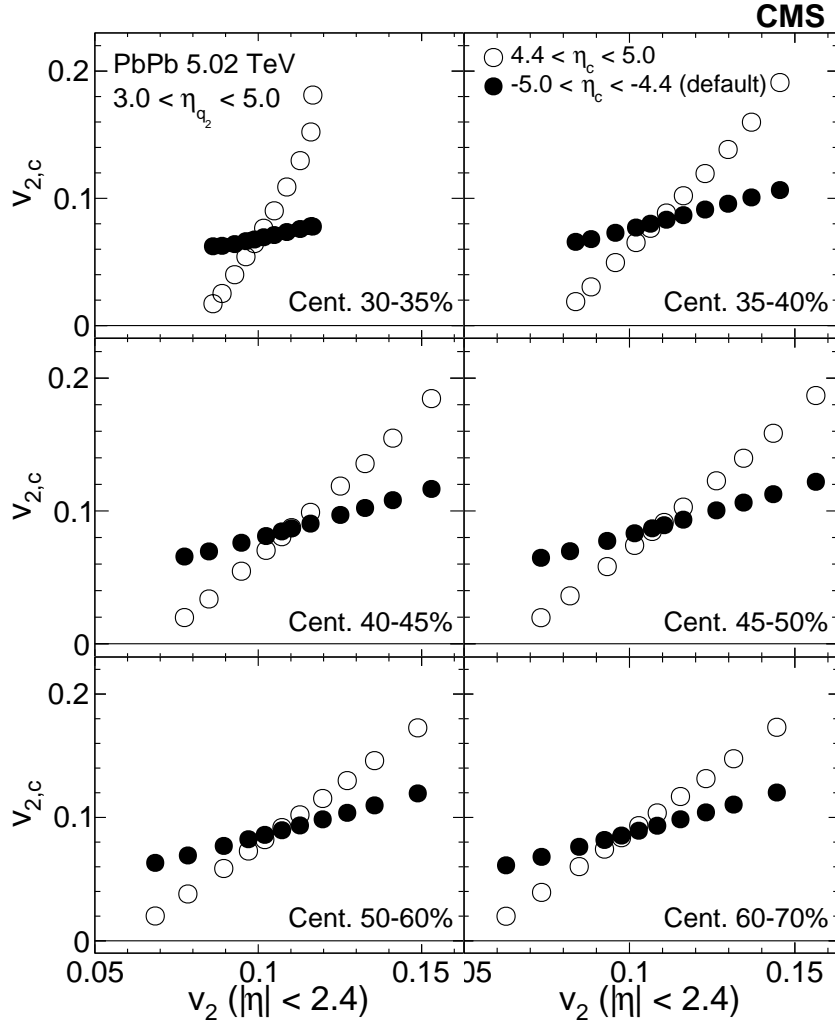


Figure 17: The $v_{2,c}$ using particle c from HF+ and HF– data are shown as a function of v_2 in the tracker region ($|\eta| < 2.4$) in PbPb collisions at $\sqrt{s_{NN}} = 5.02$ TeV.

C Three- and two-particle correlator as functions of differential variables in different multiplicity and centrality classes

The figures in Appendix C show the γ_{112} , γ_{123} , and the δ correlators as a function of $|\Delta\eta|$, $|\Delta p_T|$, and \bar{p}_T in pPb collisions at $\sqrt{s_{NN}} = 8.16$ TeV and PbPb collisions at 5.02 TeV. In pPb and PbPb collisions, the results are shown for multiplicity ranges $N_{\text{trk}}^{\text{offline}} = [120,150)$, $[150,185)$, $[185,250)$, and $[250,300)$ in Figs. 20 to 22. In PbPb collisions, the results are also shown for five centrality classes from 30–80% in Figs. 23 to 25.

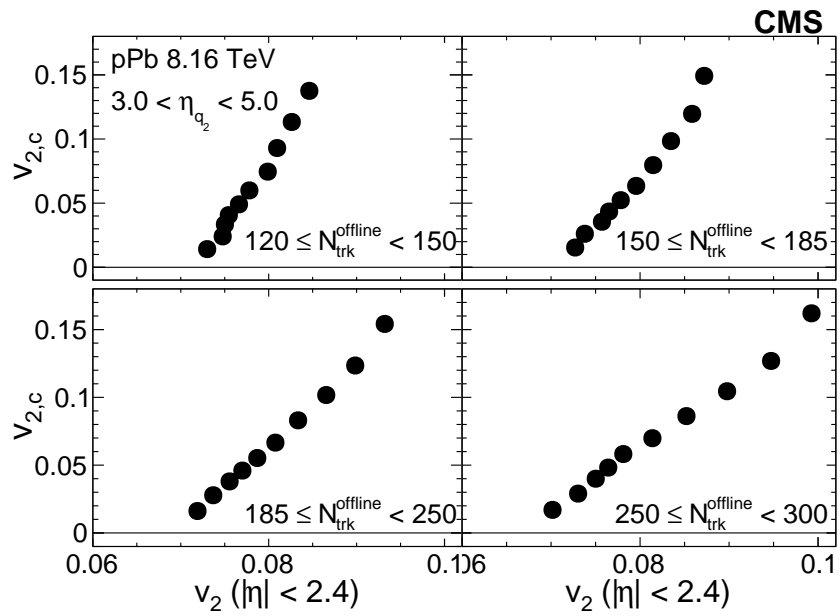


Figure 18: The $v_{2,c}$ using particle c from the Pb-going side of the HF ($4.4 < \eta < 5.0$) data are shown as a function of v_2 in the tracker region ($|\eta| < 2.4$) in pPb collisions at $\sqrt{s_{NN}} = 8.16$ TeV.

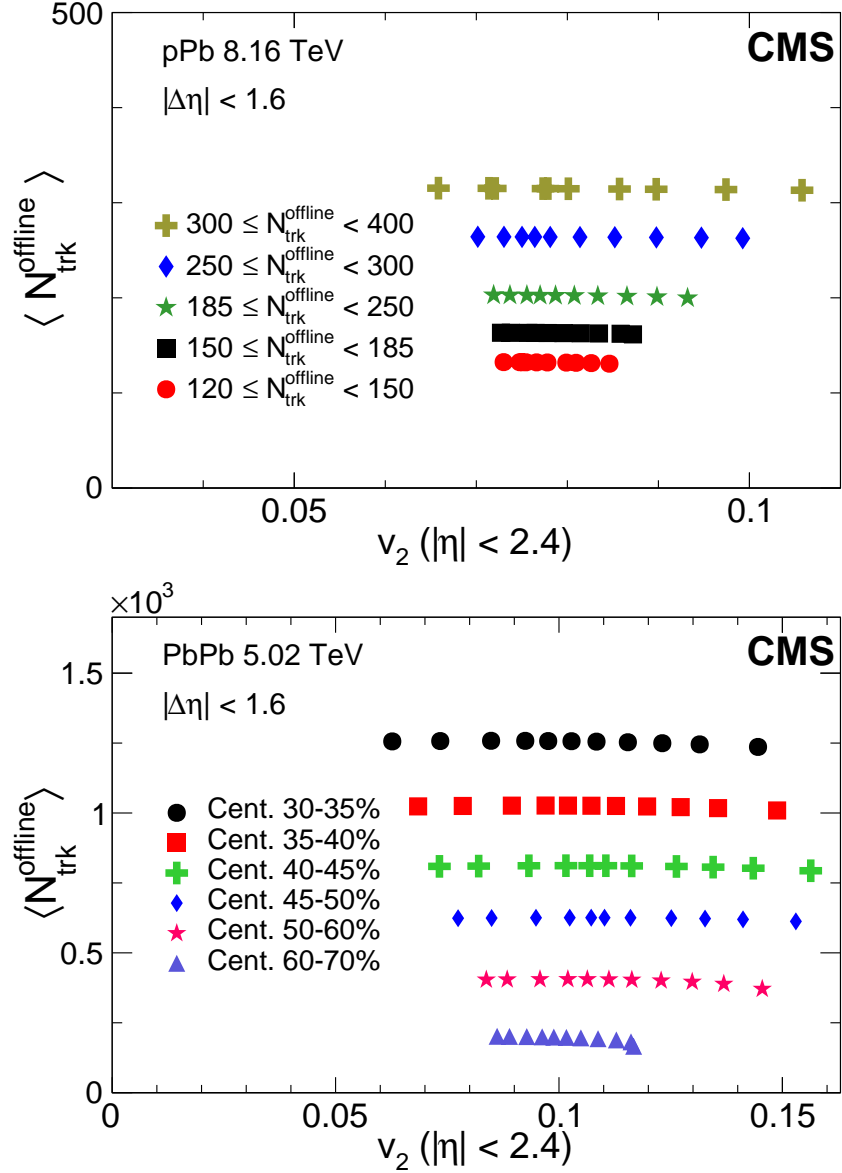


Figure 19: The average multiplicity $N_{\text{trk}}^{\text{offline}}$ as a function of v_2 evaluated in each q_2 class, for different multiplicity ranges in pPb collisions at $\sqrt{s_{\text{NN}}} = 8.16$ TeV (upper), and for different centrality classes in PbPb collisions at 5.02 TeV (lower). Statistical uncertainties are invisible on the current scale.

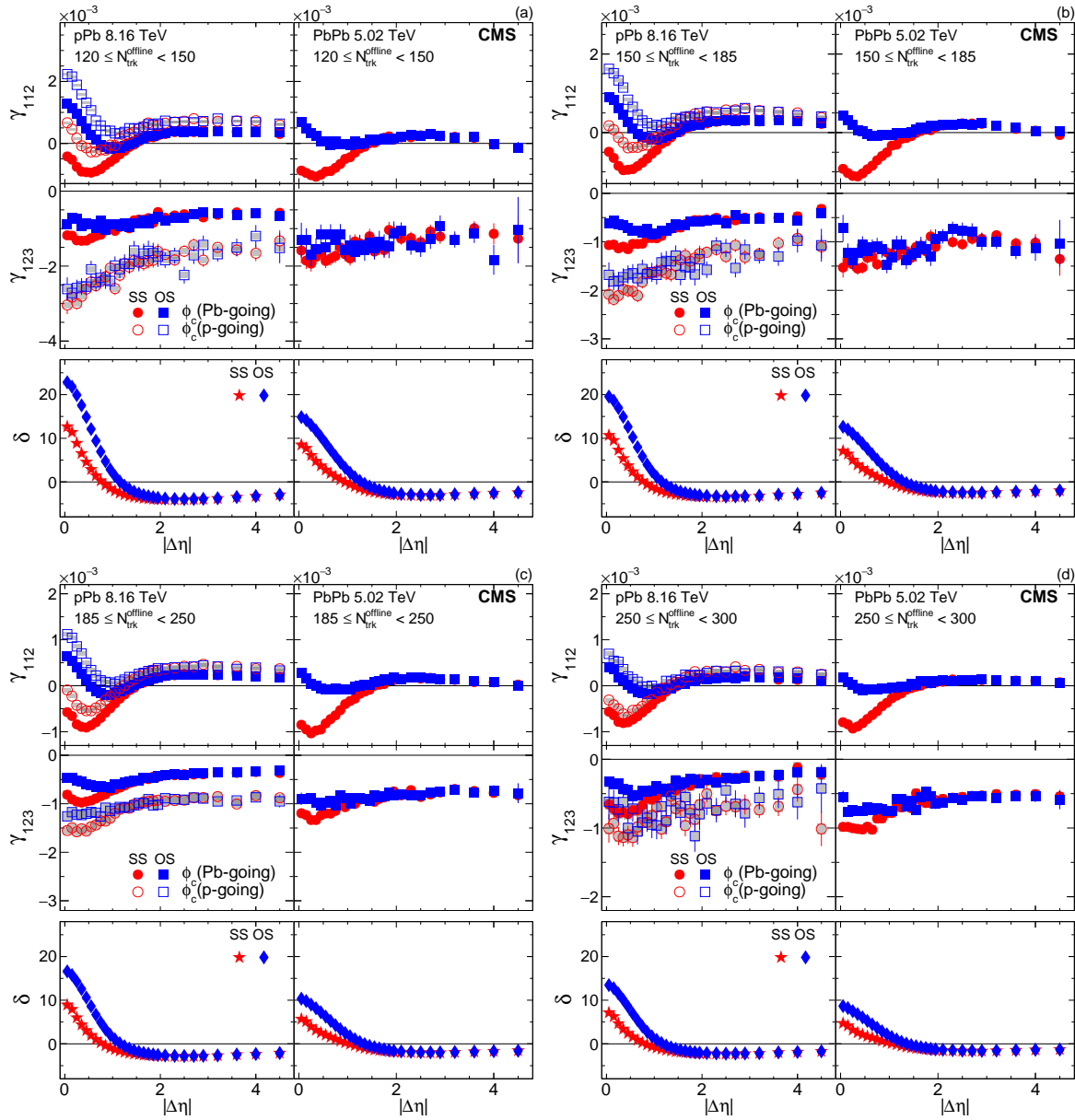


Figure 20: The SS and OS three-particle correlators, γ_{112} (upper) and γ_{123} (middle), and two-particle correlator, δ (lower), as a function of $|\Delta\eta|$ for four multiplicity ranges in pPb collisions at $\sqrt{s_{\text{NN}}} = 8.16$ TeV (left) and PbPb collisions at 5.02 TeV (right). The pPb results obtained with particle c in Pb-going (solid markers) and p-going (open markers) sides are shown separately. The SS and OS two-particle correlators are denoted by different markers for both pPb and PbPb collisions. Statistical and systematic uncertainties are indicated by the error bars and shaded regions, respectively.

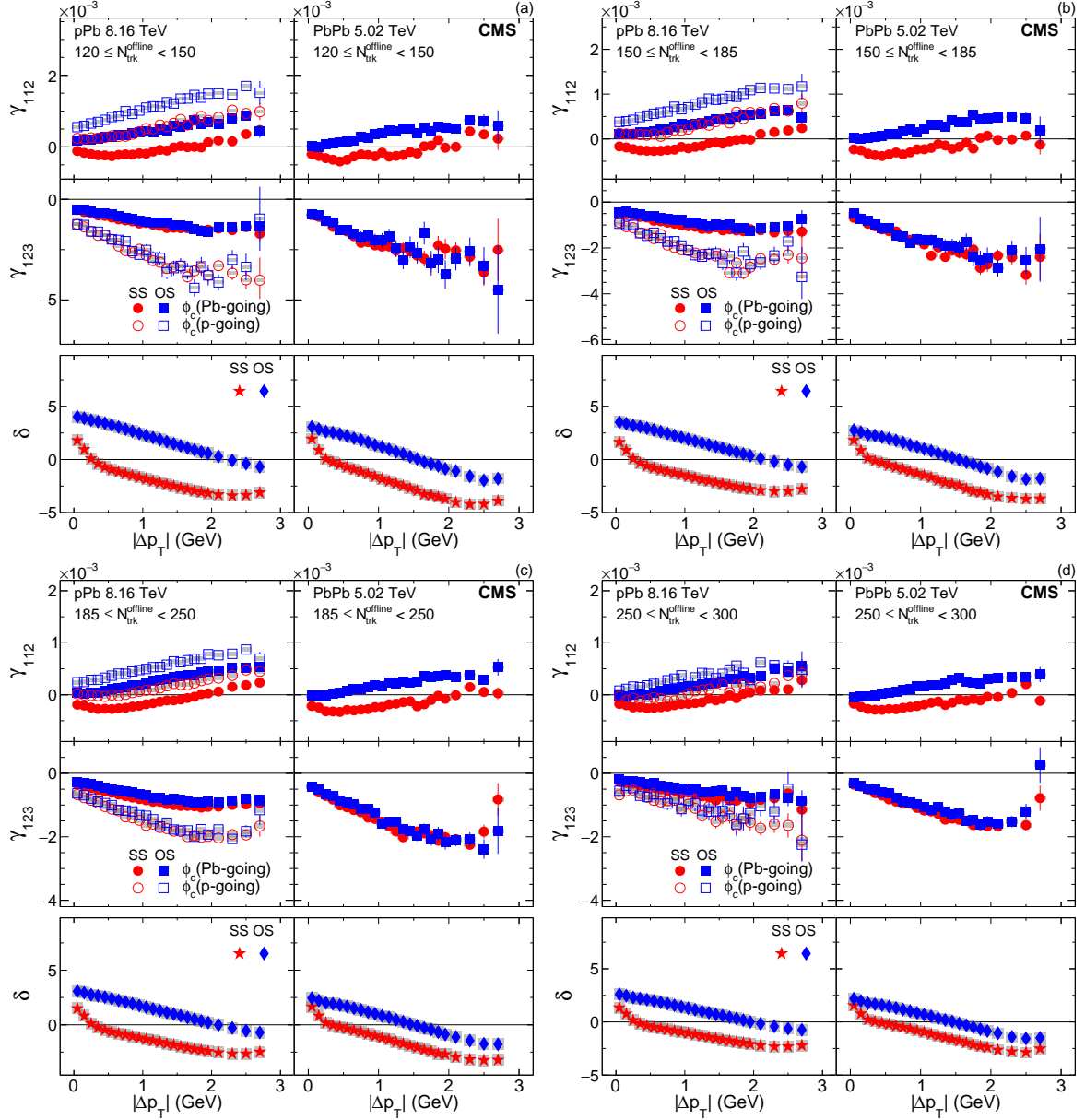


Figure 21: The SS and OS three-particle correlators, γ_{112} (upper) and γ_{123} (middle), and two-particle correlator, δ (lower), as a function of $|\Delta p_T|$ for four multiplicity ranges in pPb collisions at $\sqrt{s_{\text{NN}}} = 8.16$ TeV (left) and PbPb collisions at 5.02 TeV (right) collisions. The pPb results obtained with particle c in Pb-going (solid markers) and p-going (open markers) sides are shown separately. The SS and OS two-particle correlators are denoted by different markers for both pPb and PbPb collisions. Statistical and systematic uncertainties are indicated by the error bars and shaded regions, respectively.

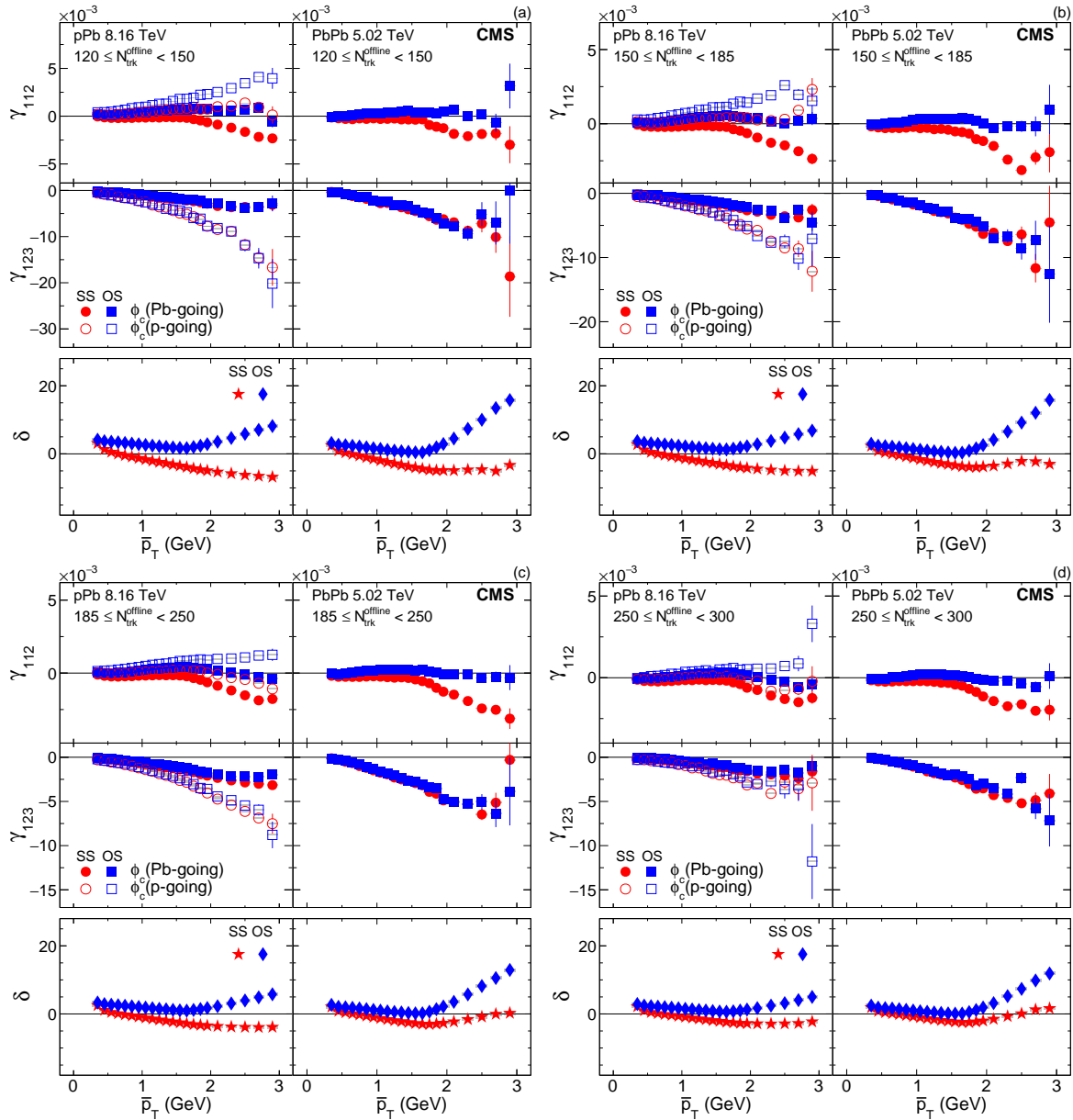


Figure 22: The SS and OS three-particle correlators, γ_{112} (upper) and γ_{123} (middle), and two-particle correlator, δ (lower), as a function of \bar{p}_T for four multiplicity ranges in pPb collisions at $\sqrt{s_{NN}} = 8.16$ TeV (left) and PbPb collisions at $\sqrt{s_{NN}} = 5.02$ TeV (right). The pPb results obtained with particle c in Pb-going (solid markers) and p-going (open markers) sides are shown separately. The SS and OS two-particle correlators are denoted by different markers for both pPb and PbPb collisions. Statistical and systematic uncertainties are indicated by the error bars and shaded regions, respectively.

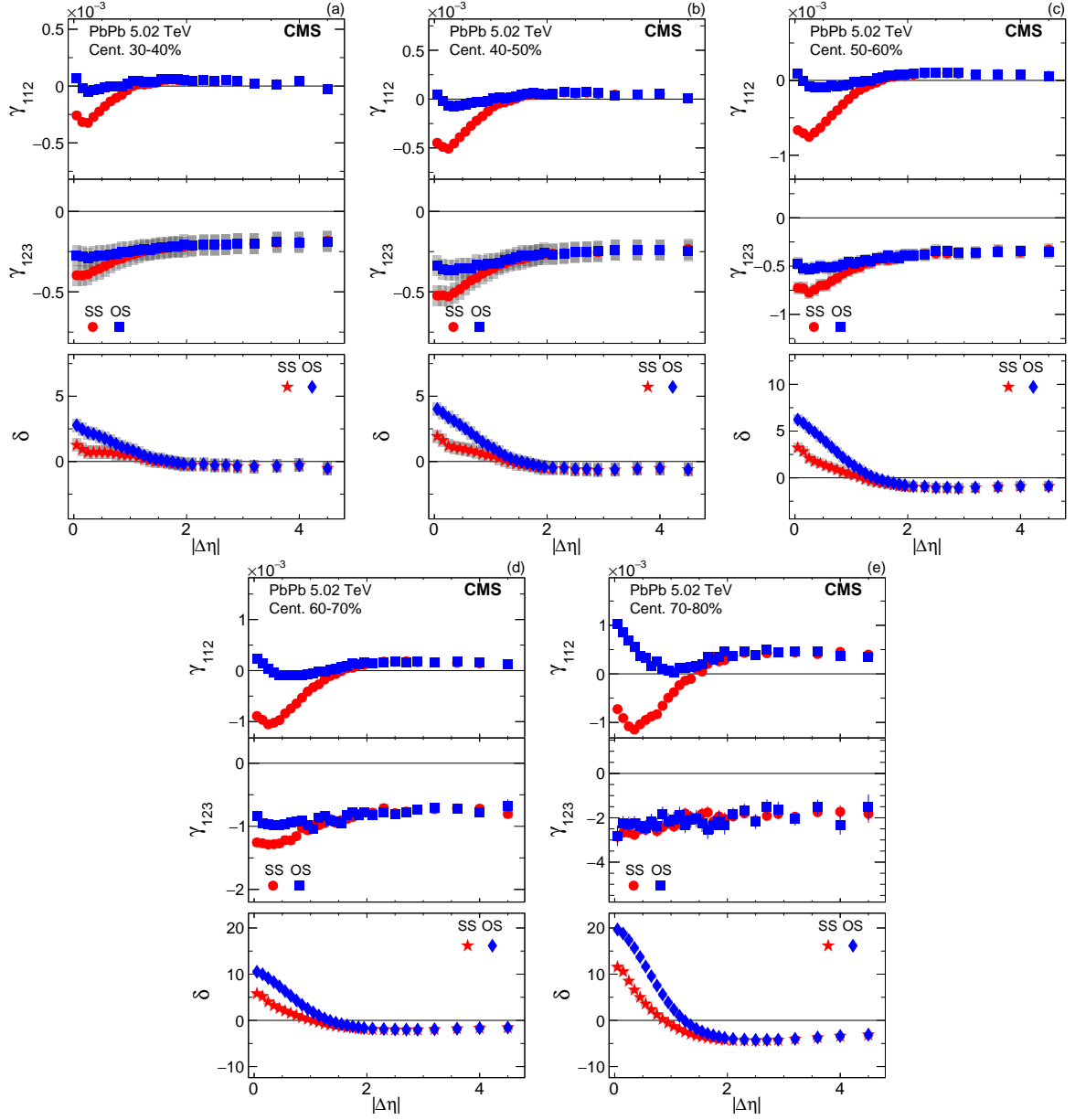


Figure 23: The SS and OS three-particle correlators, γ_{112} (upper) and γ_{123} (middle), and two-particle correlator, δ (lower), as a function of $|\Delta\eta|$ for five centrality classes in PbPb collisions at 5.02 TeV. The SS and OS two-particle correlators are denoted by different markers. Statistical and systematic uncertainties are indicated by the error bars and shaded regions, respectively.

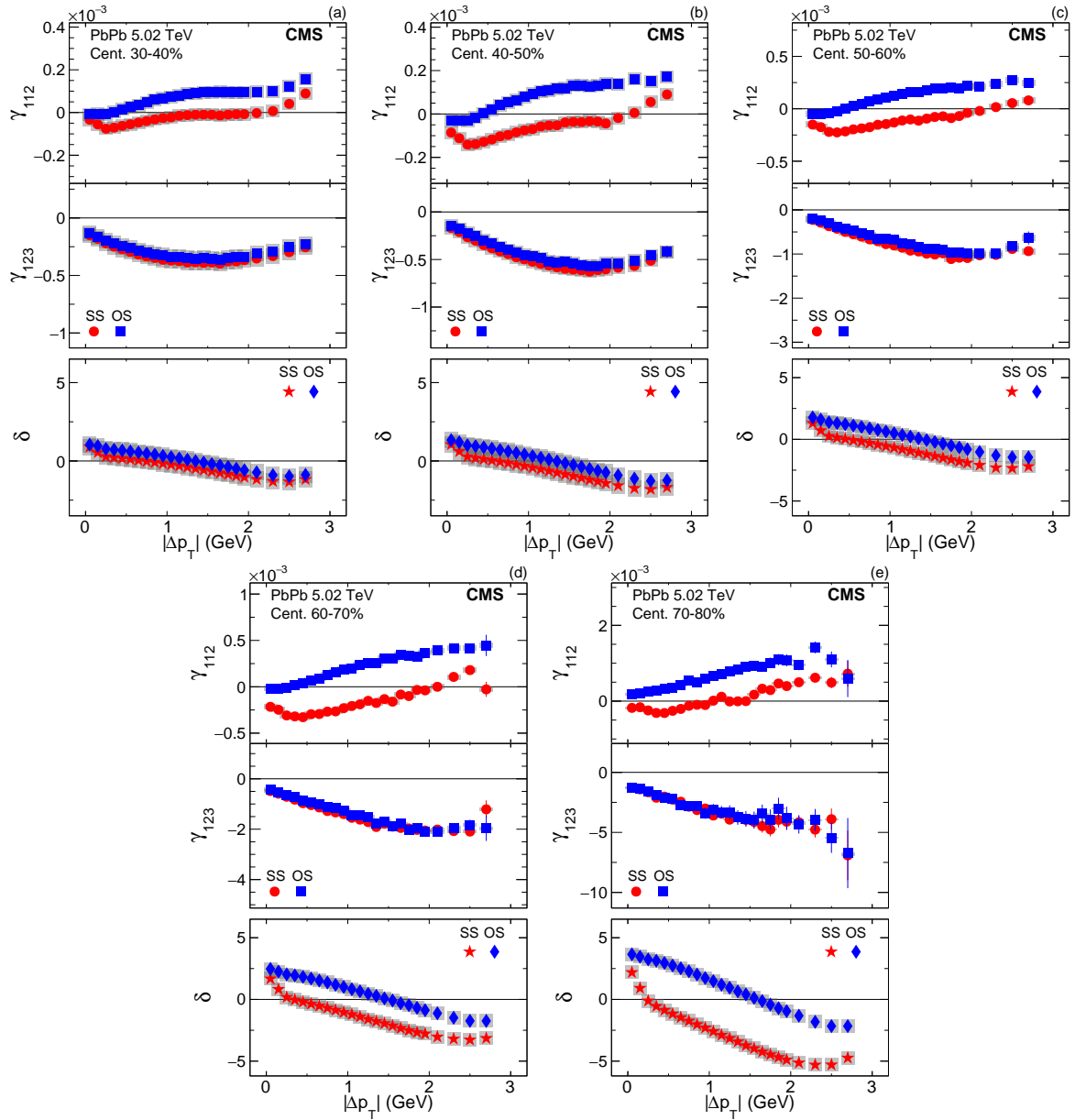


Figure 24: The SS and OS three-particle correlators, γ_{112} (upper) and γ_{123} (middle), and two-particle correlator, δ (lower), as a function of $|\Delta p_T|$ for five centrality classes in PbPb collisions at $\sqrt{s_{\text{NN}}} = 5.02$ TeV. The SS and OS two-particle correlators are denoted by different markers. Statistical and systematic uncertainties are indicated by the error bars and shaded regions, respectively.

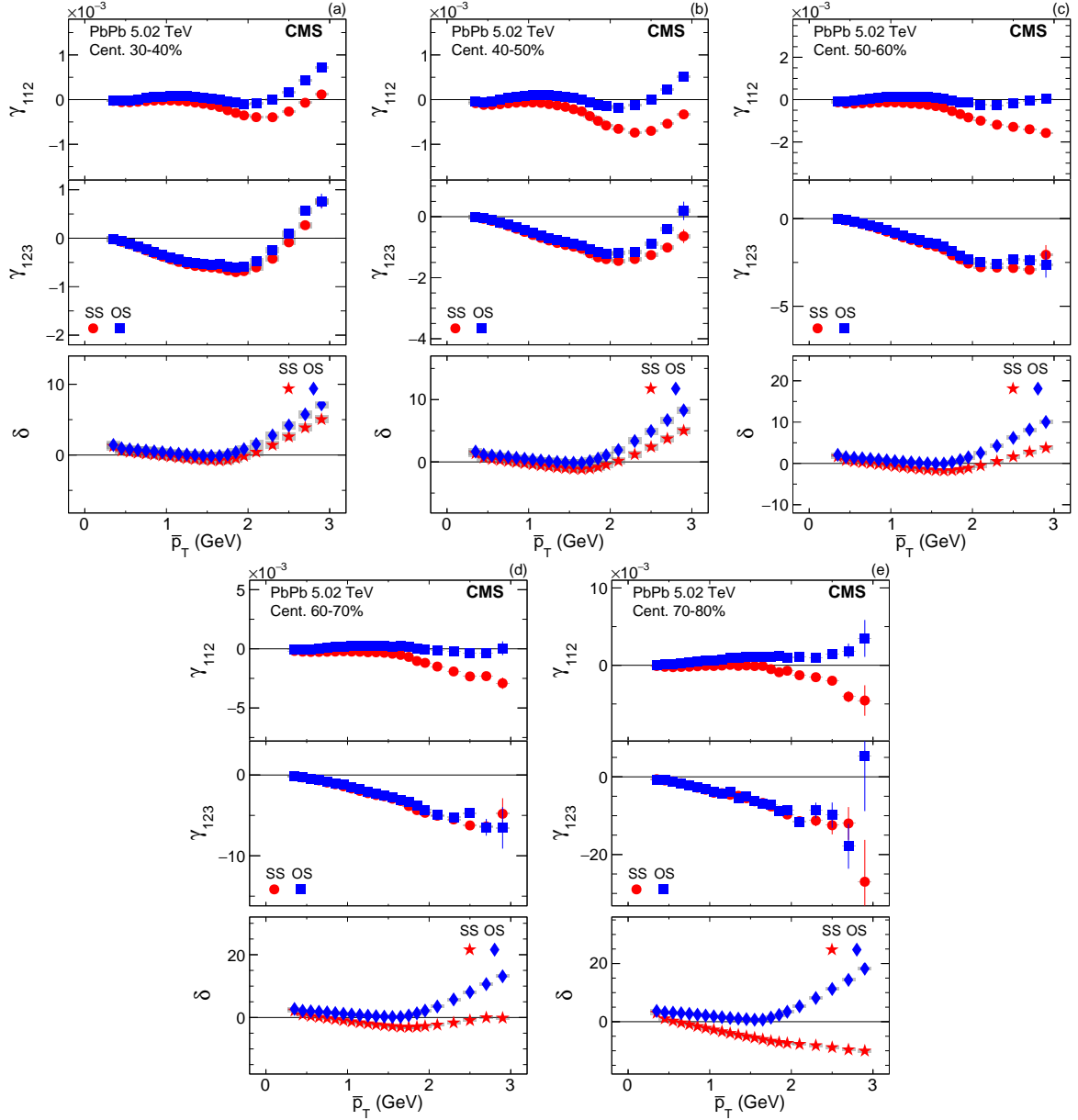


Figure 25: The SS and OS three-particle correlators, γ_{112} (upper) and γ_{123} (middle), and two-particle correlator, δ (lower), as a function of \bar{p}_T for five centrality classes in PbPb collisions at $\sqrt{s_{NN}} = 5.02$ TeV. The SS and OS two-particle correlators are denoted by different markers. Statistical and systematic uncertainties are indicated by the error bars and shaded regions, respectively.

References

- [1] T. D. Lee, "A theory of spontaneous T violation", *Phys. Rev. D* **8** (1973) 1226, doi:10.1103/PhysRevD.8.1226.
- [2] T. D. Lee and G. C. Wick, "Vacuum stability and vacuum excitation in a spin-0 field theory", *Phys. Rev. D* **9** (1974) 2291, doi:10.1103/PhysRevD.9.2291.
- [3] P. D. Morley and I. A. Schmidt, "Strong P, CP, T violations in heavy-ion collisions", *Z. Phys. C* **26** (1985) 627, doi:10.1007/BF01551807.
- [4] D. Kharzeev, R. D. Pisarski, and M. H. G. Tytgat, "Possibility of spontaneous parity violation in hot QCD", *Phys. Rev. Lett.* **81** (1998) 512, doi:10.1103/PhysRevLett.81.512, arXiv:hep-ph/9804221.
- [5] D. Kharzeev, "Parity violation in hot QCD: Why it can happen, and how to look for it", *Phys. Lett. B* **633** (2006) 260, doi:10.1016/j.physletb.2005.11.075, arXiv:hep-ph/0406125.
- [6] D. E. Kharzeev, L. D. McLerran, and H. J. Warringa, "The effects of topological charge change in heavy ion collisions: 'Event by event P and CP violation'", *Nucl. Phys. A* **803** (2008) 227, doi:10.1016/j.nuclphysa.2008.02.298, arXiv:0711.0950.
- [7] K. Fukushima, D. E. Kharzeev, and H. J. Warringa, "The chiral magnetic effect", *Phys. Rev. D* **78** (2008) 074033, doi:10.1103/PhysRevD.78.074033, arXiv:0808.3382.
- [8] B. Q. Lv et al., "Experimental discovery of Weyl semimetal TaAs", *Phys. Rev. X* **5** (2015) 031013, doi:10.1103/PhysRevX.5.031013, arXiv:1502.04684.
- [9] X. Huang et al., "Observation of the chiral-anomaly-induced negative magnetoresistance in 3D Weyl semimetal TaAs", *Phys. Rev. X* **5** (2015) 031023, doi:10.1103/PhysRevX.5.031023, arXiv:1503.01304.
- [10] Q. Li et al., "Observation of the chiral magnetic effect in ZrTe5", *Nature Phys.* **12** (2016) 550, doi:10.1038/nphys3648, arXiv:1412.6543.
- [11] STAR Collaboration, "Azimuthal charged-particle correlations and possible local strong parity violation", *Phys. Rev. Lett.* **103** (2009) 251601, doi:10.1103/PhysRevLett.103.251601, arXiv:0909.1739.
- [12] STAR Collaboration, "Observation of charge-dependent azimuthal correlations and possible local strong parity violation in heavy ion collisions", *Phys. Rev. C* **81** (2010) 054908, doi:10.1103/PhysRevC.81.054908, arXiv:0909.1717.
- [13] STAR Collaboration, "Measurement of charge multiplicity asymmetry correlations in high-energy nucleus-nucleus collisions at $\sqrt{s_{\text{NN}}} = 200$ GeV", *Phys. Rev. C* **89** (2014) 044908, doi:10.1103/PhysRevC.89.044908, arXiv:1303.0901.
- [14] STAR Collaboration, "Beam-energy dependence of charge separation along the magnetic field in Au+Au collisions at RHIC", *Phys. Rev. Lett.* **113** (2014) 052302, doi:10.1103/PhysRevLett.113.052302, arXiv:1404.1433.
- [15] STAR Collaboration, "Fluctuations of charge separation perpendicular to the event plane and local parity violation in $\sqrt{s_{\text{NN}}} = 200$ GeV Au+Au collisions at the BNL Relativistic Heavy Ion Collider", *Phys. Rev. C* **88** (2013) 064911, doi:10.1103/PhysRevC.88.064911, arXiv:1302.3802.

-
- [16] ALICE Collaboration, “Charge separation relative to the reaction plane in Pb-Pb collisions at $\sqrt{s_{\text{NN}}} = 2.76$ TeV”, *Phys. Rev. Lett.* **110** (2013) 012301, doi:10.1103/PhysRevLett.110.012301, arXiv:1207.0900.
- [17] D. E. Kharzeev, J. Liao, S. A. Voloshin, and G. Wang, “Chiral magnetic and vortical effects in high-energy nuclear collisions — a status report”, *Prog. Part. Nucl. Phys.* **88** (2016) 1, doi:10.1016/j.pnpnp.2016.01.001, arXiv:1511.04050.
- [18] F. Wang, “Effects of cluster particle correlations on local parity violation observables”, *Phys. Rev. C* **81** (2010) 064902, doi:10.1103/PhysRevC.81.064902, arXiv:0911.1482.
- [19] A. Bzdak, V. Koch, and J. Liao, “Azimuthal correlations from transverse momentum conservation and possible local parity violation”, *Phys. Rev. C* **83** (2011) 014905, doi:10.1103/PhysRevC.83.014905, arXiv:1008.4919.
- [20] S. Schlichting and S. Pratt, “Charge conservation at energies available at the BNL Relativistic Heavy Ion Collider and contributions to local parity violation observables”, *Phys. Rev. C* **83** (2011) 014913, doi:10.1103/PhysRevC.83.014913, arXiv:1009.4283.
- [21] CMS Collaboration, “Observation of charge-dependent azimuthal correlations in pPb collisions and its implication for the search for the chiral magnetic effect”, *Phys. Rev. Lett.* **118** (2017) 122301, doi:10.1103/PhysRevLett.118.122301, arXiv:1610.00263.
- [22] R. Belmont and J. L. Nagle, “To CME or not to CME? Implications of p+Pb measurements of the chiral magnetic effect in heavy ion collisions”, *Phys. Rev. C* **96** (2017) 024901, doi:10.1103/PhysRevC.96.024901, arXiv:1610.07964.
- [23] S. A. Voloshin, “Parity violation in hot QCD: How to detect it”, *Phys. Rev. C* **70** (2004) 057901, doi:10.1103/PhysRevC.70.057901, arXiv:hep-ph/0406311.
- [24] A. Bzdak, V. Koch, and J. Liao, “Charge-dependent correlations in relativistic heavy ion collisions and the chiral magnetic effect”, *Lect. Notes Phys.* **871** (2013) 503, doi:10.1007/978-3-642-37305-3_19, arXiv:1207.7327.
- [25] B. Alver and G. Roland, “Collision geometry fluctuations and triangular flow in heavy-ion collisions”, *Phys. Rev. C* **81** (2010) 054905, doi:10.1103/PhysRevC.81.054905, arXiv:1003.0194. [Erratum: doi:10.1103/PhysRevC.82.039903].
- [26] ATLAS Collaboration, “Measurement of event-plane correlations in $\sqrt{s_{\text{NN}}} = 2.76$ TeV lead-lead collisions with the ATLAS detector”, *Phys. Rev. C* **90** (2014) 024905, doi:10.1103/PhysRevC.90.024905, arXiv:1403.0489.
- [27] CMS Collaboration, “Measurement of higher-order harmonic azimuthal anisotropy in PbPb collisions at $\sqrt{s_{\text{NN}}} = 2.76$ TeV”, *Phys. Rev. C* **89** (2014) 044906, doi:10.1103/PhysRevC.89.044906, arXiv:1310.8651.
- [28] CMS Collaboration, “Multiplicity and transverse momentum dependence of two- and four-particle correlations in pPb and PbPb collisions”, *Phys. Lett. B* **724** (2013) 213, doi:10.1016/j.physletb.2013.06.028, arXiv:1305.0609.

- [29] J. Schukraft, A. Timmins, and S. A. Voloshin, “Ultra-relativistic nuclear collisions: event shape engineering”, *Phys. Lett. B* **719** (2013) 394, doi:10.1016/j.physletb.2013.01.045, arXiv:1208.4563.
- [30] CMS Collaboration, “Description and performance of track and primary-vertex reconstruction with the CMS tracker”, *JINST* **9** (2014) P10009, doi:10.1088/1748-0221/9/10/P10009, arXiv:1405.6569.
- [31] CMS Collaboration, “The CMS Experiment at the CERN LHC”, *JINST* **3** (2008) S08004, doi:10.1088/1748-0221/3/08/S08004.
- [32] CMS Collaboration, “Observation of Long-Range Near-Side Angular Correlations in Proton-Proton Collisions at the LHC”, *JHEP* **09** (2010) 091, doi:10.1007/JHEP09(2010)091, arXiv:1009.4122.
- [33] CMS Collaboration, “Observation of long-range, near-side angular correlations in pPb collisions at the LHC”, *Phys. Lett. B* **718** (2013) 795, doi:10.1016/j.physletb.2012.11.025, arXiv:1210.5482.
- [34] CMS Collaboration, “Evidence for collectivity in pp collisions at the LHC”, *Phys. Lett. B* **765** (2017) 193, doi:10.1016/j.physletb.2016.12.009, arXiv:1606.06198.
- [35] M. Gyulassy and X.-N. Wang, “HIJING 1.0: A Monte Carlo program for parton and particle production in high-energy hadronic and nuclear collisions”, *Comput. Phys. Commun.* **83** (1994) 307, doi:10.1016/0010-4655(94)90057-4, arXiv:nucl-th/9502021.
- [36] I. Selyuzhenkov and S. Voloshin, “Effects of non-uniform acceptance in anisotropic flow measurement”, *Phys. Rev. C* **77** (2008) 034904, doi:10.1103/PhysRevC.77.034904, arXiv:0707.4672.
- [37] A. Bilandzic et al., “Generic framework for anisotropic flow analyses with multiparticle azimuthal correlations”, *Phys. Rev. C* **89** (2014) 064904, doi:10.1103/PhysRevC.89.064904, arXiv:1312.3572.
- [38] ALICE Collaboration, “Event shape engineering for inclusive spectra and elliptic flow in Pb-Pb collisions at $\sqrt{s_{NN}} = 2.76$ TeV”, *Phys. Rev. C* **93** (2016) 034916, doi:10.1103/PhysRevC.93.034916, arXiv:1507.06194.
- [39] T. Pierog et al., “EPOS LHC: Test of collective hadronization with data measured at the CERN Large Hadron Collider”, *Phys. Rev. C* **92** (2015) 034906, doi:10.1103/PhysRevC.92.034906, arXiv:1306.0121.
- [40] GEANT4 Collaboration, “GEANT4 — a simulation toolkit”, *Nucl. Instrum. Meth. A* **506** (2003) 250, doi:10.1016/S0168-9002(03)01368-8.
- [41] J. Allison et al., “Geant4 developments and applications”, *IEEE Trans. Nucl. Sci.* **53** (2006) 270, doi:10.1109/TNS.2006.869826.
- [42] CMS Collaboration, “Centrality dependence of dihadron correlations and azimuthal anisotropy harmonics in PbPb collisions at $\sqrt{s_{NN}} = 2.76$ TeV”, *Eur. Phys. J. C* **72** (2012) 2012, doi:10.1140/epjc/s10052-012-2012-3, arXiv:1201.3158.

- [43] Z.-W. Lin et al., “A multi-phase transport model for relativistic heavy ion collisions”, *Phys. Rev. C* **72** (2005) 064901, doi:10.1103/PhysRevC.72.064901, arXiv:nucl-th/0411110.
- [44] G.-L. Ma and B. Zhang, “Effects of final state interactions on charge separation in relativistic heavy ion collisions”, *Phys. Lett. B* **700** (2011) 39, doi:10.1016/j.physletb.2011.04.057, arXiv:1101.1701.
- [45] G. J. Feldman and R. D. Cousins, “A unified approach to the classical statistical analysis of small signals”, *Phys. Rev. D* **57** (1998) 3873, doi:10.1103/PhysRevD.57.3873, arXiv:physics/9711021.
- [46] ALICE Collaboration, “Constraining the magnitude of the Chiral Magnetic Effect with Event Shape Engineering in Pb-Pb collisions at $\sqrt{s_{NN}} = 2.76$ TeV”, (2017). arXiv:1709.04723.

D The CMS Collaboration

Yerevan Physics Institute, Yerevan, Armenia

A.M. Sirunyan, A. Tumasyan

Institut für Hochenergiephysik, Wien, Austria

W. Adam, F. Ambrogio, E. Asilar, T. Bergauer, J. Brandstetter, E. Brondolin, M. Dragicevic, J. Erö, M. Flechl, M. Friedl, R. Frühwirth¹, V.M. Ghete, J. Grossmann, J. Hrubec, M. Jeitler¹, A. König, N. Krammer, I. Krätschmer, D. Liko, T. Madlener, I. Mikulec, E. Pree, N. Rad, H. Rohringer, J. Schieck¹, R. Schöfbeck, M. Spanring, D. Spitzbart, W. Waltenberger, J. Wittmann, C.-E. Wulz¹, M. Zarucki

Institute for Nuclear Problems, Minsk, Belarus

V. Chekhovsky, V. Mossolov, J. Suarez Gonzalez

Universiteit Antwerpen, Antwerpen, Belgium

E.A. De Wolf, D. Di Croce, X. Janssen, J. Lauwers, H. Van Haevermaet, P. Van Mechelen, N. Van Remortel

Vrije Universiteit Brussel, Brussel, Belgium

S. Abu Zeid, F. Blekman, J. D'Hondt, I. De Bruyn, J. De Clercq, K. Deroover, G. Flouris, D. Lontkovskyi, S. Lowette, S. Moortgat, L. Moreels, Q. Python, K. Skovpen, S. Tavernier, W. Van Doninck, P. Van Mulders, I. Van Parijs

Université Libre de Bruxelles, Bruxelles, Belgium

D. Beghin, H. Brun, B. Clerbaux, G. De Lentdecker, H. Delannoy, B. Dorney, G. Fasanella, L. Favart, R. Goldouzian, A. Grebenyuk, G. Karapostoli, T. Lenzi, J. Luetic, T. Maerschalk, A. Marinov, A. Randle-conde, T. Seva, E. Starling, C. Vander Velde, P. Vanlaer, D. Vannerom, R. Yonamine, F. Zenoni, F. Zhang²

Ghent University, Ghent, Belgium

A. Cimmino, T. Cornelis, D. Dobur, A. Fagot, M. Gul, I. Khvastunov³, D. Poyraz, C. Roskas, S. Salva, M. Tytgat, W. Verbeke, N. Zaganidis

Université Catholique de Louvain, Louvain-la-Neuve, Belgium

H. Bakhshiansohi, O. Bondu, S. Brochet, G. Bruno, C. Caputo, A. Caudron, P. David, S. De Visscher, C. Delaere, M. Delcourt, B. Francois, A. Giammanco, M. Komm, G. Krintiras, V. Lemaître, A. Magitteri, A. Mertens, M. Musich, K. Piotrkowski, L. Quertenmont, A. Saggio, M. Vidal Marono, S. Wertz, J. Zobec

Université de Mons, Mons, Belgium

N. Beliy

Centro Brasileiro de Pesquisas Físicas, Rio de Janeiro, Brazil

W.L. Aldá Júnior, F.L. Alves, G.A. Alves, L. Brito, M. Correa Martins Junior, C. Hensel, A. Moraes, M.E. Pol, P. Rebello Teles

Universidade do Estado do Rio de Janeiro, Rio de Janeiro, Brazil

E. Belchior Batista Das Chagas, W. Carvalho, J. Chinellato⁴, E. Coelho, E.M. Da Costa, G.G. Da Silveira⁵, D. De Jesus Damiao, S. Fonseca De Souza, L.M. Huertas Guativa, H. Malbouisson, M. Melo De Almeida, C. Mora Herrera, L. Mundim, H. Nogima, L.J. Sanchez Rosas, A. Santoro, A. Sznajder, M. Thiel, E.J. Tonelli Manganote⁴, F. Torres Da Silva De Araujo, A. Vilela Pereira

Universidade Estadual Paulista ^a, Universidade Federal do ABC ^b, São Paulo, Brazil

S. Ahuja^a, C.A. Bernardes^a, T.R. Fernandez Perez Tomei^a, E.M. Gregores^b, P.G. Mercadante^b, S.F. Novaes^a, Sandra S. Padula^a, D. Romero Abad^b, J.C. Ruiz Vargas^a

Institute for Nuclear Research and Nuclear Energy of Bulgaria Academy of Sciences

A. Aleksandrov, R. Hadjiiska, P. Iaydjiev, M. Misheva, M. Rodozov, M. Shopova, G. Sultanov

University of Sofia, Sofia, Bulgaria

A. Dimitrov, I. Glushkov, L. Litov, B. Pavlov, P. Petkov

Beihang University, Beijing, China

W. Fang⁶, X. Gao⁶, L. Yuan

Institute of High Energy Physics, Beijing, China

M. Ahmad, J.G. Bian, G.M. Chen, H.S. Chen, M. Chen, Y. Chen, C.H. Jiang, D. Leggat, H. Liao, Z. Liu, F. Romeo, S.M. Shaheen, A. Spiezia, J. Tao, C. Wang, Z. Wang, E. Yazgan, H. Zhang, S. Zhang, J. Zhao

State Key Laboratory of Nuclear Physics and Technology, Peking University, Beijing, China

Y. Ban, G. Chen, Q. Li, S. Liu, Y. Mao, S.J. Qian, D. Wang, Z. Xu

Universidad de Los Andes, Bogota, Colombia

C. Avila, A. Cabrera, L.F. Chaparro Sierra, C. Florez, C.F. González Hernández, J.D. Ruiz Alvarez

University of Split, Faculty of Electrical Engineering, Mechanical Engineering and Naval Architecture, Split, Croatia

B. Courbon, N. Godinovic, D. Lelas, I. Puljak, P.M. Ribeiro Cipriano, T. Sculac

University of Split, Faculty of Science, Split, Croatia

Z. Antunovic, M. Kovac

Institute Rudjer Boskovic, Zagreb, Croatia

V. Brigljevic, D. Ferencek, K. Kadija, B. Mesic, A. Starodumov⁷, T. Susa

University of Cyprus, Nicosia, Cyprus

M.W. Ather, A. Attikis, G. Mavromanolakis, J. Mousa, C. Nicolaou, F. Ptochos, P.A. Razis, H. Rykaczewski

Charles University, Prague, Czech Republic

M. Finger⁸, M. Finger Jr.⁸

Universidad San Francisco de Quito, Quito, Ecuador

E. Carrera Jarrin

Academy of Scientific Research and Technology of the Arab Republic of Egypt, Egyptian Network of High Energy Physics, Cairo, Egypt

Y. Assran^{9,10}, S. Elgammal¹⁰, A. Mahrous¹¹

National Institute of Chemical Physics and Biophysics, Tallinn, Estonia

R.K. Dewanjee, M. Kadastik, L. Perrini, M. Raidal, A. Tiko, C. Veelken

Department of Physics, University of Helsinki, Helsinki, Finland

P. Eerola, H. Kirschenmann, J. Pekkanen, M. Voutilainen

Helsinki Institute of Physics, Helsinki, Finland

T. Järvinen, V. Karimäki, R. Kinnunen, T. Lampén, K. Lassila-Perini, S. Lehti, T. Lindén, P. Luukka, E. Tuominen, J. Tuominiemi

Lappeenranta University of Technology, Lappeenranta, Finland

J. Talvitie, T. Tuuva

IRFU, CEA, Université Paris-Saclay, Gif-sur-Yvette, France

M. Besancon, F. Couderc, M. Dejardin, D. Denegri, J.L. Faure, F. Ferri, S. Ganjour, S. Ghosh, A. Givernaud, P. Gras, G. Hamel de Monchenault, P. Jarry, I. Kucher, C. Leloup, E. Locci, M. Machet, J. Malcles, G. Negro, J. Rander, A. Rosowsky, M.Ö. Sahin, M. Titov

Laboratoire Leprince-Ringuet, Ecole polytechnique, CNRS/IN2P3, Université Paris-Saclay, Palaiseau, France

A. Abdulsalam, C. Amendola, I. Antropov, S. Baffioni, F. Beaudette, P. Busson, L. Cadamuro, C. Charlot, R. Granier de Cassagnac, M. Jo, S. Lisniak, A. Lobanov, J. Martin Blanco, M. Nguyen, C. Ochando, G. Ortona, P. Paganini, P. Pigard, R. Salerno, J.B. Sauvan, Y. Sirois, A.G. Stahl Leitner, T. Strebler, Y. Yilmaz, A. Zabi, A. Zghiche

Université de Strasbourg, CNRS, IPHC UMR 7178, F-67000 Strasbourg, France

J.-L. Agram¹², J. Andrea, D. Bloch, J.-M. Brom, M. Buttignol, E.C. Chabert, N. Chanon, C. Collard, E. Conte¹², X. Coubez, J.-C. Fontaine¹², D. Gelé, U. Goerlach, M. Jansová, A.-C. Le Bihan, N. Tonon, P. Van Hove

Centre de Calcul de l'Institut National de Physique Nucleaire et de Physique des Particules, CNRS/IN2P3, Villeurbanne, France

S. Gadrat

Université de Lyon, Université Claude Bernard Lyon 1, CNRS-IN2P3, Institut de Physique Nucléaire de Lyon, Villeurbanne, France

S. Beauceron, C. Bernet, G. Boudoul, R. Chierici, D. Contardo, P. Depasse, H. El Mamouni, J. Fay, L. Finco, S. Gascon, M. Gouzevitch, G. Grenier, B. Ille, F. Lagarde, I.B. Laktineh, M. Lethuillier, L. Mirabito, A.L. Pequegnot, S. Perries, A. Popov¹³, V. Sordini, M. Vander Donckt, S. Viret

Georgian Technical University, Tbilisi, Georgia

A. Khvedelidze⁸

Tbilisi State University, Tbilisi, Georgia

Z. Tsamalaidze⁸

RWTH Aachen University, I. Physikalisches Institut, Aachen, Germany

C. Autermann, L. Feld, M.K. Kiesel, K. Klein, M. Lipinski, M. Preuten, C. Schomakers, J. Schulz, V. Zhukov¹³

RWTH Aachen University, III. Physikalisches Institut A, Aachen, Germany

A. Albert, E. Dietz-Laursonn, D. Duchardt, M. Endres, M. Erdmann, S. Erdweg, T. Esch, R. Fischer, A. Güth, M. Hamer, T. Hebbeker, C. Heidemann, K. Hoepfner, S. Knutzen, M. Merschmeyer, A. Meyer, P. Millet, S. Mukherjee, T. Pook, M. Radziej, H. Reithler, M. Rieger, F. Scheuch, D. Teyssier, S. Thüer

RWTH Aachen University, III. Physikalisches Institut B, Aachen, Germany

G. Flügge, B. Kargoll, T. Kress, A. Künsken, T. Müller, A. Nehr Korn, A. Nowack, C. Pistone, O. Pooth, A. Stahl¹⁴

Deutsches Elektronen-Synchrotron, Hamburg, Germany

M. Aldaya Martin, T. Arndt, C. Asawatangtrakuldee, K. Beernaert, O. Behnke, U. Behrens, A. Bermúdez Martínez, A.A. Bin Anuar, K. Borras¹⁵, V. Botta, A. Campbell, P. Connor, C. Contreras-Campana, F. Costanza, C. Diez Pardos, G. Eckerlin, D. Eckstein, T. Eichhorn, E. Eren, E. Gallo¹⁶, J. Garay Garcia, A. Geiser, A. Gzhko, J.M. Grados Luyando, A. Grohsjean, P. Gunnellini, M. Guthoff, A. Harb, J. Hauk, M. Hempel¹⁷, H. Jung, A. Kalogeropoulos, M. Kasemann, J. Keaveney, C. Kleinwort, I. Korol, D. Krücker, W. Lange, A. Lelek, T. Lenz, J. Leonard, K. Lipka, W. Lohmann¹⁷, R. Mankel, I.-A. Melzer-Pellmann, A.B. Meyer, G. Mittag, J. Mnich, A. Mussgiller, E. Ntomari, D. Pitzl, A. Raspereza, B. Roland, M. Savitskyi, P. Saxena, R. Shevchenko, S. Spannagel, N. Stefaniuk, G.P. Van Onsem, R. Walsh, Y. Wen, K. Wichmann, C. Wissing, O. Zenaiev

University of Hamburg, Hamburg, Germany

R. Aggleton, S. Bein, V. Blobel, M. Centis Vignali, T. Dreyer, E. Garutti, D. Gonzalez, J. Haller, A. Hinzmann, M. Hoffmann, A. Karavdina, R. Klanner, R. Kogler, N. Kovalchuk, S. Kurz, T. Lapsien, I. Marchesini, D. Marconi, M. Meyer, M. Niedziela, D. Nowatschin, F. Pantaleo¹⁴, T. Peiffer, A. Perieanu, C. Scharf, P. Schleper, A. Schmidt, S. Schumann, J. Schwandt, J. Sonneveld, H. Stadie, G. Steinbrück, F.M. Stober, M. Stöver, H. Tholen, D. Troendle, E. Usai, L. Vanelderen, A. Vanhoefer, B. Vormwald

Institut für Experimentelle Kernphysik, Karlsruhe, Germany

M. Akbiyik, C. Barth, S. Baur, E. Butz, R. Caspart, T. Chwalek, F. Colombo, W. De Boer, A. Dierlamm, B. Freund, R. Friese, M. Giffels, D. Haitz, M.A. Harrendorf, F. Hartmann¹⁴, S.M. Heindl, U. Husemann, F. Kassel¹⁴, S. Kudella, H. Mildner, M.U. Mozer, Th. Müller, M. Plagge, G. Quast, K. Rabbertz, M. Schröder, I. Shvetsov, G. Sieber, H.J. Simonis, R. Ulrich, S. Wayand, M. Weber, T. Weiler, S. Williamson, C. Wöhrmann, R. Wolf

Institute of Nuclear and Particle Physics (INPP), NCSR Demokritos, Aghia Paraskevi, Greece

G. Anagnostou, G. Daskalakis, T. Gerasis, V.A. Giakoumopoulou, A. Kyriakis, D. Loukas, I. Topsis-Giotis

National and Kapodistrian University of Athens, Athens, Greece

G. Karathanasis, S. Kesisoglou, A. Panagiotou, N. Saoulidou

National Technical University of Athens, Athens, Greece

K. Kousouris

University of Ioánnina, Ioánnina, Greece

I. Evangelou, C. Foudas, P. Kokkas, S. Mallios, N. Manthos, I. Papadopoulos, E. Paradas, J. Strologas, F.A. Triantis

MTA-ELTE Lendület CMS Particle and Nuclear Physics Group, Eötvös Loránd University, Budapest, Hungary

M. Csanad, N. Filipovic, G. Pasztor, O. Surányi, G.I. Veres¹⁸

Wigner Research Centre for Physics, Budapest, Hungary

G. Bencze, C. Hajdu, D. Horvath¹⁹, Á. Hunyadi, F. Sikler, V. Veszpremi, A.J. Zsigmond

Institute of Nuclear Research ATOMKI, Debrecen, Hungary

N. Beni, S. Czellar, J. Karancsi²⁰, A. Makovec, J. Molnar, Z. Szillasi

Institute of Physics, University of Debrecen, Debrecen, Hungary

M. Bartók¹⁸, P. Raics, Z.L. Trocsanyi, B. Ujvari

Indian Institute of Science (IISc), Bangalore, India

S. Choudhury, J.R. Komaragiri

National Institute of Science Education and Research, Bhubaneswar, India

S. Bahinipati²¹, S. Bhowmik, P. Mal, K. Mandal, A. Nayak²², D.K. Sahoo²¹, N. Sahoo, S.K. Swain

Panjab University, Chandigarh, India

S. Bansal, S.B. Beri, V. Bhatnagar, R. Chawla, N. Dhingra, A.K. Kalsi, A. Kaur, M. Kaur, S. Kaur, R. Kumar, P. Kumari, A. Mehta, J.B. Singh, G. Walia

University of Delhi, Delhi, India

Ashok Kumar, Aashaq Shah, A. Bhardwaj, S. Chauhan, B.C. Choudhary, R.B. Garg, S. Keshri, A. Kumar, S. Malhotra, M. Naimuddin, K. Ranjan, R. Sharma

Saha Institute of Nuclear Physics, HBNI, Kolkata, India

R. Bhardwaj, R. Bhattacharya, S. Bhattacharya, U. Bhawandeep, S. Dey, S. Dutt, S. Dutta, S. Ghosh, N. Majumdar, A. Modak, K. Mondal, S. Mukhopadhyay, S. Nandan, A. Purohit, A. Roy, D. Roy, S. Roy Chowdhury, S. Sarkar, M. Sharan, S. Thakur

Indian Institute of Technology Madras, Madras, India

P.K. Behera

Bhabha Atomic Research Centre, Mumbai, India

R. Chudasama, D. Dutta, V. Jha, V. Kumar, A.K. Mohanty¹⁴, P.K. Netrakanti, L.M. Pant, P. Shukla, A. Topkar

Tata Institute of Fundamental Research-A, Mumbai, India

T. Aziz, S. Dugad, B. Mahakud, S. Mitra, G.B. Mohanty, N. Sur, B. Sutar

Tata Institute of Fundamental Research-B, Mumbai, India

S. Banerjee, S. Bhattacharya, S. Chatterjee, P. Das, M. Guchait, Sa. Jain, S. Kumar, M. Maity²³, G. Majumder, K. Mazumdar, T. Sarkar²³, N. Wickramage²⁴

Indian Institute of Science Education and Research (IISER), Pune, India

S. Chauhan, S. Dube, V. Hegde, A. Kapoor, K. Kotheekar, S. Pandey, A. Rane, S. Sharma

Institute for Research in Fundamental Sciences (IPM), Tehran, Iran

S. Chenarani²⁵, E. Eskandari Tadavani, S.M. Etesami²⁵, M. Khakzad, M. Mohammadi Najafabadi, M. Naseri, S. Paktinat Mehdiabadi²⁶, F. Rezaei Hosseinabadi, B. Safarzadeh²⁷, M. Zeinali

University College Dublin, Dublin, Ireland

M. Felcini, M. Grunewald

INFN Sezione di Bari ^a, Università di Bari ^b, Politecnico di Bari ^c, Bari, Italy

M. Abbrescia^{a,b}, C. Calabria^{a,b}, A. Colaleo^a, D. Creanza^{a,c}, L. Cristella^{a,b}, N. De Filippis^{a,c}, M. De Palma^{a,b}, F. Errico^{a,b}, L. Fiore^a, G. Iaselli^{a,c}, S. Lezki^{a,b}, G. Maggi^{a,c}, M. Maggi^a, G. Miniello^{a,b}, S. My^{a,b}, S. Nuzzo^{a,b}, A. Pompili^{a,b}, G. Pugliese^{a,c}, R. Radogna^a, A. Ranieri^a, G. Selvaggi^{a,b}, A. Sharma^a, L. Silvestris^{a,14}, R. Venditti^a, P. Verwilligen^a

INFN Sezione di Bologna ^a, Università di Bologna ^b, Bologna, Italy

G. Abbiendi^a, C. Battilana^{a,b}, D. Bonacorsi^{a,b}, L. Borgonovi^{a,b}, S. Braibant-Giacomelli^{a,b}, R. Campanini^{a,b}, P. Capiluppi^{a,b}, A. Castro^{a,b}, F.R. Cavallo^a, S.S. Chhibra^a, G. Codispoti^{a,b}, M. Cuffiani^{a,b}, G.M. Dallavalle^a, F. Fabbri^a, A. Fanfani^{a,b}, D. Fasanella^{a,b}, P. Giacomelli^a, C. Grandi^a, L. Guiducci^{a,b}, S. Marcellini^a, G. Masetti^a, A. Montanari^a, F.L. Navarria^{a,b}, A. Perrotta^a, A.M. Rossi^{a,b}, T. Rovelli^{a,b}, G.P. Siroli^{a,b}, N. Tosi^a

INFN Sezione di Catania ^a, Università di Catania ^b, Catania, Italy

S. Albergo^{a,b}, S. Costa^{a,b}, A. Di Mattia^a, F. Giordano^{a,b}, R. Potenza^{a,b}, A. Tricomi^{a,b}, C. Tuve^{a,b}

INFN Sezione di Firenze ^a, Università di Firenze ^b, Firenze, Italy

G. Barbagli^a, K. Chatterjee^{a,b}, V. Ciulli^{a,b}, C. Civinini^a, R. D'Alessandro^{a,b}, E. Focardi^{a,b}, P. Lenzi^{a,b}, M. Meschini^a, S. Paoletti^a, L. Russo^{a,28}, G. Sguazzoni^a, D. Strom^a, L. Viliani^{a,b,14}

INFN Laboratori Nazionali di Frascati, Frascati, Italy

L. Benussi, S. Bianco, F. Fabbri, D. Piccolo, F. Primavera¹⁴

INFN Sezione di Genova ^a, Università di Genova ^b, Genova, Italy

V. Calvelli^{a,b}, F. Ferro^a, E. Robutti^a, S. Tosi^{a,b}

INFN Sezione di Milano-Bicocca ^a, Università di Milano-Bicocca ^b, Milano, Italy

A. Benaglia^a, L. Brianza^{a,b}, F. Brivio^{a,b}, V. Ciriolo^{a,b}, M.E. Dinardo^{a,b}, S. Fiorendi^{a,b}, S. Gennai^a, A. Ghezzi^{a,b}, P. Govoni^{a,b}, M. Malberti^{a,b}, S. Malvezzi^a, R.A. Manzoni^{a,b}, D. Menasce^a, L. Moroni^a, M. Paganoni^{a,b}, K. Pauwels^{a,b}, D. Pedrini^a, S. Pigazzini^{a,b,29}, S. Ragazzi^{a,b}, N. Redaelli^a, T. Tabarelli de Fatis^{a,b}

INFN Sezione di Napoli ^a, Università di Napoli 'Federico II' ^b, Napoli, Italy, Università della Basilicata ^c, Potenza, Italy, Università G. Marconi ^d, Roma, Italy

S. Buontempo^a, N. Cavallo^{a,c}, S. Di Guida^{a,d,14}, F. Fabozzi^{a,c}, F. Fienga^{a,b}, A.O.M. Iorio^{a,b}, W.A. Khan^a, L. Lista^a, S. Meola^{a,d,14}, P. Paolucci^{a,14}, C. Sciacca^{a,b}, F. Thyssen^a

INFN Sezione di Padova ^a, Università di Padova ^b, Padova, Italy, Università di Trento ^c, Trento, Italy

P. Azzi^a, N. Bacchetta^a, L. Benato^{a,b}, M. Biasotto^{a,30}, D. Bisello^{a,b}, A. Boletti^{a,b}, R. Carlin^{a,b}, P. Checchia^a, M. Dall'Osso^{a,b}, P. De Castro Manzano^a, T. Dorigo^a, U. Dosselli^a, F. Gasparini^{a,b}, U. Gasparini^{a,b}, S. Lacaprara^a, P. Lujan, M. Margoni^{a,b}, A.T. Meneguzzo^{a,b}, N. Pozzobon^{a,b}, P. Ronchese^{a,b}, R. Rossin^{a,b}, F. Simonetto^{a,b}, E. Torassa^a, M. Zanetti^{a,b}, P. Zotto^{a,b}, G. Zumerle^{a,b}

INFN Sezione di Pavia ^a, Università di Pavia ^b, Pavia, Italy

A. Braghieri^a, A. Magnani^a, P. Montagna^{a,b}, S.P. Ratti^{a,b}, V. Re^a, M. Ressegotti^{a,b}, C. Riccardi^{a,b}, P. Salvini^a, I. Vai^{a,b}, P. Vitulo^{a,b}

INFN Sezione di Perugia ^a, Università di Perugia ^b, Perugia, Italy

L. Alunni Solestizi^{a,b}, M. Biasini^{a,b}, G.M. Bilei^a, C. Cecchi^{a,b}, D. Ciangottini^{a,b}, L. Fanò^{a,b}, P. Lariccia^{a,b}, R. Leonardi^{a,b}, E. Manoni^a, G. Mantovani^{a,b}, V. Mariani^{a,b}, M. Menichelli^a, A. Rossi^{a,b}, A. Santocchia^{a,b}, D. Spiga^a

INFN Sezione di Pisa ^a, Università di Pisa ^b, Scuola Normale Superiore di Pisa ^c, Pisa, Italy

K. Androsov^a, P. Azzurri^{a,14}, G. Bagliesi^a, T. Boccali^a, L. Borrello, R. Castaldi^a, M.A. Ciocci^{a,b}, R. Dell'Orso^a, G. Fedi^a, L. Giannini^{a,c}, A. Giassi^a, M.T. Grippo^{a,28}, F. Ligabue^{a,c}, T. Lomtadze^a, E. Manca^{a,c}, G. Mandorli^{a,c}, L. Martini^{a,b}, A. Messineo^{a,b}, F. Palla^a, A. Rizzi^{a,b}, A. Savoy-Navarro^{a,31}, P. Spagnolo^a, R. Tenchini^a, G. Tonelli^{a,b}, A. Venturi^a, P.G. Verdini^a

INFN Sezione di Roma ^a, Sapienza Università di Roma ^b, Rome, Italy

L. Barone^{a,b}, F. Cavallari^a, M. Cipriani^{a,b}, N. Daci^a, D. Del Re^{a,b,14}, E. Di Marco^{a,b}, M. Diemoz^a, S. Gelli^{a,b}, E. Longo^{a,b}, F. Margaroli^{a,b}, B. Marzocchi^{a,b}, P. Meridiani^a, G. Organtini^{a,b}, R. Paramatti^{a,b}, F. Preiato^{a,b}, S. Rahatlou^{a,b}, C. Rovelli^a, F. Santanastasio^{a,b}

INFN Sezione di Torino ^a, Università di Torino ^b, Torino, Italy, Università del Piemonte Orientale ^c, Novara, Italy

N. Amapane^{a,b}, R. Arcidiacono^{a,c}, S. Argiro^{a,b}, M. Arneodo^{a,c}, N. Bartosik^a, R. Bellan^{a,b}, C. Biino^a, N. Cartiglia^a, F. Cenna^{a,b}, M. Costa^{a,b}, R. Covarelli^{a,b}, A. Degano^{a,b}, N. Demaria^a,

B. Kiani^{a,b}, C. Mariotti^a, S. Maselli^a, E. Migliore^{a,b}, V. Monaco^{a,b}, E. Monteil^{a,b}, M. Monteno^a, M.M. Obertino^{a,b}, L. Pacher^{a,b}, N. Pastrone^a, M. Pelliccioni^a, G.L. Pinna Angioni^{a,b}, F. Ravera^{a,b}, A. Romero^{a,b}, M. Ruspa^{a,c}, R. Sacchi^{a,b}, K. Shchelina^{a,b}, V. Sola^a, A. Solano^{a,b}, A. Staiano^a, P. Traczyk^{a,b}

INFN Sezione di Trieste^a, Università di Trieste^b, Trieste, Italy

S. Belforte^a, M. Casarsa^a, F. Cossutti^a, G. Della Ricca^{a,b}, A. Zanetti^a

Kyungpook National University, Daegu, Korea

D.H. Kim, G.N. Kim, M.S. Kim, J. Lee, S. Lee, S.W. Lee, C.S. Moon, Y.D. Oh, S. Sekmen, D.C. Son, Y.C. Yang

Chonbuk National University, Jeonju, Korea

A. Lee

Chonnam National University, Institute for Universe and Elementary Particles, Kwangju, Korea

H. Kim, D.H. Moon, G. Oh

Hanyang University, Seoul, Korea

J.A. Brochero Cifuentes, J. Goh, T.J. Kim

Korea University, Seoul, Korea

S. Cho, S. Choi, Y. Go, D. Gyun, S. Ha, B. Hong, Y. Jo, Y. Kim, K. Lee, K.S. Lee, S. Lee, J. Lim, S.K. Park, Y. Roh

Seoul National University, Seoul, Korea

J. Almond, J. Kim, J.S. Kim, H. Lee, K. Lee, K. Nam, S.B. Oh, B.C. Radburn-Smith, S.h. Seo, U.K. Yang, H.D. Yoo, G.B. Yu

University of Seoul, Seoul, Korea

M. Choi, H. Kim, J.H. Kim, J.S.H. Lee, I.C. Park

Sungkyunkwan University, Suwon, Korea

Y. Choi, C. Hwang, J. Lee, I. Yu

Vilnius University, Vilnius, Lithuania

V. Dudenas, A. Juodagalvis, J. Vaitkus

National Centre for Particle Physics, Universiti Malaya, Kuala Lumpur, Malaysia

I. Ahmed, Z.A. Ibrahim, M.A.B. Md Ali³², F. Mohamad Idris³³, W.A.T. Wan Abdullah, M.N. Yusli, Z. Zolkapli

Centro de Investigacion y de Estudios Avanzados del IPN, Mexico City, Mexico

Reyes-Almanza, R, Ramirez-Sanchez, G., Duran-Osuna, M. C., H. Castilla-Valdez, E. De La Cruz-Burelo, I. Heredia-De La Cruz³⁴, Rabadan-Trejo, R. I., R. Lopez-Fernandez, J. Mejia Guisao, A. Sanchez-Hernandez

Universidad Iberoamericana, Mexico City, Mexico

S. Carrillo Moreno, C. Oropeza Barrera, F. Vazquez Valencia

Benemerita Universidad Autonoma de Puebla, Puebla, Mexico

I. Pedraza, H.A. Salazar Ibarguen, C. Uribe Estrada

Universidad Autónoma de San Luis Potosí, San Luis Potosí, Mexico

A. Morelos Pineda

University of Auckland, Auckland, New Zealand

D. Krofcheck

University of Canterbury, Christchurch, New Zealand

P.H. Butler

National Centre for Physics, Quaid-I-Azam University, Islamabad, Pakistan

A. Ahmad, M. Ahmad, Q. Hassan, H.R. Hoorani, A. Saddique, M.A. Shah, M. Shoaib, M. Waqas

National Centre for Nuclear Research, Swierk, Poland

H. Bialkowska, M. Bluj, B. Boimska, T. Frueboes, M. Górski, M. Kazana, K. Nawrocki, M. Szleper, P. Zalewski

Institute of Experimental Physics, Faculty of Physics, University of Warsaw, Warsaw, PolandK. Bunkowski, A. Byszuk³⁵, K. Doroba, A. Kalinowski, M. Konecki, J. Krolikowski, M. Misiura, M. Olszewski, A. Pyskir, M. Walczak**Laboratório de Instrumentação e Física Experimental de Partículas, Lisboa, Portugal**

P. Bargassa, C. Beirão Da Cruz E Silva, A. Di Francesco, P. Faccioli, B. Galinhas, M. Gallinaro, J. Hollar, N. Leonardo, L. Lloret Iglesias, M.V. Nemallapudi, J. Seixas, G. Strong, O. Toldaiev, D. Vadrucio, J. Varela

Joint Institute for Nuclear Research, Dubna, RussiaS. Afanasiev, P. Bunin, M. Gavrilenko, I. Golutvin, I. Gorbunov, A. Kamenev, V. Karjavin, A. Lanev, A. Malakhov, V. Matveev^{36,37}, V. Palichik, V. Perelygin, S. Shmatov, S. Shulha, N. Skatchkov, V. Smirnov, N. Voytishin, A. Zarubin**Petersburg Nuclear Physics Institute, Gatchina (St. Petersburg), Russia**Y. Ivanov, V. Kim³⁸, E. Kuznetsova³⁹, P. Levchenko, V. Murzin, V. Oreshkin, I. Smirnov, V. Sulimov, L. Uvarov, S. Vavilov, A. Vorobyev**Institute for Nuclear Research, Moscow, Russia**

Yu. Andreev, A. Dermenev, S. Gninenko, N. Golubev, A. Karneyeu, M. Kirsanov, N. Krasnikov, A. Pashenkov, D. Tlisov, A. Toropin

Institute for Theoretical and Experimental Physics, Moscow, Russia

V. Epshteyn, V. Gavrilov, N. Lychkovskaya, V. Popov, I. Pozdnyakov, G. Safronov, A. Spiridonov, A. Stepenov, M. Toms, E. Vlasov, A. Zhokin

Moscow Institute of Physics and Technology, Moscow, RussiaT. Aushev, A. Bylinkin³⁷**National Research Nuclear University 'Moscow Engineering Physics Institute' (MEPhI), Moscow, Russia**R. Chistov⁴⁰, M. Danilov⁴⁰, P. Parygin, D. Philippov, S. Polikarpov, E. Tarkovskii**P.N. Lebedev Physical Institute, Moscow, Russia**V. Andreev, M. Azarkin³⁷, I. Dremin³⁷, M. Kirakosyan³⁷, A. Terkulov**Skobeltsyn Institute of Nuclear Physics, Lomonosov Moscow State University, Moscow, Russia**A. Baskakov, A. Belyaev, E. Boos, A. Ershov, A. Gribushin, A. Kaminskiy⁴¹, O. Kodolova, V. Korotkikh, I. Lokhtin, I. Miagkov, S. Obraztsov, S. Petrushanko, V. Savrin, A. Snigirev, I. Vardanyan

Novosibirsk State University (NSU), Novosibirsk, RussiaV. Blinov⁴², Y.Skovpen⁴², D. Shtol⁴²**State Research Center of Russian Federation, Institute for High Energy Physics, Protvino, Russia**

I. Azhgirey, I. Bayshev, S. Bitioukov, D. Elumakhov, V. Kachanov, A. Kalinin, D. Konstantinov, P. Mandrik, V. Petrov, R. Ryutin, A. Sobol, S. Troshin, N. Tyurin, A. Uzunian, A. Volkov

University of Belgrade, Faculty of Physics and Vinca Institute of Nuclear Sciences, Belgrade, SerbiaP. Adzic⁴³, P. Cirkovic, D. Devetak, M. Dordevic, J. Milosevic, V. Rekovic**Centro de Investigaciones Energéticas Medioambientales y Tecnológicas (CIEMAT), Madrid, Spain**

J. Alcaraz Maestre, M. Barrio Luna, M. Cerrada, N. Colino, B. De La Cruz, A. Delgado Peris, A. Escalante Del Valle, C. Fernandez Bedoya, J.P. Fernández Ramos, J. Flix, M.C. Fouz, O. Gonzalez Lopez, S. Goy Lopez, J.M. Hernandez, M.I. Josa, D. Moran, A. Pérez-Calero Yzquierdo, J. Puerta Pelayo, A. Quintario Olmeda, I. Redondo, L. Romero, M.S. Soares, A. Álvarez Fernández

Universidad Autónoma de Madrid, Madrid, Spain

J.F. de Trocóniz, M. Missiroli

Universidad de Oviedo, Oviedo, Spain

J. Cuevas, C. Erice, J. Fernandez Menendez, I. Gonzalez Caballero, J.R. González Fernández, E. Palencia Cortezon, S. Sanchez Cruz, P. Vischia, J.M. Vizan Garcia

Instituto de Física de Cantabria (IFCA), CSIC-Universidad de Cantabria, Santander, Spain

I.J. Cabrillo, A. Calderon, B. Chazin Quero, E. Curras, J. Duarte Campderros, M. Fernandez, J. Garcia-Ferrero, G. Gomez, A. Lopez Virto, J. Marco, C. Martinez Rivero, P. Martinez Ruiz del Arbol, F. Matorras, J. Piedra Gomez, T. Rodrigo, A. Ruiz-Jimeno, L. Scodellaro, N. Trevisani, I. Vila, R. Vilar Cortabitarte

CERN, European Organization for Nuclear Research, Geneva, SwitzerlandD. Abbaneo, B. Akgun, E. Auffray, P. Baillon, A.H. Ball, D. Barney, M. Bianco, P. Bloch, A. Bocci, C. Botta, T. Camporesi, R. Castello, M. Cepeda, G. Cerminara, E. Chapon, Y. Chen, D. d'Enterria, A. Dabrowski, V. Daponte, A. David, M. De Gruttola, A. De Roeck, N. Deelen, M. Dobson, T. du Pree, M. Dünser, N. Dupont, A. Elliott-Peisert, P. Everaerts, F. Fallavollita, G. Franzoni, J. Fulcher, W. Funk, D. Gigi, A. Gilbert, K. Gill, F. Glege, D. Gulhan, P. Harris, J. Hegeman, V. Innocente, A. Jafari, P. Janot, O. Karacheban¹⁷, J. Kieseler, V. Knünz, A. Kornmayer, M.J. Kortelainen, M. Krammer¹, C. Lange, P. Lecoq, C. Lourenço, M.T. Lucchini, L. Malgeri, M. Mannelli, A. Martelli, F. Meijers, J.A. Merlin, S. Mersi, E. Meschi, P. Milenovic⁴⁴, F. Moortgat, M. Mulders, H. Neugebauer, J. Ngadiuba, S. Orfanelli, L. Orsini, L. Pape, E. Perez, M. Peruzzi, A. Petrilli, G. Petrucciani, A. Pfeiffer, M. Pierini, D. Rabady, A. Racz, T. Reis, G. Rolandi⁴⁵, M. Rovere, H. Sakulin, C. Schäfer, C. Schwick, M. Seidel, M. Selvaggi, A. Sharma, P. Silva, P. Sphicas⁴⁶, A. Stakia, J. Steggemann, M. Stoye, M. Tosi, D. Treille, A. Triossi, A. Tsirou, V. Veckalns⁴⁷, M. Verweij, W.D. Zeuner**Paul Scherrer Institut, Villigen, Switzerland**W. Bertl[†], L. Caminada⁴⁸, K. Deiters, W. Erdmann, R. Horisberger, Q. Ingram, H.C. Kaestli, D. Kotlinski, U. Langenegger, T. Rohe, S.A. Wiederkehr**Institute for Particle Physics, ETH Zurich, Zurich, Switzerland**

M. Backhaus, L. Bäni, P. Berger, L. Bianchini, B. Casal, G. Dissertori, M. Dittmar, M. Donegà,

C. Dorfer, C. Grab, C. Heidegger, D. Hits, J. Hoss, G. Kasieczka, T. Klijsma, W. Luster mann, B. Mangano, M. Marionneau, M.T. Meinhard, D. Meister, F. Micheli, P. Musella, F. Nessi-Tedaldi, F. Pandolfi, J. Pata, F. Pauss, G. Perrin, L. Perrozzi, M. Quittnat, M. Reichmann, D.A. Sanz Becerra, M. Schö nenberger, L. Shchutska, V.R. Tavolaro, K. Theofilatos, M.L. Vesterbacka Olsson, R. Wallny, D.H. Zhu

Universität Zürich, Zurich, Switzerland

T.K. Aarrestad, C. Amsler⁴⁹, M.F. Canelli, A. De Cosa, R. Del Burgo, S. Donato, C. Galloni, T. Hreus, B. Kilminster, D. Pinna, G. Rauco, P. Robmann, D. Salerno, K. Schweiger, C. Seitz, Y. Takahashi, A. Zucchetta

National Central University, Chung-Li, Taiwan

V. Candelise, T.H. Doan, Sh. Jain, R. Khurana, C.M. Kuo, W. Lin, A. Pozdnyakov, S.S. Yu

National Taiwan University (NTU), Taipei, Taiwan

Arun Kumar, P. Chang, Y. Chao, K.F. Chen, P.H. Chen, F. Fiori, W.-S. Hou, Y. Hsiung, Y.F. Liu, R.-S. Lu, E. Paganis, A. Psallidas, A. Steen, J.f. Tsai

Chulalongkorn University, Faculty of Science, Department of Physics, Bangkok, Thailand

B. Asavapibhop, K. Kovitanggoon, G. Singh, N. Srimanobhas

Çukurova University, Physics Department, Science and Art Faculty, Adana, Turkey

F. Boran, S. Cerci⁵⁰, S. Damarseckin, Z.S. Demiroglu, C. Dozen, I. Dumanoglu, S. Girgis, G. Gokbulut, Y. Guler, I. Hos⁵¹, E.E. Kangal⁵², O. Kara, A. Kayis Topaksu, U. Kiminsu, M. Oglakci, G. Onengut⁵³, K. Ozdemir⁵⁴, D. Sunar Cerci⁵⁰, B. Tali⁵⁰, S. Turkcapar, I.S. Zorbakir, C. Zorbilmez

Middle East Technical University, Physics Department, Ankara, Turkey

B. Bilin, G. Karapinar⁵⁵, K. Ocalan⁵⁶, M. Yalvac, M. Zeyrek

Bogazici University, Istanbul, Turkey

E. Gülmez, M. Kaya⁵⁷, O. Kaya⁵⁸, S. Tekten, E.A. Yetkin⁵⁹

Istanbul Technical University, Istanbul, Turkey

M.N. Agaras, S. Atay, A. Cakir, K. Cankocak

Institute for Scintillation Materials of National Academy of Science of Ukraine, Kharkov, Ukraine

B. Grynyov

National Scientific Center, Kharkov Institute of Physics and Technology, Kharkov, Ukraine

L. Levchuk

University of Bristol, Bristol, United Kingdom

F. Ball, L. Beck, J.J. Brooke, D. Burns, E. Clement, D. Cussans, O. Davignon, H. Flacher, J. Goldstein, G.P. Heath, H.F. Heath, J. Jacob, L. Kreczko, D.M. Newbold⁶⁰, S. Paramesvaran, T. Sakuma, S. Seif El Nasr-storey, D. Smith, V.J. Smith

Rutherford Appleton Laboratory, Didcot, United Kingdom

A. Belyaev⁶¹, C. Brew, R.M. Brown, L. Calligaris, D. Cieri, D.J.A. Cockerill, J.A. Coughlan, K. Harder, S. Harper, E. Olaiya, D. Petyt, C.H. Shepherd-Themistocleous, A. Thea, I.R. Tomalin, T. Williams

Imperial College, London, United Kingdom

G. Auzinger, R. Bainbridge, J. Borg, S. Breeze, O. Buchmuller, A. Bundock, S. Casasso, M. Citron, D. Colling, L. Corpe, P. Dauncey, G. Davies, A. De Wit, M. Della Negra, R. Di Maria,

A. Elwood, Y. Haddad, G. Hall, G. Iles, T. James, R. Lane, C. Laner, L. Lyons, A.-M. Magnan, S. Malik, L. Mastrolorenzo, T. Matsushita, J. Nash, A. Nikitenko⁷, V. Palladino, M. Pesaresi, D.M. Raymond, A. Richards, A. Rose, E. Scott, C. Seez, A. Shtipliyski, S. Summers, A. Tapper, K. Uchida, M. Vazquez Acosta⁶², T. Virdee¹⁴, N. Wardle, D. Winterbottom, J. Wright, S.C. Zenz

Brunel University, Uxbridge, United Kingdom

J.E. Cole, P.R. Hobson, A. Khan, P. Kyberd, I.D. Reid, P. Symonds, L. Teodorescu, M. Turner, S. Zahid

Baylor University, Waco, USA

A. Borzou, K. Call, J. Dittmann, K. Hatakeyama, H. Liu, N. Pastika, C. Smith

Catholic University of America, Washington DC, USA

R. Bartek, A. Dominguez

The University of Alabama, Tuscaloosa, USA

A. Buccilli, S.I. Cooper, C. Henderson, P. Rumerio, C. West

Boston University, Boston, USA

D. Arcaro, A. Avetisyan, T. Bose, D. Gastler, D. Rankin, C. Richardson, J. Rohlf, L. Sulak, D. Zou

Brown University, Providence, USA

G. Benelli, D. Cutts, A. Garabedian, M. Hadley, J. Hakala, U. Heintz, J.M. Hogan, K.H.M. Kwok, E. Laird, G. Landsberg, J. Lee, Z. Mao, M. Narain, J. Pazzini, S. Piperov, S. Sagir, R. Syarif, D. Yu

University of California, Davis, Davis, USA

R. Band, C. Brainerd, D. Burns, M. Calderon De La Barca Sanchez, M. Chertok, J. Conway, R. Conway, P.T. Cox, R. Erbacher, C. Flores, G. Funk, M. Gardner, W. Ko, R. Lander, C. Mclean, M. Mulhearn, D. Pellett, J. Pilot, S. Shalhout, M. Shi, J. Smith, D. Stolp, K. Tos, M. Tripathi, Z. Wang

University of California, Los Angeles, USA

M. Bachtis, C. Bravo, R. Cousins, A. Dasgupta, A. Florent, J. Hauser, M. Ignatenko, N. Mccoll, S. Regnard, D. Saltzberg, C. Schnaible, V. Valuev

University of California, Riverside, Riverside, USA

E. Bouvier, K. Burt, R. Clare, J. Ellison, J.W. Gary, S.M.A. Ghiasi Shirazi, G. Hanson, J. Heilman, E. Kennedy, F. Lacroix, O.R. Long, M. Olmedo Negrete, M.I. Paneva, W. Si, L. Wang, H. Wei, S. Wimpenny, B. R. Yates

University of California, San Diego, La Jolla, USA

J.G. Branson, S. Cittolin, M. Derdzinski, R. Gerosa, D. Gilbert, B. Hashemi, A. Holzner, D. Klein, G. Kole, V. Krutelyov, J. Letts, I. Macneill, M. Masciovecchio, D. Olivito, S. Padhi, M. Pieri, M. Sani, V. Sharma, S. Simon, M. Tadel, A. Vartak, S. Wasserbaech⁶³, J. Wood, F. Würthwein, A. Yagil, G. Zevi Della Porta

University of California, Santa Barbara - Department of Physics, Santa Barbara, USA

N. Amin, R. Bhandari, J. Bradmiller-Feld, C. Campagnari, A. Dishaw, V. Dutta, M. Franco Sevilla, C. George, F. Golf, L. Gouskos, J. Gran, R. Heller, J. Incandela, S.D. Mullin, A. Ovcharova, H. Qu, J. Richman, D. Stuart, I. Suarez, J. Yoo

California Institute of Technology, Pasadena, USA

D. Anderson, J. Bendavid, A. Bornheim, J.M. Lawhorn, H.B. Newman, T. Nguyen, C. Pena, M. Spiropulu, J.R. Vlimant, S. Xie, Z. Zhang, R.Y. Zhu

Carnegie Mellon University, Pittsburgh, USA

M.B. Andrews, T. Ferguson, T. Mudholkar, M. Paulini, J. Russ, M. Sun, H. Vogel, I. Vorobiev, M. Weinberg

University of Colorado Boulder, Boulder, USA

J.P. Cumalat, W.T. Ford, F. Jensen, A. Johnson, M. Krohn, S. Leontsinis, T. Mulholland, K. Stenson, S.R. Wagner

Cornell University, Ithaca, USA

J. Alexander, J. Chaves, J. Chu, S. Dittmer, K. Mcdermott, N. Mirman, J.R. Patterson, D. Quach, A. Rinkevicius, A. Ryd, L. Skinnari, L. Soffi, S.M. Tan, Z. Tao, J. Thom, J. Tucker, P. Wittich, M. Zientek

Fermi National Accelerator Laboratory, Batavia, USA

S. Abdullin, M. Albrow, M. Alyari, G. Apollinari, A. Apresyan, A. Apyan, S. Banerjee, L.A.T. Bauerdick, A. Beretvas, J. Berryhill, P.C. Bhat, G. Bolla[†], K. Burkett, J.N. Butler, A. Canepa, G.B. Cerati, H.W.K. Cheung, F. Chlebana, M. Cremonesi, J. Duarte, V.D. Elvira, J. Freeman, Z. Gecse, E. Gottschalk, L. Gray, D. Green, S. Grünendahl, O. Gutsche, R.M. Harris, S. Hasegawa, J. Hirschauer, Z. Hu, B. Jayatilaka, S. Jindariani, M. Johnson, U. Joshi, B. Klima, B. Kreis, S. Lammel, D. Lincoln, R. Lipton, M. Liu, T. Liu, R. Lopes De Sá, J. Lykken, K. Maeshima, N. Magini, J.M. Marraffino, D. Mason, P. McBride, P. Merkel, S. Mrenna, S. Nahn, V. O'Dell, K. Pedro, O. Prokofyev, G. Rakness, L. Ristori, B. Schneider, E. Sexton-Kennedy, A. Soha, W.J. Spalding, L. Spiegel, S. Stoynev, J. Strait, N. Strobbe, L. Taylor, S. Tkaczyk, N.V. Tran, L. Uplegger, E.W. Vaandering, C. Vernieri, M. Verzocchi, R. Vidal, M. Wang, H.A. Weber, A. Whitbeck

University of Florida, Gainesville, USA

D. Acosta, P. Avery, P. Bortignon, D. Bourilkov, A. Brinkerhoff, A. Carnes, M. Carver, D. Curry, R.D. Field, I.K. Furic, S.V. Gleyzer, B.M. Joshi, J. Konigsberg, A. Korytov, K. Kotov, P. Ma, K. Matchev, H. Mei, G. Mitselmakher, D. Rank, K. Shi, D. Sperka, N. Terentyev, L. Thomas, J. Wang, S. Wang, J. Yelton

Florida International University, Miami, USA

Y.R. Joshi, S. Linn, P. Markowitz, J.L. Rodriguez

Florida State University, Tallahassee, USA

A. Ackert, T. Adams, A. Askew, S. Hagopian, V. Hagopian, K.F. Johnson, T. Kolberg, G. Martinez, T. Perry, H. Prosper, A. Saha, A. Santra, V. Sharma, R. Yohay

Florida Institute of Technology, Melbourne, USA

M.M. Baarmand, V. Bhopatkar, S. Colafranceschi, M. Hohlmann, D. Noonan, T. Roy, F. Yumiceva

University of Illinois at Chicago (UIC), Chicago, USA

M.R. Adams, L. Apanasevich, D. Berry, R.R. Betts, R. Cavanaugh, X. Chen, O. Evdokimov, C.E. Gerber, D.A. Hangal, D.J. Hofman, K. Jung, J. Kamin, I.D. Sandoval Gonzalez, M.B. Tonjes, H. Trauger, N. Varelas, H. Wang, Z. Wu, J. Zhang

The University of Iowa, Iowa City, USA

B. Bilki⁶⁴, W. Clarida, K. Dilsiz⁶⁵, S. Durgut, R.P. Gandrajula, M. Haytmyradov, V. Khristenko, J.-P. Merlo, H. Mermerkaya⁶⁶, A. Mestvirishvili, A. Moeller, J. Nachtman, H. Ogul⁶⁷, Y. Onel, F. Ozok⁶⁸, A. Penzo, C. Snyder, E. Tiras, J. Wetzel, K. Yi

Johns Hopkins University, Baltimore, USA

B. Blumenfeld, A. Cocoros, N. Eminizer, D. Fehling, L. Feng, A.V. Gritsan, P. Maksimovic, J. Roskes, U. Sarica, M. Swartz, M. Xiao, C. You

The University of Kansas, Lawrence, USA

A. Al-bataineh, P. Baringer, A. Bean, S. Boren, J. Bowen, J. Castle, S. Khalil, A. Kropivnitskaya, D. Majumder, W. Mcbrayer, M. Murray, C. Royon, S. Sanders, E. Schmitz, J.D. Tapia Takaki, Q. Wang

Kansas State University, Manhattan, USA

A. Ivanov, K. Kaadze, Y. Maravin, A. Mohammadi, L.K. Saini, N. Skhirtladze, S. Toda

Lawrence Livermore National Laboratory, Livermore, USA

F. Rebassoo, D. Wright

University of Maryland, College Park, USA

C. Anelli, A. Baden, O. Baron, A. Belloni, B. Calvert, S.C. Eno, Y. Feng, C. Ferraioli, N.J. Hadley, S. Jabeen, G.Y. Jeng, R.G. Kellogg, J. Kunkle, A.C. Mignerey, F. Ricci-Tam, Y.H. Shin, A. Skuja, S.C. Tonwar

Massachusetts Institute of Technology, Cambridge, USA

D. Abercrombie, B. Allen, V. Azzolini, R. Barbieri, A. Baty, R. Bi, S. Brandt, W. Busza, I.A. Cali, M. D'Alfonso, Z. Demiragli, G. Gomez Ceballos, M. Goncharov, D. Hsu, M. Hu, Y. Iiyama, G.M. Innocenti, M. Klute, D. Kovalskyi, Y.S. Lai, Y.-J. Lee, A. Levin, P.D. Luckey, B. Maier, A.C. Marini, C. Mcginn, C. Mironov, S. Narayanan, X. Niu, C. Paus, C. Roland, G. Roland, J. Salfeld-Nebgen, G.S.F. Stephans, K. Tatar, D. Velicanu, J. Wang, T.W. Wang, B. Wyslouch

University of Minnesota, Minneapolis, USA

A.C. Benvenuti, R.M. Chatterjee, A. Evans, P. Hansen, J. Hiltbrand, S. Kalafut, Y. Kubota, Z. Lesko, J. Mans, S. Nourbakhsh, N. Ruckstuhl, R. Rusack, J. Turkewitz, M.A. Wadud

University of Mississippi, Oxford, USA

J.G. Acosta, S. Oliveros

University of Nebraska-Lincoln, Lincoln, USA

E. Avdeeva, K. Bloom, D.R. Claes, C. Fangmeier, R. Gonzalez Suarez, R. Kamalieddin, I. Kravchenko, J. Monroy, J.E. Siado, G.R. Snow, B. Stieger

State University of New York at Buffalo, Buffalo, USA

J. Dolen, A. Godshalk, C. Harrington, I. Iashvili, D. Nguyen, A. Parker, S. Rappoccio, B. Roozbahani

Northeastern University, Boston, USA

G. Alverson, E. Barberis, A. Hortiangtham, A. Massironi, D.M. Morse, T. Orimoto, R. Teixeira De Lima, D. Trocino, D. Wood

Northwestern University, Evanston, USA

S. Bhattacharya, O. Charaf, K.A. Hahn, N. Mucia, N. Odell, B. Pollack, M.H. Schmitt, K. Sung, M. Trovato, M. Velasco

University of Notre Dame, Notre Dame, USA

N. Dev, M. Hildreth, K. Hurtado Anampa, C. Jessop, D.J. Karmgard, N. Kellams, K. Lannon, N. Loukas, N. Marinelli, F. Meng, C. Mueller, Y. Musienko³⁶, M. Planer, A. Reinsvold, R. Ruchti, G. Smith, S. Taroni, M. Wayne, M. Wolf, A. Woodard

The Ohio State University, Columbus, USA

J. Alimena, L. Antonelli, B. Bylsma, L.S. Durkin, S. Flowers, B. Francis, A. Hart, C. Hill, W. Ji, B. Liu, W. Luo, D. Puigh, B.L. Winer, H.W. Wulsin

Princeton University, Princeton, USA

S. Cooperstein, O. Driga, P. Elmer, J. Hardenbrook, P. Hebda, S. Higginbotham, D. Lange, J. Luo, D. Marlow, K. Mei, I. Ojalvo, J. Olsen, C. Palmer, P. Piroué, D. Stickland, C. Tully

University of Puerto Rico, Mayaguez, USA

S. Malik, S. Norberg

Purdue University, West Lafayette, USA

A. Barker, V.E. Barnes, S. Das, S. Folgueras, L. Gutay, M.K. Jha, M. Jones, A.W. Jung, A. Khatiwada, D.H. Miller, N. Neumeister, C.C. Peng, H. Qiu, J.F. Schulte, J. Sun, F. Wang, W. Xie

Purdue University Northwest, Hammond, USA

T. Cheng, N. Parashar, J. Stupak

Rice University, Houston, USA

A. Adair, Z. Chen, K.M. Ecklund, S. Freed, F.J.M. Geurts, M. Guilbaud, M. Kilpatrick, W. Li, B. Michlin, M. Northup, B.P. Padley, J. Roberts, J. Rorie, W. Shi, Z. Tu, J. Zabel, A. Zhang

University of Rochester, Rochester, USA

A. Bodek, P. de Barbaro, R. Demina, Y.t. Duh, T. Ferbel, M. Galanti, A. Garcia-Bellido, J. Han, O. Hindrichs, A. Khukhunaishvili, K.H. Lo, P. Tan, M. Verzetti

The Rockefeller University, New York, USA

R. Ciesielski, K. Goulianos, C. Mesropian

Rutgers, The State University of New Jersey, Piscataway, USA

A. Agapitos, J.P. Chou, Y. Gershtein, T.A. Gómez Espinosa, E. Halkiadakis, M. Heindl, E. Hughes, S. Kaplan, R. Kunnawalkam Elayavalli, S. Kyriacou, A. Lath, R. Montalvo, K. Nash, M. Osherson, H. Saka, S. Salur, S. Schnetzer, D. Sheffield, S. Somalwar, R. Stone, S. Thomas, P. Thomassen, M. Walker

University of Tennessee, Knoxville, USA

A.G. Delannoy, M. Foerster, J. Heideman, G. Riley, K. Rose, S. Spanier, K. Thapa

Texas A&M University, College Station, USA

O. Bouhali⁶⁹, A. Castaneda Hernandez⁶⁹, A. Celik, M. Dalchenko, M. De Mattia, A. Delgado, S. Dildick, R. Eusebi, J. Gilmore, T. Huang, T. Kamon⁷⁰, R. Mueller, Y. Pakhotin, R. Patel, A. Perloff, L. Perniè, D. Rathjens, A. Safonov, A. Tatarinov, K.A. Ulmer

Texas Tech University, Lubbock, USA

N. Akchurin, J. Damgov, F. De Guio, P.R. Duderø, J. Faulkner, E. Gurpinar, S. Kunori, K. Lamichhane, S.W. Lee, T. Libeiro, T. Mengke, S. Muthumuni, T. Peltola, S. Undleeb, I. Volobouev, Z. Wang

Vanderbilt University, Nashville, USA

S. Greene, A. Gurrola, R. Janjam, W. Johns, C. Maguire, A. Melo, H. Ni, K. Padeken, P. Sheldon, S. Tuo, J. Velkovska, Q. Xu

University of Virginia, Charlottesville, USA

M.W. Arenton, P. Barria, B. Cox, R. Hirosky, M. Joyce, A. Ledovskoy, H. Li, C. Neu, T. Sinthuprasith, Y. Wang, E. Wolfe, F. Xia

Wayne State University, Detroit, USA

R. Harr, P.E. Karchin, N. Poudyal, J. Sturdy, P. Thapa, S. Zaleski

University of Wisconsin - Madison, Madison, WI, USA

M. Brodski, J. Buchanan, C. Caillol, S. Dasu, L. Dodd, S. Duric, B. Gomber, M. Grothe, M. Herndon, A. Hervé, U. Hussain, P. Klabbers, A. Lanaro, A. Levine, K. Long, R. Loveless, G. Polese, T. Ruggles, A. Savin, N. Smith, W.H. Smith, D. Taylor, N. Woods

†: Deceased

1: Also at Vienna University of Technology, Vienna, Austria

2: Also at State Key Laboratory of Nuclear Physics and Technology, Peking University, Beijing, China

3: Also at IRFU, CEA, Université Paris-Saclay, Gif-sur-Yvette, France

4: Also at Universidade Estadual de Campinas, Campinas, Brazil

5: Also at Universidade Federal de Pelotas, Pelotas, Brazil

6: Also at Université Libre de Bruxelles, Bruxelles, Belgium

7: Also at Institute for Theoretical and Experimental Physics, Moscow, Russia

8: Also at Joint Institute for Nuclear Research, Dubna, Russia

9: Also at Suez University, Suez, Egypt

10: Now at British University in Egypt, Cairo, Egypt

11: Now at Helwan University, Cairo, Egypt

12: Also at Université de Haute Alsace, Mulhouse, France

13: Also at Skobeltsyn Institute of Nuclear Physics, Lomonosov Moscow State University, Moscow, Russia

14: Also at CERN, European Organization for Nuclear Research, Geneva, Switzerland

15: Also at RWTH Aachen University, III. Physikalisches Institut A, Aachen, Germany

16: Also at University of Hamburg, Hamburg, Germany

17: Also at Brandenburg University of Technology, Cottbus, Germany

18: Also at MTA-ELTE Lendület CMS Particle and Nuclear Physics Group, Eötvös Loránd University, Budapest, Hungary

19: Also at Institute of Nuclear Research ATOMKI, Debrecen, Hungary

20: Also at Institute of Physics, University of Debrecen, Debrecen, Hungary

21: Also at Indian Institute of Technology Bhubaneswar, Bhubaneswar, India

22: Also at Institute of Physics, Bhubaneswar, India

23: Also at University of Visva-Bharati, Santiniketan, India

24: Also at University of Ruhuna, Matara, Sri Lanka

25: Also at Isfahan University of Technology, Isfahan, Iran

26: Also at Yazd University, Yazd, Iran

27: Also at Plasma Physics Research Center, Science and Research Branch, Islamic Azad University, Tehran, Iran

28: Also at Università degli Studi di Siena, Siena, Italy

29: Also at INFN Sezione di Milano-Bicocca; Università di Milano-Bicocca, Milano, Italy

30: Also at Laboratori Nazionali di Legnaro dell'INFN, Legnaro, Italy

31: Also at Purdue University, West Lafayette, USA

32: Also at International Islamic University of Malaysia, Kuala Lumpur, Malaysia

33: Also at Malaysian Nuclear Agency, MOSTI, Kajang, Malaysia

34: Also at Consejo Nacional de Ciencia y Tecnología, Mexico city, Mexico

35: Also at Warsaw University of Technology, Institute of Electronic Systems, Warsaw, Poland

36: Also at Institute for Nuclear Research, Moscow, Russia

37: Now at National Research Nuclear University 'Moscow Engineering Physics

Institute' (MEPhI), Moscow, Russia

38: Also at St. Petersburg State Polytechnical University, St. Petersburg, Russia

39: Also at University of Florida, Gainesville, USA

40: Also at P.N. Lebedev Physical Institute, Moscow, Russia

41: Also at INFN Sezione di Padova; Università di Padova; Università di Trento (Trento), Padova, Italy

42: Also at Budker Institute of Nuclear Physics, Novosibirsk, Russia

43: Also at Faculty of Physics, University of Belgrade, Belgrade, Serbia

44: Also at University of Belgrade, Faculty of Physics and Vinca Institute of Nuclear Sciences, Belgrade, Serbia

45: Also at Scuola Normale e Sezione dell'INFN, Pisa, Italy

46: Also at National and Kapodistrian University of Athens, Athens, Greece

47: Also at Riga Technical University, Riga, Latvia

48: Also at Universität Zürich, Zurich, Switzerland

49: Also at Stefan Meyer Institute for Subatomic Physics (SMI), Vienna, Austria

50: Also at Adiyaman University, Adiyaman, Turkey

51: Also at Istanbul Aydin University, Istanbul, Turkey

52: Also at Mersin University, Mersin, Turkey

53: Also at Cag University, Mersin, Turkey

54: Also at Piri Reis University, Istanbul, Turkey

55: Also at Izmir Institute of Technology, Izmir, Turkey

56: Also at Necmettin Erbakan University, Konya, Turkey

57: Also at Marmara University, Istanbul, Turkey

58: Also at Kafkas University, Kars, Turkey

59: Also at Istanbul Bilgi University, Istanbul, Turkey

60: Also at Rutherford Appleton Laboratory, Didcot, United Kingdom

61: Also at School of Physics and Astronomy, University of Southampton, Southampton, United Kingdom

62: Also at Instituto de Astrofísica de Canarias, La Laguna, Spain

63: Also at Utah Valley University, Orem, USA

64: Also at Beykent University, Istanbul, Turkey

65: Also at Bingol University, Bingol, Turkey

66: Also at Erzincan University, Erzincan, Turkey

67: Also at Sinop University, Sinop, Turkey

68: Also at Mimar Sinan University, Istanbul, Istanbul, Turkey

69: Also at Texas A&M University at Qatar, Doha, Qatar

70: Also at Kyungpook National University, Daegu, Korea